Studies on relationships between malignant behaviors and ezrin activity in tissues of canine osteosarcoma patients and a xenograft nude mouse model

(犬骨肉腫の臨床例およびヌードマウス移植モデルにおける悪性挙動と
ezrin 活性の関連に関する研究)

Tassanee   Jaroensong

タッサニー　ジャロンソン

Studies on relationships between malignant behaviors and ezrin activity in tissues of canine osteosarcoma patients and a xenograft nude mouse model

(犬骨肉腫の臨床例およびヌードマウス移植モデルにおける悪性挙動と ezrin 活性の関連に関する研究)

Laboratory of Veterinary Surgery

Department of Veterinary Medical Sciences

Graduate School of Agricultural and Life Sciences

The University of Tokyo

東京大学大学院農学生命科学研究科

獣医学専攻博士課程 獣医外科学研究科室

平成 19 年度入学

Tassanee　Jaroensong

タッサニー　ジャロンソン

Contents

General Introduction

General Introduction

Canine osteosarcoma (OS) is an aggressive primary bone tumor in dogs, accounting for up to 85% of malignancies originating from the skeleton (Withrow and Vail, 2007). Metastasis of canine OS occurs mainly to the lung via the hematogenous route and is the most common cause of death (Withrow and Vail, 2007). Lymph nodes are involved less commonly (4.4-9%) (Hillers *et al*., 2005; Spodnick *et al*., 1992).

Despite of advances in various managements of canine OS including limb amputation/ sparing, chemotherapy and palliative radiotherapy, prognosis remains poor because almost 90% of dogs will develop predominantly pulmonary metastasis with median survival times ranging from 3 months to 1 year and less than 20% of dogs survive for more than 2 years following diagnosis (Boston *et al*., 2007; Straw and Withrow, 1996).

Metastasis, the spread of malignant cells from the primary tumor to distant sites, is the most serious problem for cancer treatment and is the main cause of death for cancer patients. To metastasize successfully, tumor cells must overcome a series of challenges. Tumor cells must be released from the primary tumor and invade into the local environment, followed by directional motility to enter the circulation. While in the circulation, tumor cells must evade damage and death from physical stress, immune-

medianed destruction, and induction of cell death resulting from anoikis. At a distant site, tumor cells must arrest and leave the circulation and survive in the new environment. Tumor cells must proliferate within the organ parenchyma, develop a vascular network, evade destruction by immune responses, and then complete the metastatic process (Hunter, 2004; Withrow and Vail, 2007).

Xenograft models of canine OS cells injected into immunocompromised mice are necessary for a greater understanding of the biology of metastasis to improve the outcomes for canine OS patients. These models can demonstrate the interaction between cancer cells and the surrounding microenvironment that is necessary for metastasis (Welch, 1997). Moreover, they also provide opportunities to evaluate novel therapeutics. However, the nature of models prevents the study of several biologically important processes, including immune responses to OS and failure to produce spontaneous metastasis. Nowadays, orthotopic transplantation is accepted to be reproducible and reliable methodology for the studies of OS biology, metastasis and therapy.

Identification of the genes that are associated with metastasis is inevitable not only for a basic understanding of the molecular and cellular processes involved, but also to provide the novel therapeutic targets. Microarray analysis identified 53 genes (out of 3166 unique cDNAs) that were differentially expressed in the primary tumors between

more aggressive (K7M2) and less aggressive (K12) OS models (Khanna *et al*., 2001).

K7M2 exhibited increased cellular motility and cytoskeletal changes, earlier heterotypic

adherence, and enhanced tumor angiogenesis compared with K12. Ten genes were

assigned on the basis of this functional and metastasis-related characterization. *Ezrin*

was one of these 10 genes and frequently identified as a key molecule during the onset

and progression of the metastatic cascade. This report suggests that ezrin expression is

necessary for metastatic behavior in a murine model of OS.

Ezrin (cytovillin/p81/80k/Villin-2), a member of the ezrin–radixin–moesin

(ERM) proteins family, provides the link between transmembrane receptor and the actin

cytoskeleton; it also allows the tumor cells to interact with tumor microenvironments

(Bretscher *et al*., 2002; Hunter, 2004). This linker function makes ezrin essential for

many fundamental cellular processes, including the cell adhesion, motility, invasion and

integration of membrane transport with signaling pathways, such as Rho-, Akt-, and

MAPK-signaling pathway (del Pozo *et al*., 1996; Orian-Rousseau *et al*., 2007).

It is clearly demonstrated that ERM exists in two forms: inactive and active

forms. The difference between these two forms depends on the conformation of the

protein. Two domains are involved in intra- and inter-molecular interactions. ERM

proteins exist in the cytoplasm in the inactive form, in which the 107 carboxy-terminal

residues known as C-ERMAD (C-ERM associated domain) binds to the 296 amino-

terminal residues known as N-ERMAD (N-ERM associated domain) (Pearson *et al*., 2000). The activation of ERM proteins is mediated by both C-terminal threonine phosphorylation (T567 in ezrin, T564 in radixin, T558 in moesin) and exposure to polyphosphoinositides (Fievet *et al*., 2004; Pearson *et al*., 2000). Activated ERM allows the tumor cells to interact with tumor microenvironments (Bretscher *et al*., 2002; Hunter, 2004). This linker function makes ERM proteins essential for many fundamental cellular processes and support signal transduction through membrane-bound signaling proteins. A model for ezrin activation is shown in Figure 1(Khanna and Helman, 2006).

Several protein kinases have been found to phosphorylate the C-terminal threonine residues of ERM proteins, including PKCα (Ng *et al*., 2001), PKCθ (Pietromonaco *et al*., 1998), PKCι (Wald *et al*., 2008), Rho kinases/ROCK (Matsui *et al*., 1998), G-protein-coupled receptor kinase 2 (GRK2) (Cant and Pitcher, 2005) and myotonic dystrophy kinase-related Cdc42-binding kinase (MRCK) (Nakamura *et al*., 2000).

Despite of expression of other ERM proteins, the suppression of ezrin in several murine and human cancer models resulted in the inhibition of metastasis (Khanna *et al*., 2004; Yu *et al*., 2004). This suggests that ezrin, rather than other ERM proteins, is a unique protein and plays a key role in tumor metastasis.

Ezrin overexpression was associated with malignancy and metastatic potential in various human cancers, including rhabdomyosarcoma, Ewing sarcoma, soft-tissue sarcoma, melanoma, pancreatic cancer, breast cancer, colorectal carcinoma, serous ovarian carcinoma, and brain tumors (Bohling *et al*., 1996; Elliott *et al*., 2005; Elzagheid *et al*., 2008; Ilmonen *et al*., 2005; Krishnan *et al*., 2006; Meng *et al*., 2010; Moilanen *et al*., 2003; Weng *et al*., 2005; Yu *et al*., 2004). Ezrin overexpression on OS is promising as a negative prognostic factor for survival in humans (Khanna *et al*., 2004; Kim *et al*., 2009; Kim *et al*., 2007) and associated with early development of metastasis in dogs (Khanna *et al*., 2004).

According to these backgrounds, a series of studies is carried out to study the role of ezrin activity in metastasis of canine OS. In chapter 1, the relationship between the expressions of ezrin, phosphorylated ERM (p-ERM), Ki-67 (proliferation index: PI) in the primary tissues excised from spontaneous canine OS patients and clinicopathological parameters are evaluated to determine the involvement of ezrin in canine OS patients. In chapter 2, to evaluate the effect of microenvironment at the transplantation site on tumor growth and pulmonary metastatic potential of canine OS cell lines in nude mice, expressions of ezrin, p-ERM, Ki-67, Ras, B-Raf, C-Raf, p-ERK1/2, ERK1/2, and PKCα are investigated. Finally in chapter 3, chelerythrine (CHE), a pharmacological PKC inhibitor, is used to inhibit the phosphorylation of ERM

in canine OS cells, then the changes of tumor characteristics are evaluated in both *in vitro* and *in vivo* experiments.
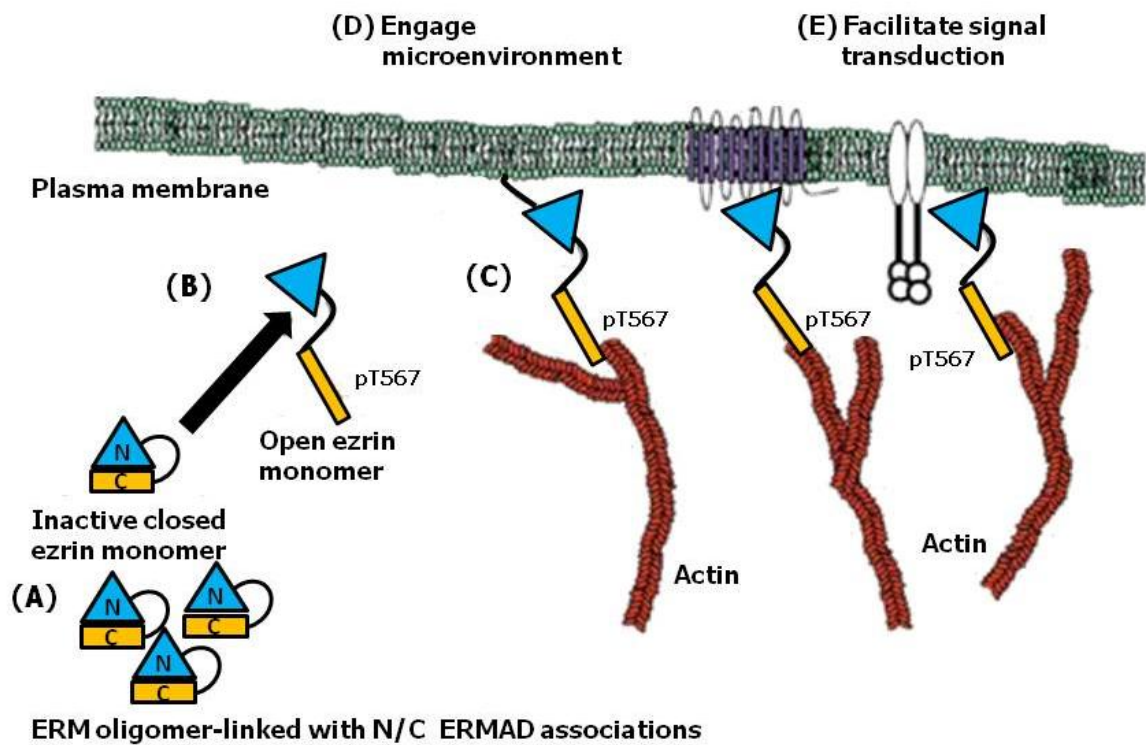
Figure 1. A model of ezrin activation. (A) Ezrin and ERM family members are inactive as monomers or oligomers where the N and C termini of the proteins either self-associate or associate with other family members. (B) Ezrin activation begins with the acquisition of an open protein conformation that results from phosphorylation of ezrin. The C-terminal threonine 567 of ezrin is believed to be a critical site of phosphorylation in this activation step. (C) In its open conformation, actin binding sites at the C terminus of ezrin bind actin. The N terminus can either bind to the cell membrane directly or to integral membrane-binding proteins. (D) This linkage of the cell membrane to the actin cytoskeleton results in a connection of the cell to its membrane, which facilitates interaction with the microenvironment. (E) The linkage is also necessary to support signal transduction through membrane-bound signaling proteins (Khanna and Helman, 2006).

Chapter 1

Investigation of ezrin and phosphorylated ERM (p-ERM) expressions in primary tumor tissues of canine OS patients

Introduction

Canine OS often develops in large and giant breeds such as Rottweiler, Great Dane, Greyhound, Saint Bernard and Doberman pinscher (McNeill *et al*., 2007; Norrdin *et al*., 1989; Ru *et al*., 1998). Males are more often affected than females (ratio 1.5:1) and the median age at presentation with clinical signs is 7-10 years old (Boston *et al*., 2006; Spodnick *et al*., 1992), though younger dogs with 18-24 months old also affect OS (Evans, 1983). The tumor arises approximately 75% in the appendicular skeleton (Liptak *et al*., 2004), followed by 24% in the axial skeleton and 1% in soft tissues (Dickerson *et al*., 2001; Hammer *et al*., 1995). The forelimbs are affected twice as often as the hindlimbs, and the distal radius and proximal humerus are the most common sites, followed by the distal femur and proximal and distal tibia (Straw *et al*., 1990; Withrow and Vail, 2007). Dogs often present lameness due to bone destruction by OS, and in some cases, pathological fracture of the affected bone with radiographic evidence of both osteoproductive and osteolytic lesions is found.

The current diagnosis for OS is made on histopathology and classified based on the formation of osteoid matrix with their predominant pattern of cell type. The histopathological classification for canine OS is as follows: poorly differentiated, osteoblastic, chondroblastic, fibroblastic, telangiectatic, and giant cell types (Slayter *et al*., 1994; Withrow and MacEwen, 1989).

The prognosis of canine OS is poor, mainly due to its earlier metastasis in the course of disease. By the time OS is found at the primary site, most have already metastasized (Ling *et al*., 1974). Negative prognostic factors associated with a shorter survival time include young age ($\leq$ 5 years) (Loukopoulos and Robinson, 2007), elevated pre-treatment total and bone-specific serum alkaline phosphatase (ALP) activities (Hillers *et al*., 2005; Kirpensteijn *et al*., 2002; Selvarajah *et al*., 2009), metastatic spread to the lung (Boston *et al*., 2006) or regional lymph nodes (Hillers *et al*., 2005), increased tumor mitotic index (Hammer *et al*., 1995; Kirpensteijn *et al*., 2002; Moore *et al*., 2007), high histological grade (grade III) (Kirpensteijn *et al*., 2002), humeral involvement (Bergman, *et al*. 1996), higher body weight ($>$ 40 kg) (Bergman *et al*., 1996; Moore *et al*., 2007), incompleteness of excision (Hammer *et al*., 1995), extension of the tumor into the adjacent soft tissue (Misdorp and Hart, 1979), increased tumor volume (Misdorp and Hart, 1979), and vascular invasion (Kirpensteijn *et al*., 2002). Although histiological subtype does not appear to influence on the clinical behavior of OS, fibroblastic subtype may have more favorable prognosis than other subtypes (Misdorp and Hart, 1979). Recently, the differential diagnosis and prognosis for OS has become increasingly reliant on molecular diagnostics and immunohistochemistry.

Ki-67 expression on immunohistochemistry has been commonly used to evaluate proliferation index (PI) in tumors. Ki-67 is expressed throughout the cell cycle (late G1, S, G2, and M), but absent in G0. Ki-67 was associated with negative prognosis in several canine neoplasms, including melanomas, mast cell tumors, cutaneous epithelial tumors, and OS (Laprie *et al*., 2001; Ohta *et al*., 2004; Sakai *et al*., 2002; Sakai *et al*., 2001).

Ezrin is known to play an important role in the metastasis of OS. Ezrin has been reported to have 100% specificity in differentiating human chondroblastic OS from chondrosarcoma (Salas *et al*., 2009). Ezrin was detected in 83% of primary canine OS and its presence was associated with early pulmonary metastasis and a shorter median disease-free interval compared to those with low ezrin expression, and a significant association with high ezrin expression and poor outcome was also found in pediatric OS (Khanna *et al*., 2004). In other studies on primary human OS, ezrin overexpression predicted lung metastasis (Xu-Dong *et al*., 2009). Moreover, ezrin overexpression predicted patients that responded to chemotherapy but had poor overall survival, relative to patients with tumors that did not express ezrin (Kim *et al*., 2009). One study found that 43.7% of high grade OS expressed high levels of ezrin and the risk of metastatic relapse was 80% greater for those patients, while no low grade OS expressed ezrin (Park *et al*., 2006). Patients in stage IIB (high grade) OS showed 51.6% of ezrin

expression and 66.7% of these patients had distant metastasis (Kim *et al*., 2007). In addition, 62% of human OS were positive for ezrin expression and ezrin was an independent prognostic factor for event-free and overall survival rate (Salas *et al*., 2007). Accordingly, ezrin has been suggested to be a molecule involved in the metastasis of OS. However, there have been only a few reports regarding the expression of ezrin in canine OS or its relationship with the clinicopathological parameters and PI.

The aim of this chapter is to investigate the expression of ezrin and p-ERM using immunohistochemical staining and to evaluate their expression in relation to clinicopathological features and PI of primary tumor tissues of canine OS patients.

Materials and Methods

Patients and tumor specimens

Fifteen canine OS tissue specimens were obtained from 15 dogs underwent surgical resection at Veterinary Medical Center, the University of Tokyo, between 2006 and 2010. The clinical information of these patients, including age, gender, breed, body weight, serum ALP, lung metastasis and survival time was obtained from the medical records and telephone interviews to the owners or referred veterinarians.

Histological classification according to World Health Organization (WHO) was made by diplomates of Japanese College of Veterinary Pathologist of the Laboratory of Veterinary Pathology, the University of Tokyo. Pulmonary metastasis was confirmed on thoracic radiography or histopathological examination after autopsy. Survival time was defined as the time from diagnosis to death.

Antibodies

The primary antibodies used for immunohistochemistry were as follows: mouse monoclonal anti-human ezrin (dilution 1:500; Sigma-Aldrich Inc., St. Louis, MO, USA); rabbit monoclonal anti-human phosphorylated ezrin/radixin/moesin (p-ERM)

(dilution1:100; Cell Signaling Technology, Danvers, MA, USA); and mouse monoclonal anti-human Ki-67 (dilution 1:100; DAKO, Glostrup, Denmark).

Histology and immunohistochemistry

All specimens were fixed in 10% neutral buffered formalin, decalcified with 10% EDTA and then paraffin-embedded using a standard protocol. The tissues were sectioned into 6-μm thickness and mounted on glass slides. The OS tissue sections were stained with hematoxyline and eosin (HE) and examined with a light microscope (Oympus BX51, Tokyo, Japan)

Immunohistochemistry was performed using DAKO ENVISION+ kit/HRP (DAKO Diagnostics Japan Inc., Kyoto, Japan). Formalin-fixed paraffin-embedded sections were deparaffinized in xylene and rehydrated through a graded ethanol series, followed by distilled water. Sections were antigen-retrieved by incubating in 10 mM sodium citrate buffer, pH 6.0, at 121 °C for 10 minutes, followed by cooling on the bench for 30 minutes. The sections were treated with 0.3% hydrogen peroxide at room temperature for 10 minutes to inactivate endogenous peroxidase. Nonspecific protein binding was saturated using 5% normal goat serum (Sigma-Aldrich Inc.) in Tris-Buffered Saline and Tween 20 (TBS-T) at room temperature for 1 hour. All sections were incubated with primary antibodies at 4°C overnight. After washing with TBS-T,

sections were incubated with labeled polymer solution containing HRP-conjugated antibodies against mouse or rabbit immunoglobulin (EnVision[TM]-HRP labeled polymer, DAKO North America Inc., Carpinteria, CA, USA) for 30 minutes at room temperature. Sections were visualized with liquid 3, 3'-diaminobenzidine (DAB)/hydrogen peroxidase solution (DAKO North America Inc.) and then washed with distilled water. Hematoxylin was used for nuclear counterstaining. Canine normal lung for ezrin and p-ERM, and the tonsil for Ki-67 were used as positive controls to assess the specification of the reactions. The absence of primary antibody was used as a negative control.

Evaluation of ezrin, p-ERM and Ki-67 expressions

The immunohistochemical staining for tissue sections were analyzed by a light microscopy (Olympus BX51, Tokyo, Japan) with a 400× magnification. The percentage of the positive cell staining area over the total field area for each field was calculated by Image J (NIH, Bethesda, MA, USA).

For the evaluation of ezrin and p-ERM expressions, the positive cell ratio was evaluated in 5 random high-power fields in each tissue specimen. The mean ratio of 5 fields was used as the percentage of positive cells in the tissues. The ezrin expression was graded as follows: negative (no staining), low (positive staining 1-32%), moderate

(positive staining between 33 to 67%) and high (positive staining between 68 to 100%) (Cui *et al*., 2010).

For the evaluation of Ki-67, 5 random high-power fields were selected and 1,000 OS cells were counted in each tissue specimen as the total field area. The ratio of Ki-67-positive nuclei was calculated. The median values for the percentage of Ki-67-positive cells of the whole specimens were used as the cutoff points as used in the previous study (Mohammed *et al*., 2007). If the percentage of positive cells was equal to or higher than the cutoff value, it was defined as high. In contrast, if the percentage of positive cells was lower than the cutoff value, it was defined as low.

Statistical analysis

The mean $\pm$ standard deviation (SD) values of the percentage of ezrin-, p-ERM-, and Ki-67- positive cells were calculated. Multiple regression analyses were performed to evaluate the relationship between the clinicopathological characteristics and the expressions of ezrin, p-ERM, and Ki-67 on the tissues of canine OS patients.

Kaplan-Meier method and log-rank test using StatView for Windows version 5.0 (SAS Institute Inc., Cary, NC, USA.) were performed to compare survival time between OS patients with high and low expression of ezrin, p-ERM, and Ki-67.

Spearman's rank correlation test was used for analyzing the correlation between

the expressions of ezrin, p-ERM, and Ki-67. Statistical difference was set at $p < 0.05$.

Data analysis was carried out using NCSS 2007 (Kaysville, UT, USA).

Results

Clinicopathological features of canine OS patients

Clinicopathological features of 15 canine OS patients are shown in Table 1.1. The median age at the time of diagnosis was 10.1 years (range: 1.9 ~ 14.4 years). The females were affected twice as often as males. The breed distribution was as follows: 5 Golden Retriever, 1 Labrador Retriever, 1 Flat Coated Retriever, 2 Border Collie, 1 Boxer, 1 Akita and 4 mixed breeds. The median body weight was 27.3 (range 9 ~ 34 kg). The primary site distribution was as follows: 2 humerus, 1 radius, 3 femur, 4 tibia, 1 maxilla, 1 mandible, 1 vertebra, and 2 ribs. Histological types were diagnosed as follows: 10 osteoblastic, 1 chondroblastic, 3 fibroblastic and 1 giant cell types. The median value of serum ALP was 306 U/L (range: 77~1,925 U/L). From these patients, 11 (73%) patients had a higher serum ALP than normal range (normal ranges of serum ALP are between 69 and 333 U/L in dogs younger than 1 year and between 47 and 254 U/L in dogs older than 1 year).

For the lung metastasis at diagnosis, 10 (67%) patients were non-metastatic and 5 (33%) patients were metastatic on radiography. The median survival time calculated from the day at diagnosis to death from 15 patients was 290 days (range: 28 ~ 1,174 days).

Correlation between the expressions of ezrin, p-ERM, and Ki-67 and clinicopathological characteristics

Table 1.2 shows the correlation between the expressions of ezrin, p-ERM, and Ki-67 and clinicopathological characteristics. Typical immunohistochemical findings of ezrin, p-ERM, and Ki-67 are shown in Figure 1.1.

The expression of ezrin and clinicopathological characteristics

All samples were found to be ezrin positive. The median value of ezrin-positive cells was 94%. Thirteen of 15 samples (87%) showed high ezrin expression. Ezrin was localized diffusely in the cytoplasm and cell membrane. There was no significant correlation between ezrin expression and variables including age, gender, breed, body weight, primary site, histological type, ALP, and lung metastasis. The survival rate of 13 dogs of the high ezrin expression group tended to be worse than that of 2 dogs of the low ezrin expression group. The survival curve for those with high and low ezrin did not show significant difference ($p = 0.2606$) (Figure 1.2A).

The expression of p-ERM and clinicopathological characteristics

All samples were found to be p-ERM positive. The median value of p-ERM-positive cells was 90%. Thirteen of 15 samples (87%) exhibited high expression. The expression of p-ERM was detectable throughout the cytoplasm and cell membrane, especially near the cell membrane. There were no significant correlation between high or low percentages of p-ERM-positive cells and variables including age, gender, breed, body weight, primary site, histological type, ALP, and lung metastasis. The survival rate of 13 dogs of the high p-ERM expression group tended to be worse than that of 2 dogs of the low p-ERM expression group. The survival curve for those with high and low p-ERM did not show significant difference ($p = 0.2606$) (Figure 1.2B).

The expression of Ki-67 and clinicopathological characteristics

All samples were found to be Ki-67 positive. The median value of Ki-67 was 5.8% (range: 0.3~23.7%). Eight of 15 samples (53.3%) exhibited high percentages of Ki-67-positive cells. There was no significant correlation between the expression of Ki67 and variables of any clinicopathological features. The survival rate of 8 dogs of the high Ki-67 expression group seemed similar to that of 7 dogs of the low Ki-67 expression group. The survival curve for those with high and low Ki-67 did not show significant difference ($p = 0.6874$) (Figure 1.2C).

Correlation among the expressions of ezrin, p-ERM, and Ki-67

Figure 1.3 shows the correlation between the expressions of ezrin, p-ERM, and Ki-67. The ezrin-positive cell percentages had significant correlation (correlation coefficient $r = 0.9932$, $p = 0.0000$) with p-ERM-positive cell percentages (Figure 1.3A). On the contrary, there was no significant correlation (correlation coefficient $r = 0.2640$, $p = 0.3417$) between ezrin- and Ki-67-positive cell percentages (Figure 1.3B).

Discussion

In this study, I examined the expression of ezrin, p-ERM, and Ki-67 in the tissues of canine OS patients and their correlation with clinicopathological features was evaluated.

According to clinical data from 15 patients, canine OS was more common in dogs older than 5 years old in large breeds such as Golden Retriever whose body weight was over 25 kg. The results were mostly similar to those in previous studies though the number of case was too small (McNeill *et al*., 2007; Norrdin *et al*., 1989; Ru *et al*., 1998; Spodnick *et al*., 1992). Contrast to one study (Boston *et al*., 2006), I found that females were more commonly affected than males, though the sample size was again too small. In this study, the primary tumors developed in the appendicular skeleton in 66.7% of patients and in the axial skeleton in the remaining patients. This result was similar to another study (Liptak *et al*., 2004). In the appendicular skeleton, the hindlimbs were affected twice as often as the forelimbs in which the tibia was the most common site, though the previous reports indicated that the forelimbs were more common (Straw *et al*., 1990; Withrow and Vail, 2007). For histology, a predominance of osteoblastic type was over the other histological types. This finding agreed with the previous report (Hammer *et al*., 1995). Elevated ALP was detected in 73% of patients. This result was similar to another study (Garzotto *et al*., 2000).

In this chapter, the expression of ezrin was found in all canine OS tissue specimens examined. There was no significant correlation between ezrin expression and clinicopathological features. However, the survival rate of the high ezrin expression group tended to be worse than that of the low ezrin expression group.

These results were similar to the previous study, in which high ezrin expression was detected in 83% of primary tissues in canine OS patients and its presence was associated with a shorter disease-free interval compared to those with low ezrin expression. Moreover, a significant association with high ezrin expression and poor prognostic outcome was also found in pediatric OS (Khanna *et al*., 2004).

Recent studies suggest that the mechanism by which ezrin contributes to metastasis requires the phosphorylation of ezrin in several human tumors, including pancreatic ductal adenocarcinoma, Ewing's sarcoma, and OS (Cui *et al*., 2010; Krishnan *et al*., 2006; Ren *et al*., 2009). The positive expression of p-ERM was found in all canine OS tissues in this study and high expression was also found in tissues with high expression of ezrin on the same specimens. Statistical analyses showed no significant correlation between p-ERM expression and clinicopathological characteristics. The survival rate of the high p-ERM expression group tended to be worse than that of the low p-ERM expression group. This result supported the

expression of p-ERM may reflect the active status or the serious behavior of OS patients. However in recent time, there is no report of p-ERM expression in canine OS.

Assessment of proliferative potential in canine OS tissues using immunohistochemistry for Ki-67 in one study suggested that the expression of Ki-67 correlated positively with tumor proliferation and a shorter survival time (Ohta *et al*., 2004). There was a positive correlation between expression of ezrin and Ki-67 as well as tumor proliferation in human chondrosarcoma (Hameetman *et al*., 2005; Soderstrom *et al*., 2010). However in this study, the expression of Ki-67 was not significantly associated with any clinicopathological features. Moreover, unlike ezrin and p-ERM, the high expression of Ki-67 was found only 8 of 15 patients (53.3%). With regard to the correlation among ezrin, p-ERM, and Ki-67 expressions, ezrin was significantly associated with p-ERM, but not with Ki-67. In addition, with regard to the correlation between survival time and these proteins, the survival curve for those with high and low ezrin, p-ERM and Ki-67 expression did not show significant difference. However, the survival rate of the high ezrin and p-ERM expression groups tended to be worse than that of the low ezrin and p-ERM expression groups.

Despite of the limitations of this study, such as a small sample size and a shorter follow up period, the results contributed the important data that canine OS patients who expressed ezrin and p-ERM on the primary tissues had a shorter survival time. In

addition, ezrin and p-ERM may play a role in development of malignant behaviors of canine OS. In this chapter, it was difficult to conclude that ezrin and p-ERM expression in canine OS patients was a prognostic factor, but these proteins may be indicated to predict the outcome of canine OS patients. The roles and the mechanism of ezrin and p-ERM expressions should be further clarified.

Variables	Values
Number of patients	15
Median age at diagnosis (years)	10.1 (1.9 - 14.5)
< 5	2 (13%)
≥ 5	13 (87%)
Gender	
Male	5 (33%)
Female	10 (67%)
Breed	
Golden Retriever	5 (33%)
Labrador Retriever	1 (6.7%)
Flat Coated Retriever	1 (6.7%)
Border Collie	2 (13%)
Boxer	1 (6.7%)
Akita	1 (6.7%)
Mixed breed	4 (27%)
Median body weight (kg)	27.3 (9 – 34)
< 25	6 (40%)
≥ 25	9 (60%)
The primary site	
Humerus	2 (13%)
Radius	1 (6.7%)
Femur	3 (20%)
Tibia	4 (27%)
Maxilla	1 (6.7%)
Mandible	1 (6.7%)
Vertebra	1 (6.7%)
Rib	2 (13%)
Histological type	
Osteoblastic	10 (67%)
Chondroblastic	1 (6.7%)
Fibroblastic	3 (20%)
Giant cell	1 (6.7%)
ALP (U/L)	306 (77-1,925)
Normal	4 (27%)
High	11 (73%)
Pulmonary metastasis	
Negative	10 (67%)
Positive	5 (33%)
Survival time (day)	290 (28 – 1,174)
death	12 (80%)
alive	3 (20%)

**Table 1.1.** Clinicopathological characteristics of canine OS patients.

		Ezrin			p-ERM			Ki-67		
	Total	High	Low	*p*	High	Low	*p*	High	Low	*p*
Number of patients	15	13	2		13	2		8	7	
Age (years)				0.473			0.456			0.1188
< 5	2	2	0		2	0		2	0	
≥ 5	13	11	2		11	2		6	7	
Gender				0.4595			0.4337			0.4376
Male	5	4	1		4	1		3	2	
Female	10	9	1		9	1		5	5	
Breed				0.6463			0.7875			0.3809
Retrievers	7	6	1		6	1		2	5	
Others	8	7	1		7	1		6	2	
Body weight (kg)				0.997			0.8205			0.5356
< 25	6	5	1		5	1		4	2	
≥ 25	9	8	1		8	1		4	5	
Primary site				0.1478			0.131			0.1167
Appendicular	10	8	2		8	2		5	5	
Others	5	5	0		5	0		3	2	
Histological type				0.144			0.1249			0.6845
Osteoblastic	10	10	0		10	0		5	5	
Others	5	3	2		3	2		3	2	
ALP				0.1652			0.1659			0.0713
Normal	4	3	1		3	1		1	3	
High	11	10	1		10	1		7	4	
Pulmonary metastatasis				0.6235			0.8265			0.9835
Negative	10	9	1		9	1		4	6	
Positive	5	4	1		4	1		4	1	

Table 1.2. Correlation between ezrin, p-ERM, or Ki-67 and clinicopathological characteristics of canine OS patients. There were no significant differences between either ezrin, p-ERM, or Ki-67 and clinicopathological characteristics.

High   **Low**

Ezrin (A, B)
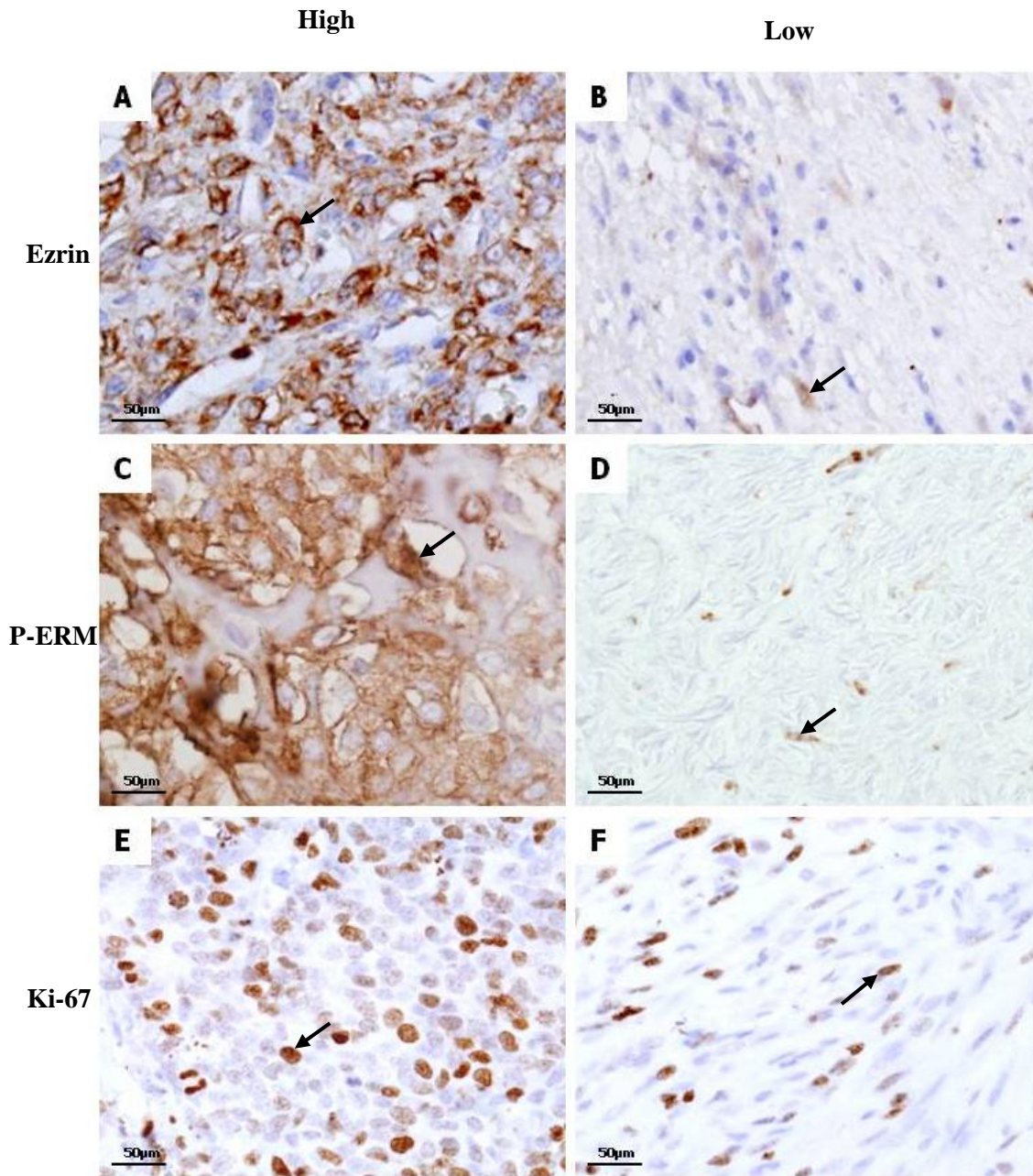
P-ERM (C, D)

Ki-67 (E, F)

Figure 1.1. Typical immunohistochemical findings of ezrin (A, B), p-ERM (C, D), and Ki-67 (E, F) in the primary tissues of canine OS patients. Arrows indicate positive cells. Original magnification, 400×.
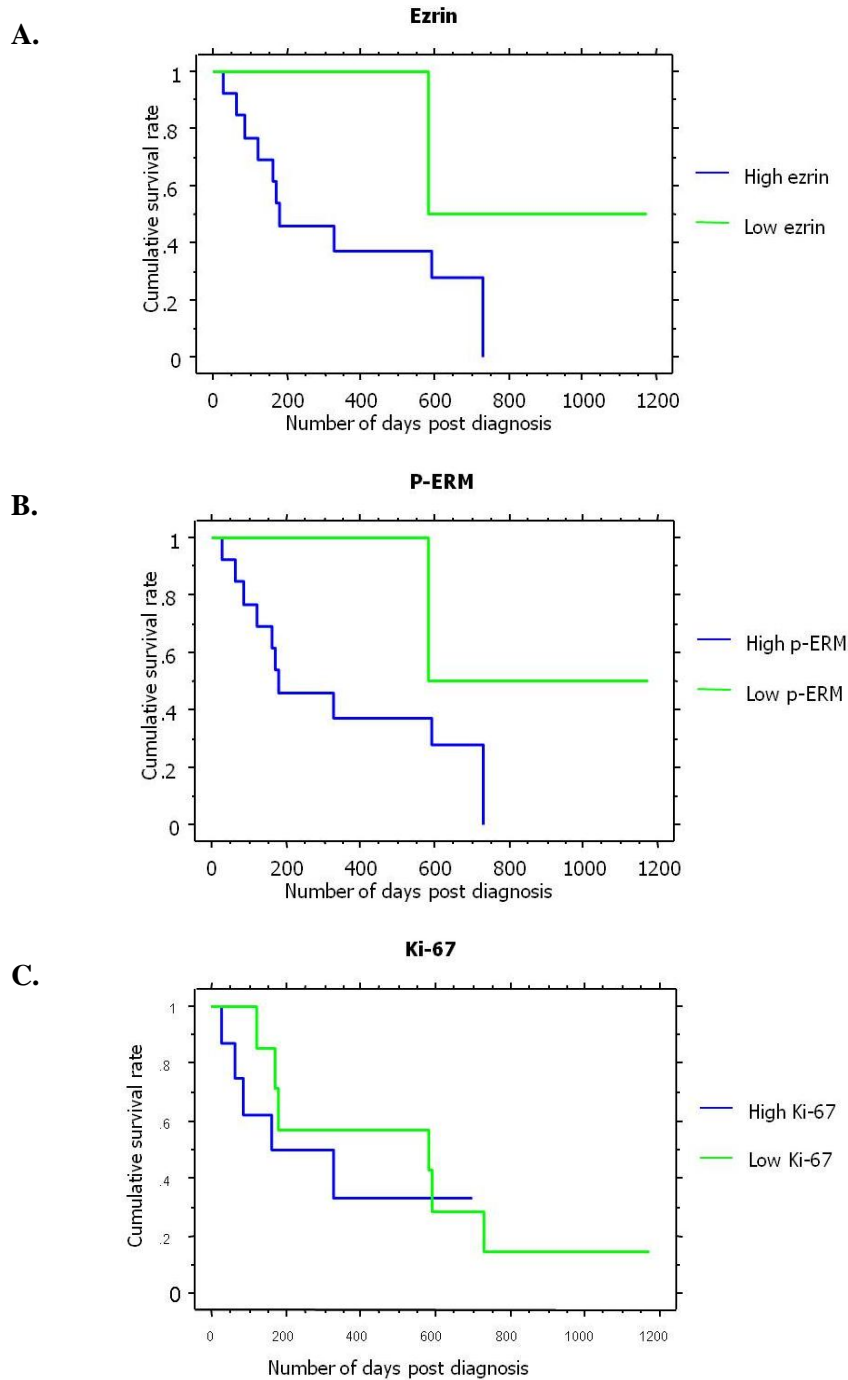
Figure 1.2. Kaplan-Meier survival time between high and low ezrin, p-ERM, or Ki-67 expressions in canine OS patients. (A) High ezrin expression, n = 13; Low ezrin expression, n = 2 (Log rank *p* = 0.2606); (B) High p-ERM expression, n = 13; Low p-ERM expression, n = 2 (Log rank *p* = 0.2606); and (C) High Ki-67 expression, n = 8; Low p-ERM expression, n = 7 (Log rank *p* = 0.6874). There were no significant differences between high and low ezrin, p-ERM, or Ki-67 expressions in canine OS patients.

A.

B.
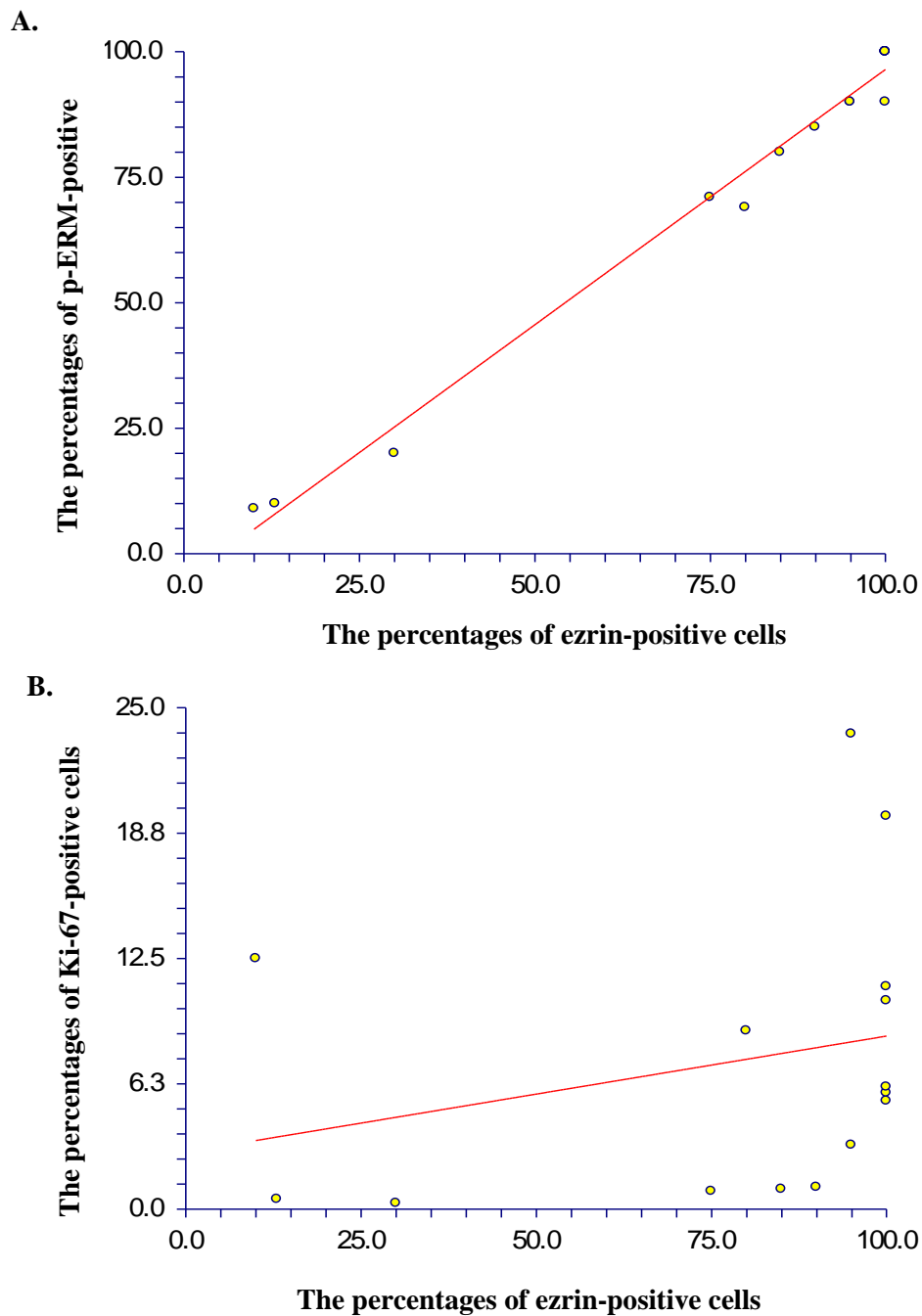
Figure 1.3. Correlation between ezrin- and p-ERM-positive cell percentages and ezrin- and Ki-67-positive cell percentages. (A) Statistical analysis demonstrated positive correlation between the percentages of ezrin-positive cells and p-ERM-positive cells (correlation coefficient $r = 0.9932$, $p = 0.0000$). (B) Statistical analysis demonstrated no correlation between the percentages of ezrin-positive cells and Ki-67-positive cells (correlation coefficient $r = 0.2640$, $p = 0.3417$).

Chapter 2

Effects of microenvironment at transplantation sites

on the growth and metastasis in a canine OS cell-

xenografted mouse model

Introduction

In the previous chapter, I investigated the clinicopathological characteristics and the expression of ezrin, p-ERM, and PI in tissues of canine OS patients. Although the results suggested that the expression of ezrin and p-ERM tended to correlate with the survival time, there were a few limitations in the first chapter.

Mouse models have been commonly used to study on the biology of tumor behaviors. Basic and clinical cancer studies can provide insight into the mechanisms underlying the development of primary tumor growth and metastasis as well as testing novel therapeutic agents. Tumor progression in a murine OS model may be faster than that in canine OS (Khanna and Hunter, 2005), which is more preferable for investigating the mechanism of OS development.

The transplantation site used in the mouse model has been investigated to clarify the effect of microenvironment on the malignant behaviors of tumor cells. Spontaneous metastasis is produced by transplanting the tumor cells into orthotopic sites. However, the same tumor cells transplanted into the subcutaneous tissue (ectopic site) sometimes fail to produce metastasis (Killion *et al*., 1998). Transplantation into orthotopic sites has been frequently used to develop many human tumor models with spontaneous metastasis in colon, bladder, lung, pancreas, prostate, and bone tumors (Berlin *et al*., 1993; Cui *et al*., 2006; Kubota, 1994; Nakamura *et al*., 2007; Togo *et al*., 1995).

The orthotopic transplantation of human small-cell lung carcinoma revealed a different chemosensitivity pattern compared with the subcutaneousely inoculated model (Kuo *et al*., 1993). This suggests different pharmacodynamics in the orthotopic lung and ectopic subcutaneous tissue. Primary tumors grown in the subcutis are sensitive to doxorubicin, whereas experimental metastatic tumors in the lungs are not. When human colon carcinoma cells were injected into the subcutaneous site, they did not produce any visceral metastases; however, when they were transplanted into the cecum, they metastasized to regional mesenteric lymph nodes and the liver (Nakajima *et al*., 1990). In the report, the microenvironment of the subcutis was found to potentially contain low levels of type IV collagenase and heparanase, whereas that of the cecal wall potentially contained high levels of both. These results suggest that factors in the environment at the transplantation site may affect tumor extracellular matrix-degrading enzymes. Furthermore, these factors may alter the metastatic potential of human colon carcinoma cells in nude mice.

Recently, several orthotopic models of OS in nude mice have been made in human and murine OS cells (Khanna *et al*., 2000). However, there have been no reports that compare the primary tumor growth and lung metastatic potential of canine OS cell lines between ectopic and orthotopic transplantation.

In a mouse model of OS and breast cancer, ezrin was found to be necessary for development of metastases (Elliott *et al*., 2005; Khanna *et al*., 2004). Ezrin-mediated early metastatic survival of mouse OS cell lines was partially dependent on activation of mitogen-activated protein kinase (MAPK) family members ERK1/2 (Khanna *et al*., 2004). B- and C-Raf are two of several Raf kinase isoforms that mediate cell growth, proliferation, and survival signaling downstream of Ras in the MAPK pathway. They are the cellular proto-oncogene homologue of a retroviral oncogene v-Raf and are the central component of the MAPK cascade (Heidecker *et al*., 1990; Morrison and Cutler, 1997). However, the detailed signal transduction pathways of phosphorylated ezrin remain unclear. Ezrin was not only associated with MAPK pathway, but relationship between ezrin and PKCα was also reported in the other study. PKCα is one of several protein kinases that can regulate ezrin during metastatic progression in human and murine OS (Ren *et al*., 2009).

In the section 1 of this chapter, tumor growth and pulmonary metastatic potential of 3 canine OS cell lines (HMPOS, OOS, and CHOS) are evaluated after transplanting to different transplantation sites of nude mice. The expression levels of ezrin and p-ERM are evaluated in both *in vitro* and *in vivo*. In the section 2, to study the roles and mechanisms of ezrin activity, PI in primary tissues of HMPOS/OOS/CHOS-xenografted mice and lung metastatic tissues of HMPOS-xenografted mice, the expression of

molecules in Ras/Raf/ERK pathway (Ras, B-Raf, C-Raf, p-ERK1/2, and ERK1/2) and

PKCα are also evaluated on 3 canine OS cell lines and tissues of mice xenografted with

HMPOS cells.

Section 1: Effects of transplantation sites on tumor growth, pulmonary metastatic potential, and the expression of ezrin and p-ERM in canine OS cells xenografted into nude mice

Materials and Methods

Cell lines and culture conditions

Three canine OS cell lines, HMPOS (Barroga *et al*., 1999), OOS, and CHOS (Hong *et al*., 1998), established from spontaneous canine OS patients were used in this study. The HMPOS cell line was derived from a cloned POS cell line from spontaneous femoral OS. The OOS and CHOS cell lines were derived from mandibular and scapular OS, respectively. The cells were maintained in RPMI-1640 (Wako Pure Chemical Industries Ltd., Osaka, Japan) supplemented with 10% heat inactivated fetal bovine serum (Gibco BRL, Grand Island, NY, USA) and 5 mg/L gentamicin (Sigma-Aldrich Inc.) at 37°C in a humidified atmosphere with 5% CO_2.

Antibodies

The primary antibodies for ezrin and p-ERM used for Western blot analysis, immunocytochemistry, and immuohistochemistry were the same as in chapter 1. The dilutions of these antibodies in each experiment were shown in the following table:

Antibodies	Dilutions		
	WB	ICC	IHC
Ezrin	1:4,000	1:500	1:500
P-ERM	1:1,000	1:200	1:100
Actin	1:10,000	-	-

WB, Western blot analysis; ICC, Immunocytochemistry; IHC, Immunohistochemistry

Western blot analysis

Tumor cells in sub-confluent condition were collected and washed 3 times in ice-cold phosphate buffer saline (PBS). Then cells were lysed in RIPA buffer [50 mM Tris-HCl, 150 mM NaCl, 5 mM EDTA, 1% Triton-X, 0.1% SDS, 4 mM Pefabloc SC (Roche Diagnostics K.K., Basel, Switzerland), 5 μg/ml aprotinin, 5 μg/ml leupeptin, 10 mM NaF, 2 mM Na_3VO_4 and 1 complete mini tablet (Roche Diagnostic)/10 ml H_2O]. Lysates were centrifuged at 15,000 rpm at 4^oC for 20 minutes. Protein concentrations of

supernatants were measured by a spectrophotometer using BCA protein assay reagent (Thermo Fisher Scientific Inc., Rockford, IL, USA). Cell lysates were denatured at $98^{\circ}C$ for 5 minutes in $2\times$sample loading buffer. Equal amount of proteins were resolved on SDS-polyacrylamide gel electrophoresis (PAGE) and transferred onto polyvinylidine fluoride (PVDF) membranes (Bio-Rad Laboratories, Hercules, CA, USA). The membranes were blocked with 5% non-fat dry milk in TBS-T for 1 hour at room temperature. The blots were incubated with primary antibodies over night at $4^{\circ}C$ with agitation. A mouse monoclonal anti-actin (Millipore, Tenecula, CA, USA.) was used as an internal control. The membranes were rinsed in TBS-T and incubated with the horseradish peroxidase (HRP)-conjugated antibodies against mouse or rabbit IgG (GE Healthcare, Piscataway, NJ, USA) for 1 hour at room temperature with vigorous agitation. The antigen-antibody complex of proteins was visualized by using the enhanced chemiluminescence (ECL) Plus detection system (GE Healthcare).

Immunocytochemistry

Three canine OS cells at a density of 2.5×10^3 cells/well were cultured in Lab Tek II 8-well chamber slides (Thermo Fisher Scientific Inc., Waltham, MA, USA) coated with poly-L-lysine, and allowed to adhere for 24 hours. Culture media were removed and the wells were flushed gently with phosphate buffer solution (PBS) 3

times. Then OS cells were fixed with 4% paraformaldehyde in PBS at room temperature

for 30 minutes. After washing 3 times with PBS, the sections were treated with 0.3%

hydrogen peroxide in distilled water at room temperature for 10 minutes to inactivate

endogenous peroxidase. Nonspecific protein binding was saturated using 5% normal

goat serum (Sigma-Aldrich Inc.) in PBS-T at room temperature for 45 minutes. All

sections were incubated with primary antibodies at $4^{o}C$ overnight. After being washed

with PBS-T 3 times, sections were incubated with labeled polymer solution containing

HRP-conjugated antibodies against mouse or rabbit immunoglobulin (EnVision^{TM}-HRP

labeled polymer, DAKO North America Inc.) at room temperature for 30 minutes.

Sections were visualized with liquid 3,3'-diaminobenzidine (DAB)/hydrogen

peroxidase solution (DAKO North America, Inc.) and then washed with distilled water.

Hematoxylin was used for nuclear counterstaining. Appropriate positive controls were

the same as in immunohistochemistry in chapter 1. The absence of primary antibody

was used as a negative control.

Cell transplantation

Five-week-old female BALB/c nude mice (SLC, Tokyo, Japan) were maintained

under specific pathogen-free conditions and given sterilized food and water *ad libitum*.

To examine the effects of different transplantation sites on primary tumor growth and

metastasis *in vivo*, the mice were divided into 3 groups according to the transplantation sites as shown in Figure 2.1.1: subcutaneous (SC group), intratibial (IT group) and intravenous (IV group) transplantation. In the SC group, 2×10^6 OS cells in 200 μL medium without serum were injected into the subcutis of the right lateral flank. In the IT group, 2×10^6 cells in 10 μL medium were injected into the right proximal tibia. To assess experimental metastasis, the IV group was injected with 2×10^6 cells in 100 μL medium into the lateral tail vein. Total number of mice in this study was 135 mice (n = 5/time point/transplantation site/cell line).

Evaluation of primary tumor growth and metastasis

Primary tumors developed in nude mice were measured twice a week after transplantation until the time of sacrifice. Tumor diameter was measured in 2 perpendicular dimensions: D1 and D2. In the IT group, D1 was anteroposterior length and D2 was the lateral plane. In the SC group, D1 was tumor length and D2 was tumor width. The tumor volume was calculated according to the following formula (Berlin *et al.*, 1993):

$$\text{Tumor volume (mm}^3) = 4/3 \cdot \pi [1/4 \cdot (D1 + D2)]^2$$

The number of mice in this study was 5 mice in each transplantation site at each sacrificed time. Mice were sacrificed 1, 2, and 4 weeks after transplantation. Primary

41

tumors and lung lesions were subsequently harvested and grossly assessed for evidence of primary tumor development and lung metastasis. Radiograms of the affected tibias of IT-xenografted mice were taken immediately after euthanization to obtain images of the bone lesions. Animal handling and all experimental procedures were in accordance with Guidelines for Animal Experiments by the Graduate School of Agricultural and Life Sciences, the University of Tokyo.

Histopathology and Immunohistochemistry

All tissues were fixed in 10% neutral buffered formalin for 24 hours. The lesions of the tibia were decalcified for 2 weeks in 10% EDTA. All tissues were cut into 4 to 6 µm sections and stained with HE for histopathology.

For immunohistochemistry and evaluation of the ezrin and p-ERM expressions, tissue sections were treated as described in chapter 1.

Statistical analysis

The mean, SD, and standard error (SE) values of primary tumor volumes, the number of lung metastatic nodules, and the percentage of ezrin- and p-ERM-positive cells were calculated. The Tukey-Kramer multiple comparison test and analysis of

variance (ANOVA) were used for statistical analysis among the different groups. Statistical difference was set at $p < 0.05$. Data analysis was carried out using NCSS 2007 (Kaysville, UT, USA).

Results

Morphology of canine OS cells

Figure 2.1.2 shows morphological appearance of canine OS cell lines. HMPOS cell line was medium-sized and polygonal in shape. OOS cell line consisted of spherical cells, fibroblast-like cells, large or small polygonal cells, and multinucleated giant cells. CHOS cell line consisted of elongated fibroblastic cells.

Western blot analysis for ezrin and p-ERM

Figure 2.1.3 shows the expression of ezrin and p-ERM in HMPOS, OOS, and CHOS cells. Ezrin was expressed in all canine OS cell lines. P-ERM was expressed in HMPOS and OOS cells, but not in CHOS cells.

Immunocytochemistry for ezrin and p-ERM

Figure 2.1.4 shows immunocytochemical findings for ezrin and p-ERM. Ezrin and p-ERM were distributed throughout the cytosol and cell membrane. Ezrin was expressed in all cell lines. P-ERM was expressed in HMPOS and OOS cells, but not in CHOS cells.

Primary tumor development in canine OS-xenografted mice

Primary tumor masses were developed in all nude mice after SC and IT transplantation of OS cells. Figure 2.1.5 shows the typical mice at 4 weeks after transplantation with HMPOS, OOS, and CHOS cells via SC and IT sites. Both SC and IT transplantation, HMPOS cells were significantly more tumorigenic than OOS and CHOS cells.

Figure 2.1.6 shows the histological findings at 2 weeks and radiographic images at 4 weeks after transplantation. Tissues produced by xenograft of HMPOS and OOS cells were mainly composed of osteoblastic spindloid tumor cells, while those produced by CHOS cells were composed of fibroblastic elongated spindle cells. Radiography revealed that the tibial lesions in IT-xenografted mice with HMPOS cells exhibited less osteolysis with more soft-tissue swelling and much osteoid tissue (Figure 2.1.6G); those with OOS and CHOS cells exhibited severe osteolysis with less soft-tissue swelling (Figure 2.1.6H and I).

Figure 2.1.7 shows the increases in tumor volume after the transplantation of each cell line via IT or SC. The primary tumors developed by xenograft of HMPOS and OOS exhibited a gradual increase in tumor volume, although the masses formed by HMPOS were significantly larger ($p < 0.05$) than those formed by OOS and CHOS cells. In addition, the tumor volumes in IT-xenografted mice were significantly larger (p

< 0.05) than those in SC-xenografted mice. In nude mice xenografted with CHOS cells, the tumor mass and volume developed by SC injection decreased 2 weeks after transplantation.

Pulmonary metastasis

Figure 2.1.8 shows gross findings of lung metastatic nodules at 4 weeks after transplantation. IT- and IV-xenografted mice with HMPOS and OOS cells showed variably sized metastatic nodules on the lung surface, whereas SC-xenografted mice with the same cells did not. There was no macroscopic metastasis on the surface of the lung in CHOS-xenografted mice with all transplantation sites.

Figure 2.1.9 shows the number of gross metastatic nodules at 2 and 4 weeks after transplantation of each cell line. IT-xenografted mice with HMPOS cells produced a considerably larger number of visible lung metastatic nodules at 4 weeks, while SC-xenografted mice with HMPOS cells did not produce any visible nodules by this time; meanwhile, the correct number of metastatic nodules could not be counted at 4 weeks in IT- and IV-xenografted mice due to too many nodules. In HMPOS-xenografted mice, the number of lung metastatic nodules by IT transplantation was significantly lower ($p < 0.05$) than those by IV transplantation at 2 weeks after transplantation. However at 4 weeks after transplantation, the number of lung metastatic nodules through IT and IV

xenografts were similar. In OOS-xenografted mice, the number of lung metastatic nodules was similar in IT- and IV- xenografted mice at 2 and 4 weeks after transplantation. In mice xenografted with OOS cells via SC, there were no visible lung metastases even 4 weeks after transplantation. In mice xenografted with CHOS cells, there were no visible lung metastases in any transplantation routes.

Histologically, lung metastases were found in all mice xenografted with HMPOS cells and 2 of 5 mice xenografted with OOS cells at 1 week after IT and IV transplantation, respectively. In the SC group, no histological lung metastases were found in mice xenografted with OOS or CHOS cells and only 1 of 5 mice xenografted with HMPOS cells developed micrometastases at 4 weeks after transplantation.

Ezrin and p-ERM immunohistochemistry in primary and lung metastatic tissues

Figure 2.1.10 and 2.1.11 show typical immunohistochemical findings for ezrin and p-ERM in primary and metastatic lesions. The expressions of both ezrin and p-ERM were localized at the cytosol and cell membrane of the tumor cells in primary and lung metastatic tissues produced by any OS cell lines via any transplantation routes. Figure 2.1.12 shows the ratio of ezrin and p-ERM-positive cells in these tissues.

At 4 weeks, more than 90% of cells in the primary lesions in IT-xenografted mice with HMPOS and OOS cells were ezrin positive, and significantly higher ($p <$ 0.05) than that of SC-xenografted mice with the same cell lines as well as IT-xenografted mice with CHOS cells (Figure 2.1.12A).

In the primary tissues of IT-xenografted mice with HMPOS and OOS cells, 59% and 54% of cells were p-ERM positive, respectively, which were significantly higher ($p <$ 0.05) than that of IT-xenografted mice with CHOS cells (15%); there was no significant difference in the percentage between the tissues of SC- and IT-xenografted mice with HMPOS and OOS cells (Figure 2.1.12B).

Changes in expression ratios of ezrin and p-ERM in the primary lesions of SC- and IT-xenografted mice as well as lung metastatic lesions in IT-xenografted mice with HMPOS cells at 4 weeks after transplantation are shown in Figure 2.1.12C and D. The percentages of ezrin-positive cells in the primary tissues of SC-xenografted mice were 55–75% and significantly lower ($p <$ 0.05) than those in the primary and metastatic tissues of IT-xenografted mice at any time after transplantation. The percentages of p-ERM-positive cells significantly decreased in all tissues of IT-xenografted mice after transplantation in a time-dependent manner. Among the tissues, the percentages of p-ERM-positive cells in the primary tissues of SC-xenografted mice were about 40–60% and were significantly lower ($p <$ 0.05) than those in the primary tissues of IT-

xenografted mice at 1 and 2 weeks after transplantation. In IT-xenografted mice, the

percentages of p-ERM-positive cells in the lung metastatic tissues were >80% and were

as high as those in the primary tissues 1 week after transplantation. However, the

percentages of p-ERM-positive cells in the lung metastatic tissues were 20–30%, which

were significantly lower ($p < 0.05$) than those in the primary tissues at 2 and 4 weeks

after transplantation.

Discussion

In this experiment, a xenografted nude mouse model was developed by transplanting tumor cells into ectopic and orthotopic sites, in which spontaneous metastasis was expected in an orthotopic xenograft model. In addition, experimental pulmonary metastasis was made in mice receiving an intravenous injection. To the best of my knowledge, this is the first report to compare the tumor growth and pulmonary metastatic potential among nude mice transplanted with canine OS cells at different sites. One high-metastatic (HMPOS) and 2 low-metastatic (OOS and CHOS) cell lines were used to determine the differences in primary tumor growth and lung metastatic potential in relation to their characteristics.

Among the 3 cell lines, HMPOS cells produced significantly larger tumor masses 4 weeks after transplantation than OOS and CHOS cells when transplanted into IT and SC sites. HMPOS is a cloned cell line derived from a dog with femoral OS that is highly malignant (Barroga *et al*., 1999). Meanwhile, the OOS and CHOS cell lines are derived from patients with mandibular and scapular OS, respectively, and are less malignant than HMPOS (Hong *et al*., 1998). These results suggested that the tumor growth in this mouse model was dependent on the characteristics of the cell lines. In addition, CHOS cells produced only small primary masses in both the IT and SC groups and did not exhibit any lung metastases in any mice.

50

These results were similar to those in previous reports in which approximately 50–75% of tumor cells in SC xenografts survived and exhibited growth (Khanna *et al*., 2000; Luu *et al*., 2005). The IT xenograft site is a metaphyseal region that is constantly undergoing bone remodeling, which releases growth factors from the matrix. OS cells interact with the cells in the bone microenvironment including osteoblasts, osteoclasts, hematopoietic cells, stromal cells, cytokines and transient cells of the immune system that support OS cell growth (Bussard *et al*., 2008). It is reported that paracrine growth factors including insulin-like growth factor I, insulin-like growth factor binding protein 3 and transforming growth factor-β, are present in the tumor microenvironment of OS cells (Ferracini *et al*., 1995; Hirschfeld and Helman, 1994; Seitz *et al*., 1992). Therefore, the environment of IT xenografts appears to facilitate OS cell growth more than that of SC xenografts.

The disadvantages of SC xenografts include an abundance of false-positive responses to drugs as well as the absence of metastasis and negligible host infiltration and a tumor microenvironment (Killion *et al*., 1998). Studies using SC-xenografted mice with PC-3 human prostatic carcinoma cell line found that local tumor growth can only be produced when the cells are administered in large numbers or with the addition of bone marrow-derived fibroblasts (Chackal-Roy *et al*., 1989).

In the IT and IV groups, histological micrometastases in the lung were observed 1 week after transplantation and macroscopic metastatic nodules were first detected at 2 weeks after transplantation in mice xenografted with HMPOS and OOS cells. On the other hand, mice in the SC group with HMPOS cells exhibited low incidence of lung micrometastases (1/5) at 4 weeks after transplantation. This result also demonstrated the advantages of orthotopic transplantation for investigating the mechanism of lung metastasis in OS-xenografted mice.

Tail vein injection was used as a control to determine the important features of the steps involved in the cascade of metastasis as well as the processes of cellular extravasation and survival at distant metastatic sites (Chambers *et al*., 2000). However, this model has a disadvantage in that the early steps in the metastatic cascade are eliminated.

In the first report on the spontaneous metastasis of human OS cells in a xenograft model, cells were orthotopically transplanted into the bone using a v-Ki-ras-transformed HOS cell line (KRIB or 143B) (Berlin *et al*., 1993). There are numerous subsequent reports on human OS mice models (Dass *et al*., 2006; Luu *et al*., 2005; Yuan *et al*., 2009). These IT xenograft models demonstrated highly reproducible and consistent rates and sizes of tumor formation. On the other hand, in the subcutaneous injection models, the MNNG/HOS and 143B human OS cells only formed tumor

masses in 50% of the xenografted mice with a large variation in tumor sizes and there were no spontaneous lung metastases (Khanna *et al*., 2000). The results in this chapter of the IT and SC groups were similar to those of previous reports.

Bone is an ideal and fertile environment for tumor cell migration and colonization. The specialized microvasculature of bone marrow is adapted for the easy passage of cells in and out of it (Bussard *et al*., 2008). The growth-stimulating effect of bone marrow on primary tumors was essential for both local tumor growth and the metastasis of OS. Therefore, IT transplantation may lead to more local tumor growth and metastatic potential than ectopic transplantation.

IT transplantation with HMPOS and OOS cells produced primary tumor tissues and lung metastases that exhibited increased expression of ezrin and p-ERM. In contrast, SC transplantation of those cell lines produced tumor tissues with decreased expression of ezrin and p-ERM. Ezrin and p-ERM may play important roles in multiple metastatic steps associated with adhesion, motility, invasion, and activation of the signaling pathway crucial for OS progression and metastasis (Khanna *et al*., 2001; Khanna *et al*., 2004). Their expression levels in this study may support the malignant behaviors of the tumors produced by IT xenografts. In addition, non-metastatic CHOS cells did not produce any lung metastases with either IT or SC transplantation and exhibited little or no ezrin or p-ERM expression. These results suggested that the

transplantation site may influence the malignant behavior of metastatic OS cells, although the potential of non-metastatic OS cells did not change according to the injection site. Moreover, these results were corroborated by those of other reports regarding the association of ezrin expression and metastasis in OS cells (Khanna *et al*., 2004) and other cancers including rhabdomyosarcoma, uveal malignant melanoma, and pancreatic cancers (Hunter, 2004).

Interestingly, the strong expression of p-ERM in primary and lung metastatic lesions decreased according to the time after transplantation. The expression of p-ERM was quite high at 1 week after transplantation of metastatic HMPOS cells. However, at 2 and 4 weeks after transplantation, the primary tumor size and number of metastatic nodules increased, while the expression level of p-ERM decreased, especially at the centers of tumor tissues. These data suggest that p-ERM plays an essential role in metastasis at the early phase after arrival of canine OS cells at the lung. In murine and human OS models, it is reported that metastatic OS cells expressed p- ERM early after their arrival at the lung, and only at the invasive front of larger metastatic lesions later on (Ren *et al*., 2009). The authors of that report speculated that the loss of p-ERM over time was required for the development of cell–cell contacts required during the progression of OS cells to multicellular clusters. Although the re-expression of p-ERM was not clearly observed in this study, the results suggest that p-ERM is not required

throughout the total metastatic process and that it may be regulated by some molecular factors at transplantation sites; this should be investigated in the future. Further studies focusing on the other factors related to regulation or enhancing ezrin and p-ERM expressions should also be conducted to extend more understanding of the mechanisms of ezrin activity and lung metastasis.

SC　　　　　　**IT**　　　　　　**IV**
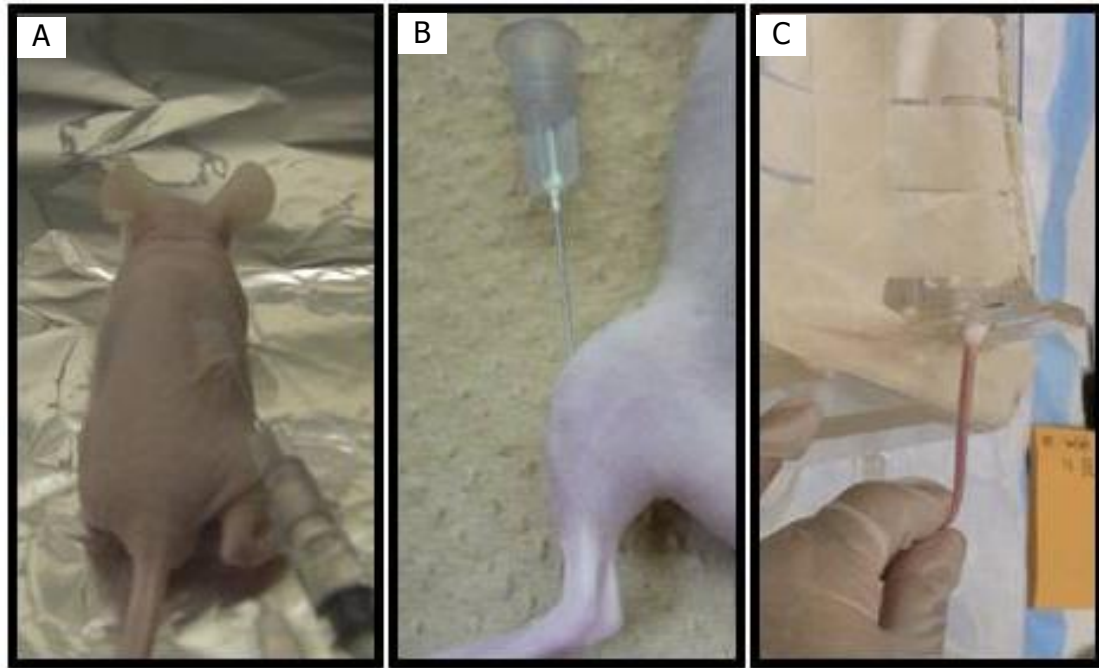
Figure 2.1.1. Cell transplantation into nude mice. (A) SC transplantation into right flank; (B) IT transplantation into right proximal tibia; (C) IV transplantation into lateral tail vein.
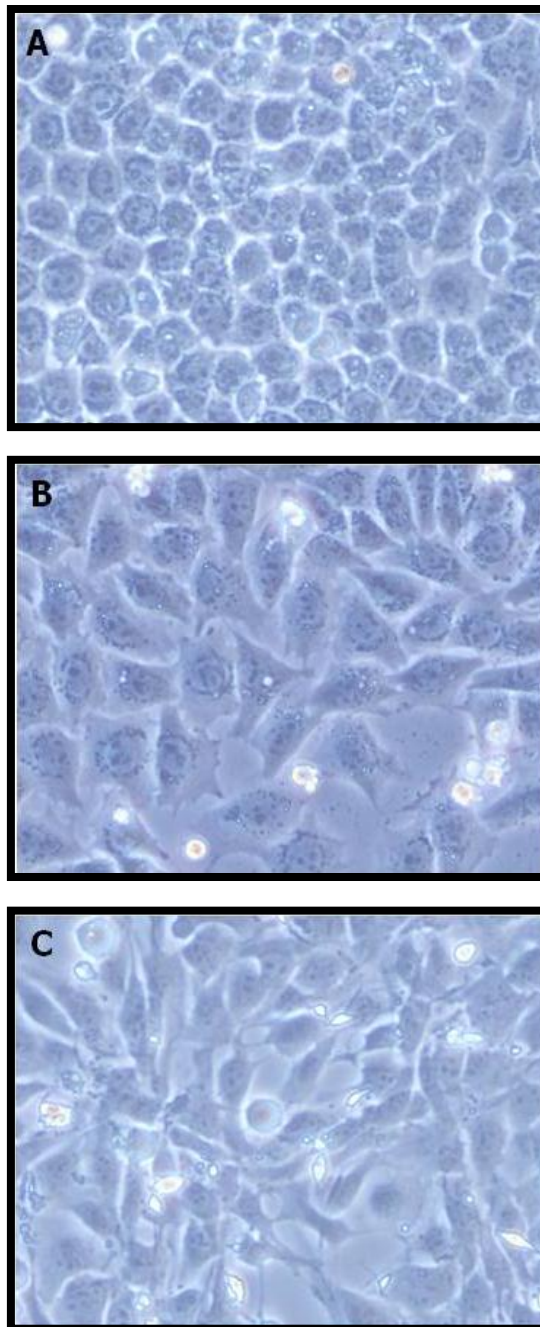
Figure 2.1.2. Morphological appearance of canine OS cell lines. (A) HMPOS cells show a medium- sized polygonal cell type; (B) OOS cells show a mixed cell type consisted of spherical cells, fibroblast-like cells, large or small polygonal cells, and multinucleated giant cells; (C) CHOS cells show a fibroblastic cell type. Original magnification, 400×.
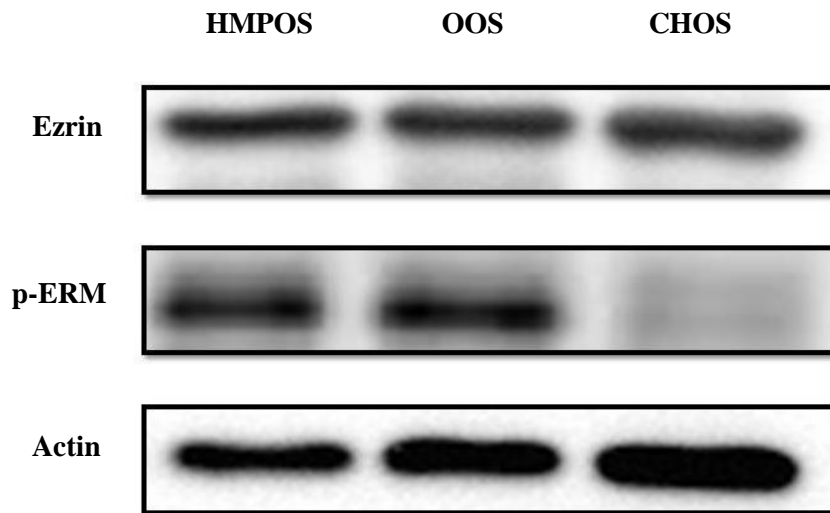
Figure 2.1.3. Western blot analysis shows expression of ezrin and p-ERM in HMPOS, OOS, and CHOS cell lines. Ezrin was expressed in all canine OS cells, while p-ERM did not express in CHOS cells.
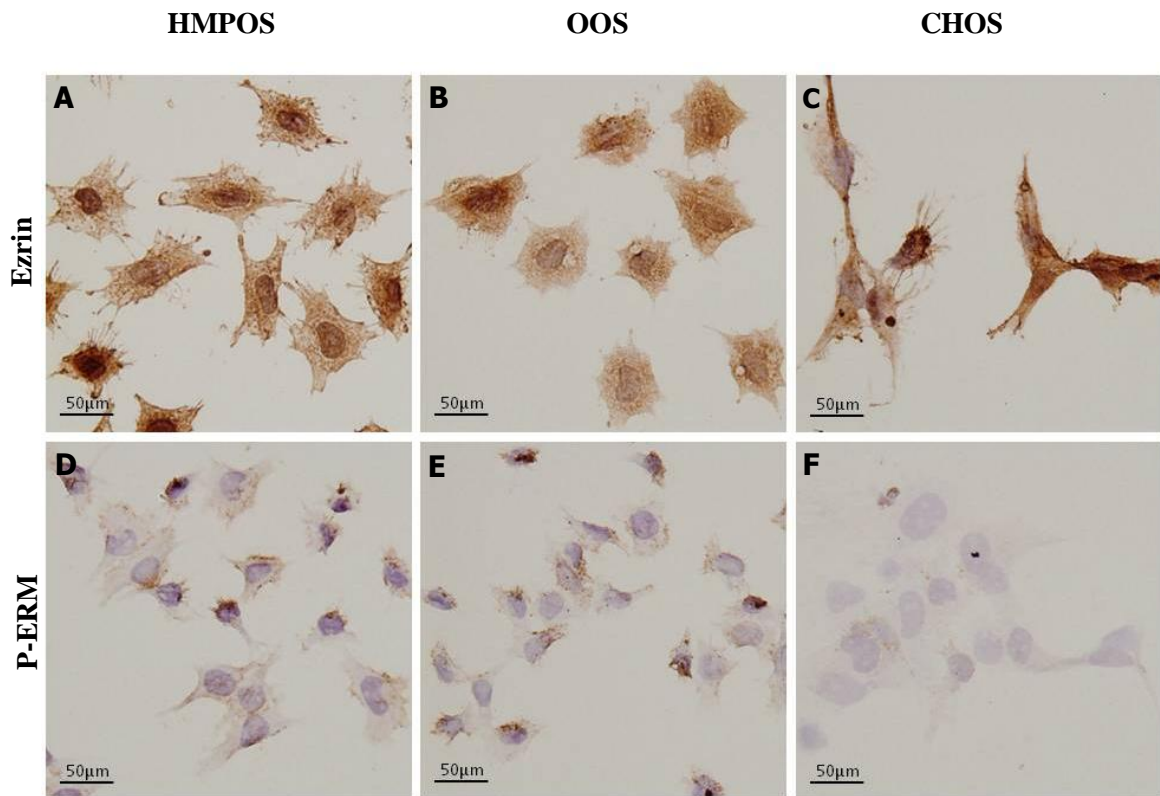
Figure 2.1.4. Immunocytochemistry for ezrin and p-ERM in HMPOS, OOS, and CHOS cell lines (original magnification, 400×). (A,B,C) Ezrin and (D,E,F) p-ERM expression distributed throughout the cytosol and cell membrane. Ezrin expressed in all canine OS cells, while p-ERM did not express in CHOS cells.
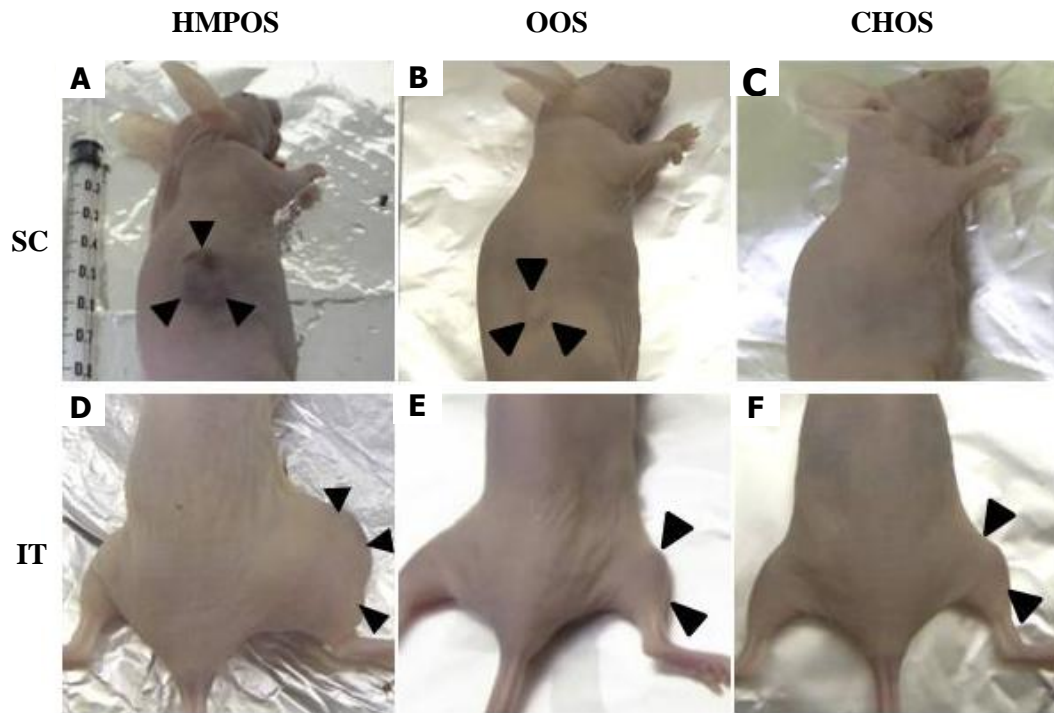
Figure 2.1.5. The typical mice at 4 weeks after transplantation with HMPOS, OOS, and CHOS cells via SC and IT sites. (A,B,C) the primary lesion of SC-xenografted mouse with HMPOS cells shows a larger tumor size than SC-xenografted mouse with OOS cells and SC-xenografted mouse with CHOS cells does not show any lesion; (D,E and F) the primary lesion of IT-xenografted mouse with HMPOS cells shows a larger tumor size than IT-xenografted mice with OOS and CHOS cells.
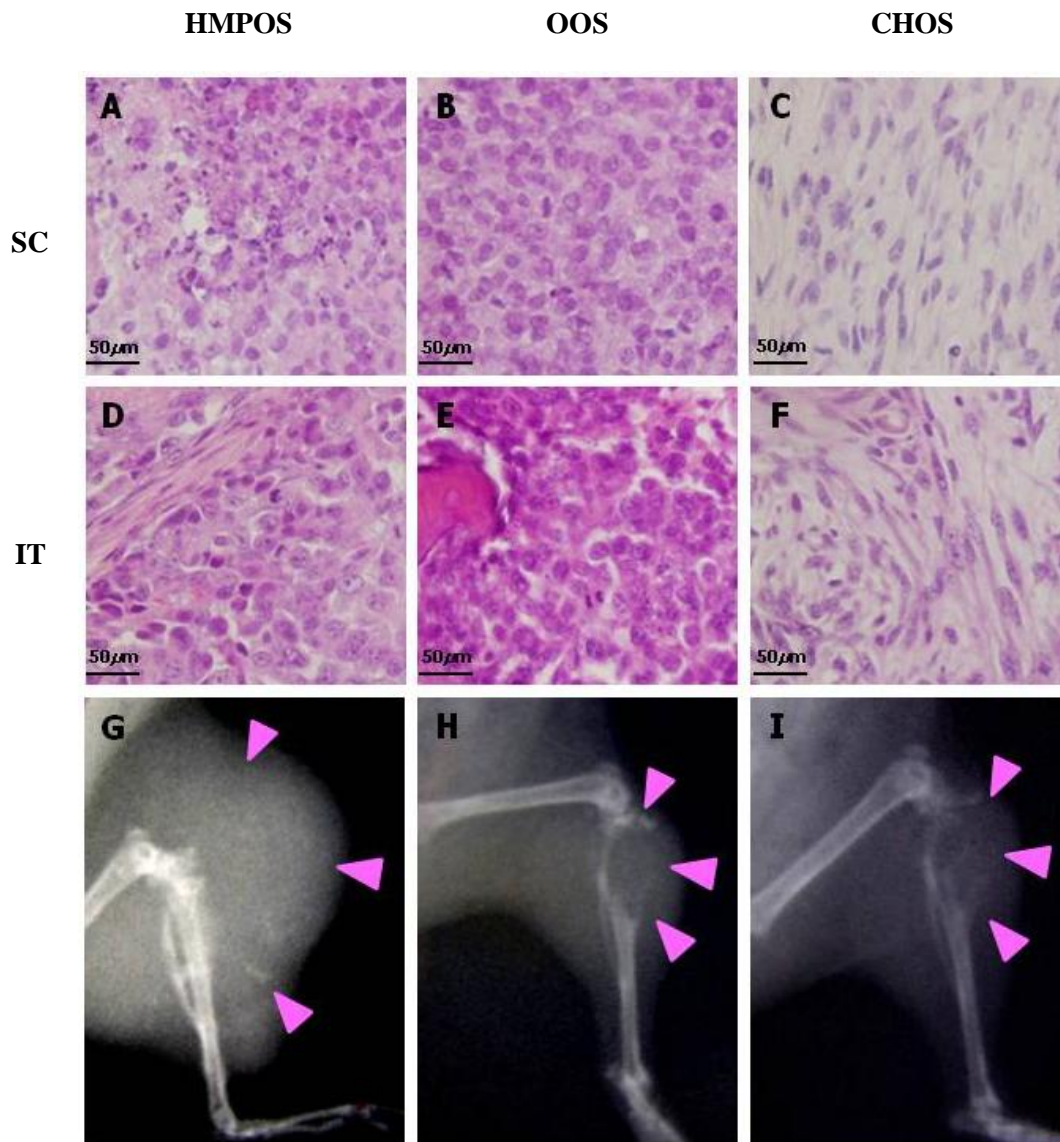
Figure 2.1.6. The primary tumor masses at 2 weeks after transplantation in mice xenografted with OS cell at each site. The histological appearance of primary tumor tissues and tumor cell characteristics by SC xenografts (A, B, and C) and IT xenografts (D, E, and F). HE, original magnification 400×. The radiographs of tibias (G, H, and I) xenografted with HMPOS, OOS and CHOS cells after 4 weeks show differences between cell lines.
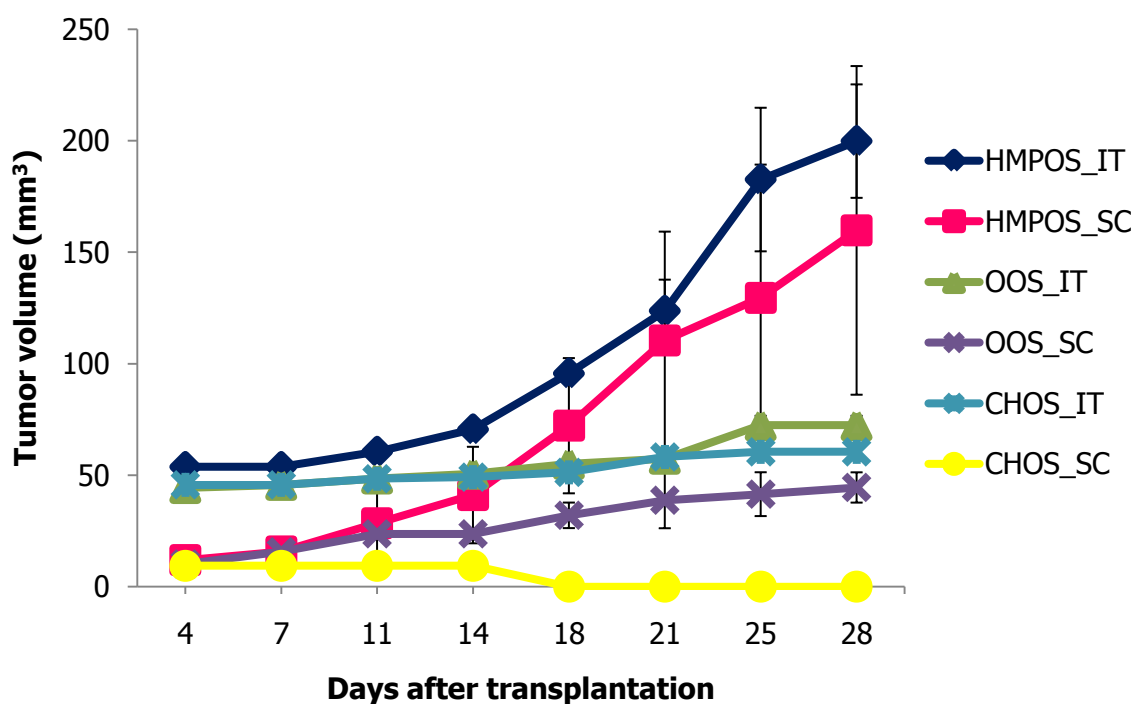
Cell lines	Transplantation sites	Tumor volume $\pm$ SE (mm^3) after transplantation			
		Day 7	Day 14	Day 21	Day 28
HMPOS	SC	15.8±5.5	41.1±21.6	110.5±48.7	159.8±73.7
	IT	53.76±3.2	70.58±3	123.72±14	199.83±25.4
OOS	SC	15.7±1	23.7±2.5	38.8±12.6	44.5±6.8
	IT	44.68+1.4	50.69±2.2	57.4±1.6	72.42±4.2
CHOS	SC	9.4±0	9.4±0	0	0
	IT	45.68±1.4	49.2±1.4	58.2±1.9	60.53±1

Figure 2.1.7. Primary tumor growth curves and table after SC and IT transplantation of HMPOS, OOS, and CHOS cells. The masses formed by HMPOS xenografts were significantly larger ($p < 0.05$) than those formed by OOS and CHOS cells. Tumor volumes of IT xenograft were significantly larger ($p < 0.05$) than SC xenograft. In CHOS xenograft, the tumor volume of SC injection decreased 2 weeks after transplantation. * Significant difference ($p < 0.05$); error bars represent SE.
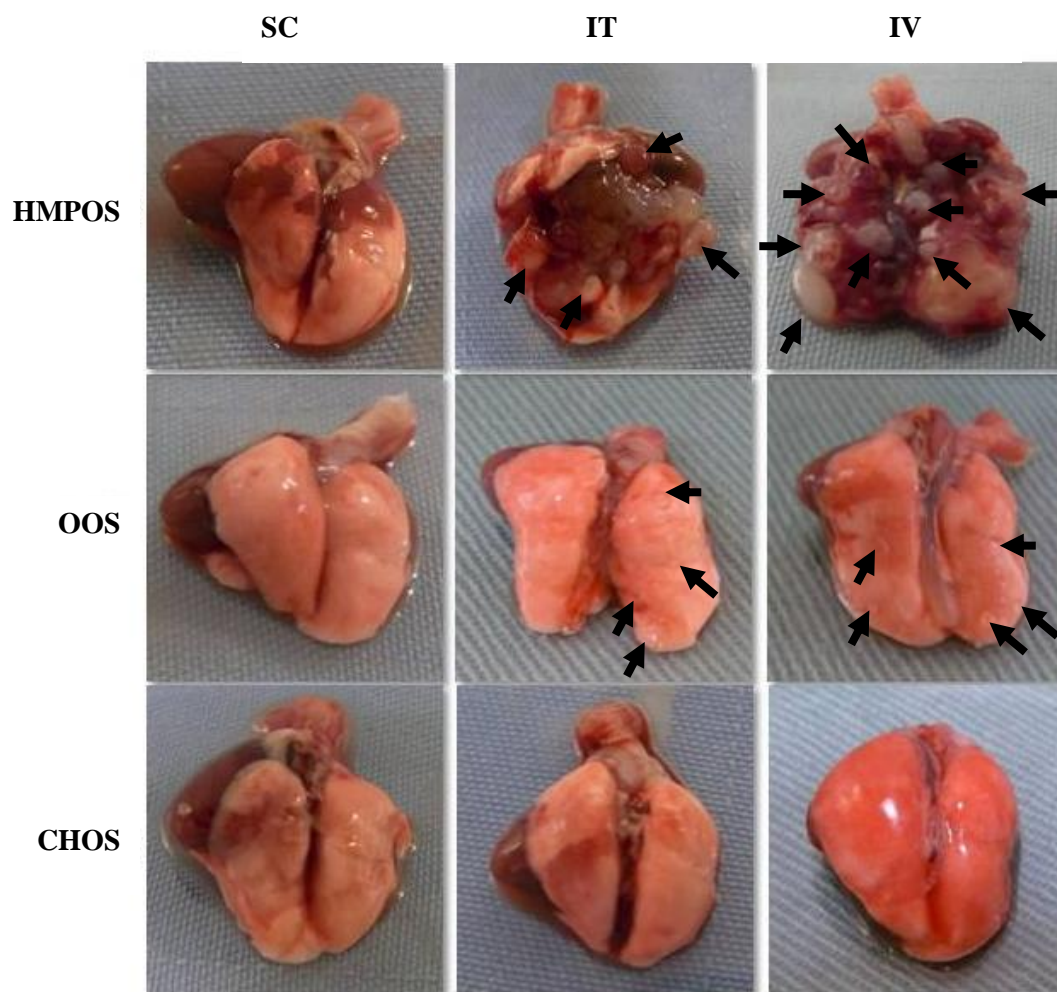
Figure 2.1.8. Gross findings of lung metastatic nodules developed in xenografted mice 4 weeks after SC, IT, or IV injection with CHOS, OOS, and HMPOS cells. Lung metastatic nodules could be observed in IT- and IV-xenografted mice with HMPOS and OOS cells, but not in SC-xenografted mice. There was no lung metastatic nodule in CHOS-xenografted mice.
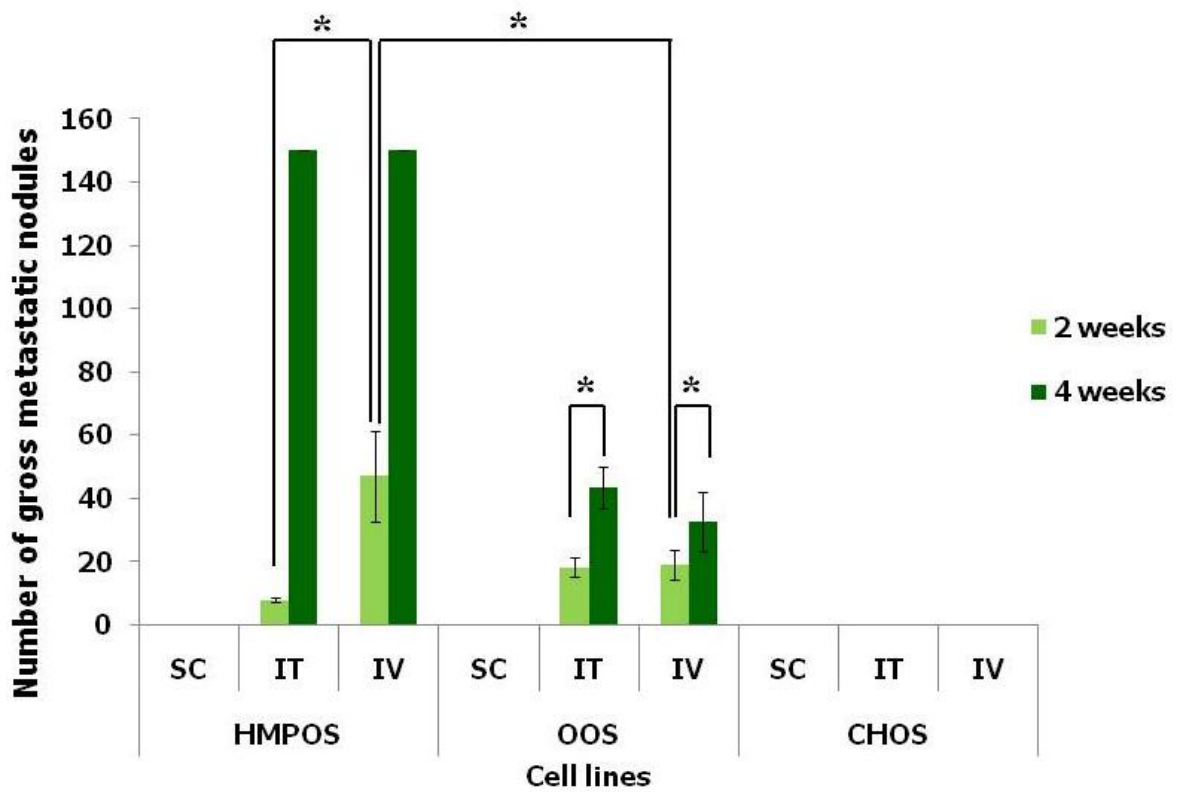
Figure 2.1.9. The number of gross metastatic nodules 2 and 4 weeks after the transplantation of each cell line. * Significant difference ($p < 0.05$); error bars represent SE.
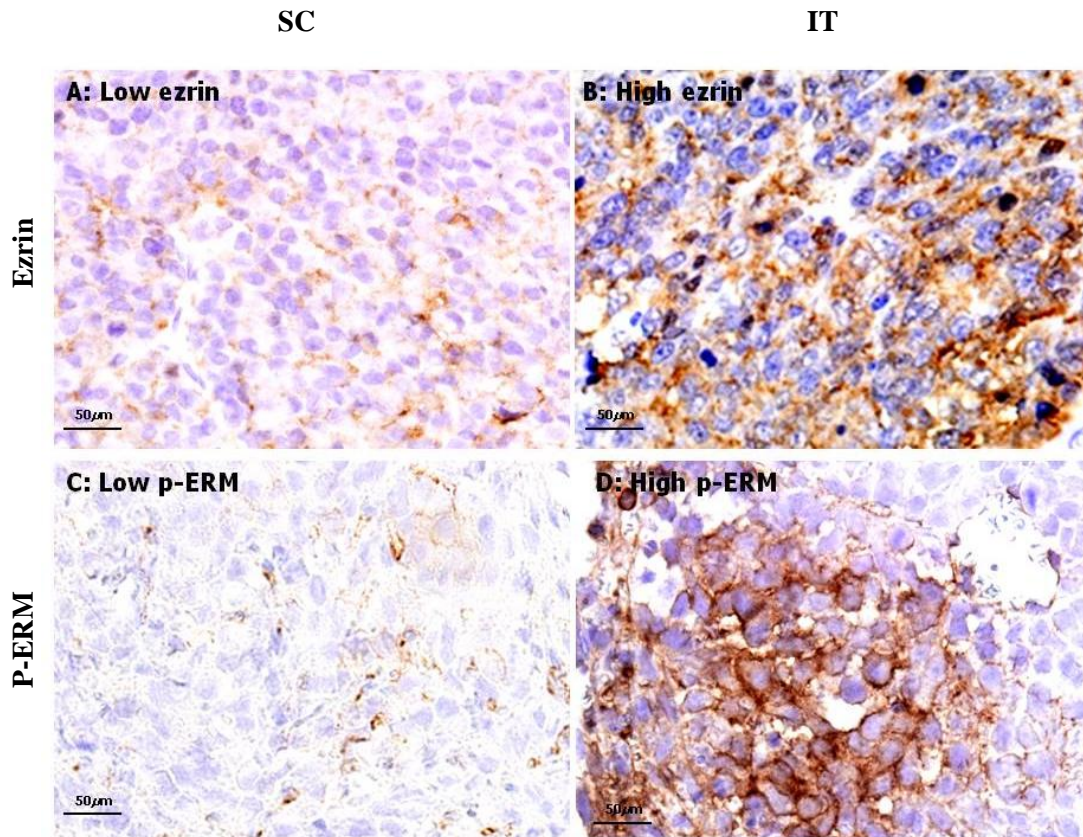
Figure 2.1.10. Typical immunohistochemical findings of ezrin and p-ERM (original magnification, 400×). The expression of both ezrin and p-ERM was localized at the cytosol and cell membrane of the tumor cells in primary and lung metastatic tissues produced by OS cell lines via all transplantation routes. (A) Low ezrin expression; (B) high ezrin expression; (C) low p-ERM expression; (D) high p-ERM expression.
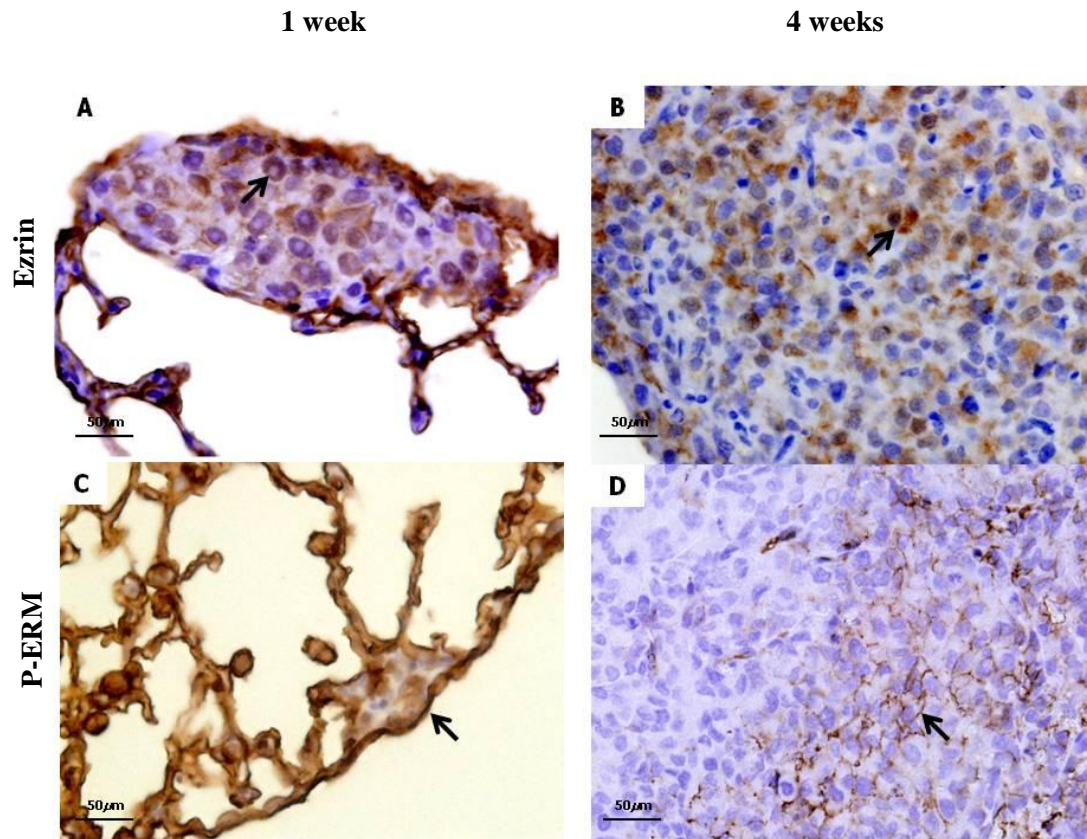
1 week   **4 weeks**

Figure 2.1.11. Typical immunohistochemical findings of ezrin and p-ERM in lung metastatic tissues produced by OS cell lines via IT route at 1 and 4 weeks after transplantation (original magnification, 400×). (A) high ezrin expression at 1 week; (B) high ezrin expression at 4 weeks; (C) high p-ERM expression at 1 week; (D) loss of p-ERM expression in the center of the lesion with low expression at the border at 4 weeks.
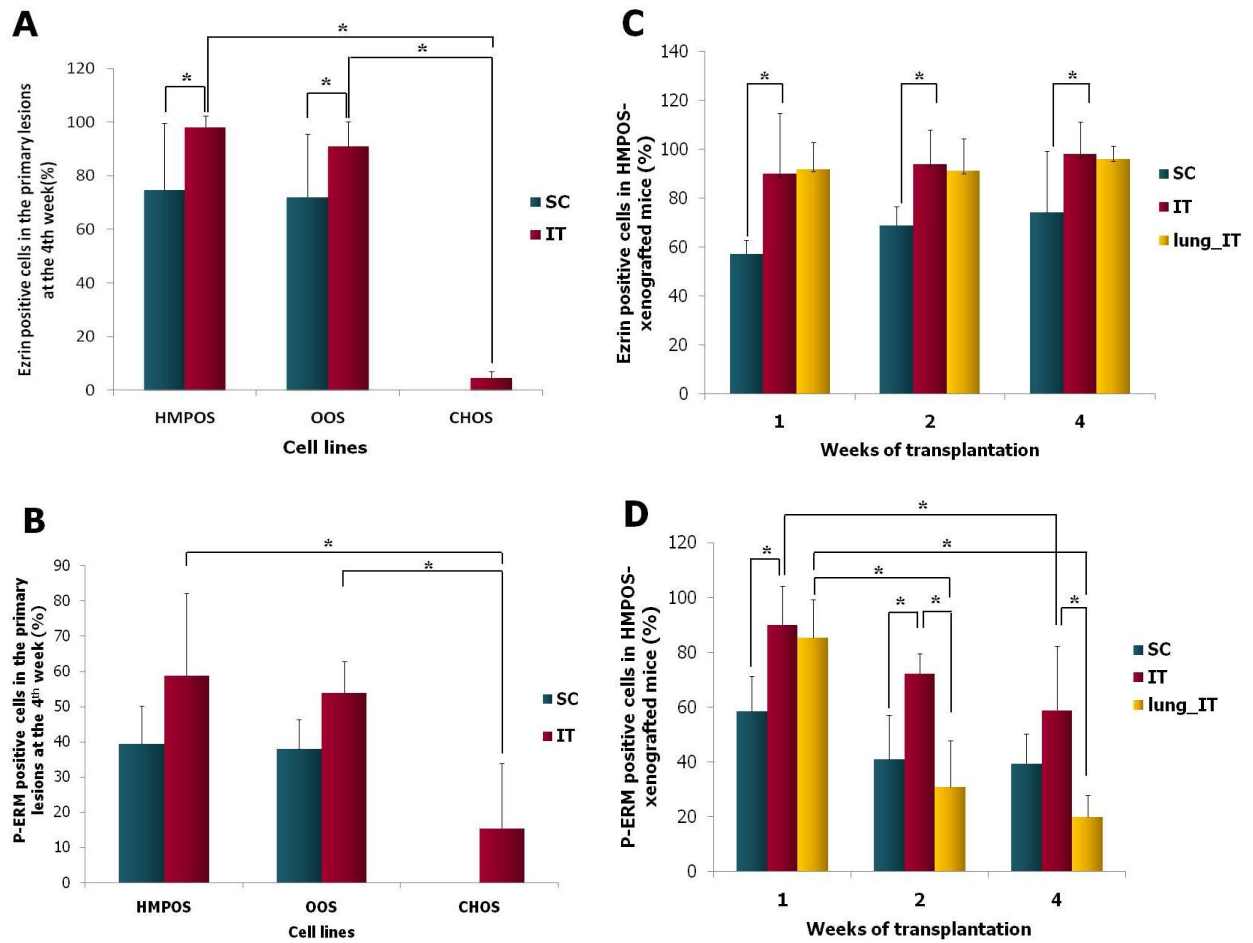
Figure 2.1.12. The ratios of ezrin- and p-ERM-positive cells in each tissue. (A, B) The percentages of ezrin- and p-ERM-positive cells in primary lesions of IT-xenografted mice with HMPOS and OOS cells at 4 weeks after transplantation were significantly higher ($p < 0.05$) than those xenografted with CHOS cells. (C, D) The changes in ezrin- and p-ERM-positive cell percentages in the primary and lung metastatic lesions of HMPOS-xenografted mice via each transplantation route. (C) The percentages of ezrin-positive cells in primary lesions of SC-xenografted mice were significant lower than IT- xenografted mice, whereas those in IT primary and lung metastatic tissues were not significantly different. (D) The percentages of p-ERM-positive cells decreased after transplantation in all tissues in a time-dependent manner. The percentages of p-ERM-positive cells of primary lesions in SC-xenografted mice were significantly lower than those of IT-xenografted mice 1 and 2 weeks after transplantation, but there were no significant differences after 4 weeks. * Significant difference ($p < 0.05$); error bars represent SDs.

Section 2: Relationship between ezrin and p-ERM expression and proliferation index, Ras/Raf/ERK MAPK pathway, and PKCα in tissues developed in xenografted mice

Materials and Methods

Antibodies

The primary antibodies used for Western blot analysis, immunocytochemistry, and immunohistochemistry were as follows: mouse monoclonal anti-Ki-67 (Dako, the same as chapter 1); mouse monoclonal anti-Ras and C-Raf (BD Biosciences, San Diego, CA, USA)**;** rabbit polyclonal anti-B-Raf (Santa Cruz Biotechnoloy Inc., Santa Cruz, CA, USA); rabbit monoclonal anti-p-ERK1/2 and ERK1/2 (Cell Signaling Technology, Danvers, MA, USA); and mouse momoclonal anti-PKCα and actin (Millipore, Temecula, CA, USA).

The dilutions of these antibodies were shown in the following.

Antibodies	Dilutions		
	WB	ICC	IHC
Ki-67	-	-	1:100
Ras	1:2,000	1:250	1:250
B-Raf	1:200	1:200	1:50
C-Raf	1:2,000	1:20	1:20
P-ERK1/2	1:2,000	1:200	1:200
ERK1/2	1:1,000	1:100	-
PKCα	1:1,000	1:100	1:100
Actin	1:10,000	-	-

WB, Western blot analysis; ICC, Immunocytochemistry; IHC, Immunohistochemistry

Western blot analysis, immunocytochemistry, and immunohistochemistry

Western blot analysis and immunocytochemistry for 3 OS cell lines were performed as described in section 1. Immunohistochemistry was performed as described in chapter 1 and section 1 for Ki-67 in primary tissues of HMPOS/OOS/CHOS-xenografted mice and lung metastatic tissues of IT-xenografted mice with HMPOS. On the other hand, immunohistochemistry for Ras, B-Raf, C-Raf, p-ERK1/2, and PKCα was performed in primary and lung metastatic tissues of HMPOS-xenografted mice. Lung metastatic tissues of IT-xenografted mice with HMPOS cells were used in this

69

section because the lung metastasis was producible after using this cell line at every time points.

For immunohistochemistry, canine tonsil for Ki-67, canine prostate gland for Ras and B-Raf, mouse bone marrow for C-Raf, p-ERK1/2 and ERK1/2 and mouse brain for PKCα, respectively, were used as positive controls to assess the specification of the reactions. The absence of primary antibody was used as a negative control. For evaluation the level of Ki-67, Ras, B-Raf, C-Raf, p-ERK1/2, ERK1/2, and PKCα expressions, tissue sections were performed as described in chapter 1 and section 1.

Statistical analysis

The mean and SD values of the percentages of Ki-67, Ras-, B-Raf, C-Raf, p-ERK1/2, and PKCα-positive cells were calculated. The Tukey-Kramer multiple comparison test and analysis of variance (ANOVA) were used for statistical analysis among the different groups.

Spearman's rank correlation test was used for evaluating the correlations between the expression of Ki-67 and tumor volume, number of lung metastatic nodules, ezrin and p-ERM expressions were evaluated. Moreover, the correlations between expressions of Ras, B-Raf, C-Raf, p-ERK1/2, and PKCα and tumor volume, number of lung metastatic nodules, ezrin, p-ERM, and PI were also evaluated. Statistical difference

was set at $p < 0.05$. Data analysis was carried out using NCSS 2007 (Kaysville, UT, USA).

Results

Western blot analysis for Ras, B-Raf, C-Raf, p-ERK1/2, ERK1/2, and PKCα

Results of Western blot analysis for Ras, B-Raf, C-Raf, p-ERK1/2, and ERK1/2 in 3 canine OS cells are shown in Figure 2.2.1. Ras and ERK1/2 expressions were detected in all cell lines. B-Raf was not detected in CHOS. C-Raf expression in HMPOS and OOS cells was stronger than that in CHOS cells. PKCα expression in HMPOS was stronger than that in OOS and CHOS cells. On the contrary, p-ERK1/2 was not expressed in HMPOS and OOS cells.

Immunocytochemistry for Ras, B-Raf, C-Raf, p-ERK1/2, ERK1/2, and PKCα

Immunocytochemical findings for Ras, B-Raf, C-Raf, p-ERK1/2, ERK1/2, and PKCα are shown in Figure 2.2.2. As observed in Western blot analysis, the expressions of Ras and ERK1/2 were detected in all cell lines. B-Raf was not detected in CHOS. C-Raf and PKCα expressions in HMPOS and OOS cells were stronger than those in CHOS cells. On the contrary, p-ERK1/2 was not expressed in HMPOS and OOS cells.

Immunohistochemistry for Ki-67 in primary and lung metastatic tissues of xenografted mice

Figure 2.2.3 shows the expression of Ki-67 in primary and lung metastatic tissues of HMPOS-xenografted mice and the percentage of Ki-67-positive cells (PI) in primary tissues of SC- and IT-xenografted mice with HMPOS, OOS, and CHOS cells at 4 weeks after transplantation. Moreover, PI of primary and lung metastatic tissues in HMPOS-xenografted mice was evaluated at 1, 2, and 4 weeks after transplantation.

Figure 2.2.3A shows the immunohistochemical findings for Ki-67 in the primary tissues at 1, 2, and 4 weeks after transplantation via SC (a,b,c) and IT (d,e,f) routes. The expression of Ki-67 was localized in nuclei of tumor cells in primary and lung metastatic tissues produced by any OS cell lines via any transplantation routes.

Figure 2.2.3B shows the percentages of Ki-67-positive cells in these tissues. At 4 weeks after transplantation, the expression of Ki-67-positive cells in the primary tissues of IT-xenografted mice with HMPOS cells was 20.1% and significantly higher ($p < 0.05$) than that of IT-xenografted mice with OOS (15.5%) and CHOS (10.5%) cells, respectively.

Changes in expression of Ki-67 in the primary lesions of SC- and IT-xenografted mice with HMPOS cells are shown in Figure 2.2.3C. The percentages of

Ki-67-positive cells gradually increased in all tissues after transplantation in a time-dependent manner. In IT-xenografted mice with HMPOS at 4 weeks after transplantation, the percentage of Ki-67-positive cells in the primary tissues of SC-xenografted mice was 16.2% and significantly lower ($p < 0.05$) than that in IT-xenografted mice (20.1%). There was no significant difference in the percentages between the primary tissues of SC- and IT-xenografted mice with OOS and CHOS cells.

The comparison of Ki-67-positive cells between primary and lung metastatic lesions was also conducted. There was no significant difference in the percentages of Ki-67-positive cells between primary lesions (20.1%) and lung metastatic lesions (20.2%) in IT-xenografted mice with HMPOS cells at 4 weeks after transplantation.

Table 2.2.1 shows Spearman's rank correlation between expression of Ki-67 and tumor volume, number of lung metastatic nodules, and expressions of ezrin and p-ERM in primary tumor tissues of all mice. The expression of Ki-67 was significantly correlated with the tumor volume (correlation coefficient $r = 0.5301$, $p < 0.001$), number of lung metastatic nodules (correlation coefficient $r = 0.5630$, $p < 0.001$), and ezrin expression (correlation coefficient $r = 0.6905$, $p < 0.001$). On the contrary, the expression Ki-67 was not significantly correlated with p-ERM expression (correlation coefficient $r = 0.2207$, $p > 0.05$).

Immunohistochemistry for Ras/Raf/ERK pathway

Figure 2.2.4 shows the expression of Ras on immunohistochemistry and the percentages of Ras-positive cells in the primary and lung metastatic tissues of HMPOS-xemografted mice at 1, 2, and 4 weeks after transplantation. The expression of Ras was localized throughout the cytoplasm of OS cells. The percentages of Ras-positive cells increased in all tissues of SC- and IT-xenografted mice after transplantation. The percentage of Ras-positive cells in IT-xenografted mice with HMPOS cells (90.7%) was significantly higher ($p < 0.01$) than that in SC-xenografted mice (15.1%) at 2 weeks after transplantation. On the contrary, there was no significant difference between SC- and IT-xenografed mice at 1 and 4 weeks after transplantation. The percentages of Ras-positive cells in primary and lung metastatic tissues of IT-xenografted mice with HMPOS were not significantly different at any time points.

Figure 2.2.5 shows the expression of B-Raf on immunohistochemistry and the percentages of B-Raf-positive cells in the primary tissues of HMPOS-xemografted mice at 1, 2, and 4 weeks after transplantation. The expression of B-Raf was weak and localized throughout the cytoplasm of OS cells. The percentages of B-Raf-positive cells decreased in all tissues of SC- and IT-xenografted mice after transplantation in a time-dependent manner. The percentages of B-Raf-positive cells in IT-xenografted mice with HMPOS cells were 72.2% and 23.4% at 1 and 2 weeks, respectively, and were higher

than those in SC-xenografted mice (70% and 14%, respectively). However, B-Raf expression of both SC- and IT-xenografts was negative at 4 weeks after transplantation and there was no significant difference in the percentage of positive cells between the tissues of SC- and IT-xenografted mice with HMPOS cells at any time points. B-Raf was not expressed in lung metastatic tissues of IT-xenografted mice with HMPOS.

Figure 2.2.6 shows the expression of C-Raf on immunohistochemistry and the percentages of C-Raf-positive cells in the primary and lung metastatic tissues of HMPOS-xemografted mice at 1, 2, and 4 weeks after transplantation. The expression of C-Raf was localized throughout the cytoplasm of OS cells. The percentages of C-Raf-positive cells increased in all tissues of SC- and IT-xenografted mice after transplantation in a time-dependent manner. The percentages of C-Raf-positive cells in IT-xenografted mice with HMPOS cells were 28.8% and 73.6% at 2 and 4 weeks after transplantation, respectively, and were significantly higher ($p < 0.01$) than those in SC-xenograftd mice (7.5% and 14.9%, respectively). On the contrary, the expression of C-Raf was weak in all tissues and there was no significant difference between SC- and IT-xenografted mice at 1 week after transplantation The percentages of C-Raf-positive cells in primary and lung metastatic tissues of IT-xenografted mice with HMPOS were not significantly different at any time points.

Figure 2.2.7 shows the expression of p-ERK1/2 on immunohistochemistry and the percentages of p-ERK1/2-positive cells in the primary and lung metastatic tissues of HMPOS-xemografted mice at 1, 2, and 4 weeks after transplantation. The expression of p-ERK1/2 was localized in the nucleus and cytoplasm of OS cells. The percentages of p-ERK1/2-positive cells increased in all tissues of SC- and IT-xenografted mice after transplantation in a time-dependent manner. The percentages of p-ERK1/2-positive cells in primary tissues of IT-xenografted mice with HMPOS cells were 27.8% and 41% at 2 and 4 weeks after transplantation, respectively and were significantly higher ($p < 0.01$) than those in primary tissues of SC-xenograftd mice (7.8% and 10%, respectively) and those in lung metastatic tissues of IT-xenografted mice (1.5% and 5%, respectively). On the contrary, the expression of p-ERK1/2 was weak and there was no significant difference among all tissues of HMPOS-xenografted mice at 1 week after transplantation.

Immunohistochemistry for PKCα

Figure 2.2.8 shows the expression of PKCα on immunohistochemistry and the percentages of PKCα-positive cells in the primary and lung metastatic tissues of HMPOS-xemografted mice at 1, 2, and 4 weeks after transplantation. The expression of PKCα was localized in the cytoplasm and cell membrane of OS cells. The percentages

of PKCα-positive cells in IT-xenografted mice with HMPOS cells were 87% and 96% at 1 and 2 weeks after transplantation, respectively and were significantly higher ($p < 0.01$) than those in SC-xenografted mice (16.5% and 16.9%, respectively). However, there was no significant difference between SC- and IT-xenografted mice at 4 weeks after transplantation. The percentages of PKCα-positive cells in primary and lung metastatic tissues of IT-xenografted mice with HMPOS were not significantly different at any time points.

Correlation between expressions of Ras/Raf/ERK pathway, PKCα, tumor volume, number of lung metastatic nodules, ezrin, p-ERM, and PI.

Table 2.2.2 shows Spearman's rank correlation between expressions of Ras, B-Raf, C-Raf, p-ERK1/2, and PKCα and variables of malignant behaviors, including tumor volume, number of lung metastatic nodules, expressions of ezrin, p-ERM, and PI, in primary tissues of all mice.

The expressions of Ras, C-Raf, and p-ERK1/2 were correlated with the tumor volume and the expression of ezrin and PI. In contrast, the expressions of Ras, C-Raf, and p-ERK1/2 were not correlated with p-ERM expression. Although the expressions of Ras and C-Raf were correlated with number of lung metastatic nodules, p-ERK1/2 was not. The expression of B-Raf was not correlated with tumor volume, number of lung metastatic nodules, expressions of ezrin, and PI, but was correlated with p-ERM

expression. The expression of PKCα was correlated with tumor volume, number of lung

metastatic nodules, expressions of ezrin, p-ERM, and PI.

Discussion

To focus on the other factors related to ezrin and p-ERM expression, PI in primary tissues of HMPOS/OOS/CHOS-xenografted mice and lung metastatic tissues of HMPOS-xenografted mice was evaluated in section 2. Moreover, molecules in Ras/Raf/ERK pathway (Ras, B-Raf, C-Raf, and p-ERK1/2) and PKCα were investigated in 3 OS cell lines, primary and lung metastatic tissues of HMPOS-xenografted mice for more understanding of relationship between malignant behaviors and ezrin activity in different transplantation sites.

The expression of Ki-67 in the previous chapter that evaluated PI in the tissues of canine OS patients was not correlated with the expression of ezrin and p-ERM. However, the result was not enough to conclude the correlation among those molecules. Therefore, in this chapter, Ki-67 was evaluated again in the nude mouse model. I found that Ki-67 was significantly correlated with malignant behaviors in IT-xenografted mice. In addition, Ki-67 was significantly correlated with the expression of ezrin. This result suggested that microenvironment at IT transplantation site or the expression of ezrin but not p-ERM may play a role in proliferation of canine OS cells in the mouse model. This result was similar to earlier studies that demonstrated significant correlations between ezrin overexpression and PI in human chondrosarcoma, melanoma and OS (Ilmonen *et al*., 2005; Soderstrom *et al*., 2010).

The previous study reported that ezrin-mediated early metastatic survival advantage for mouse OS cells was partially dependent on activation of MAPK (Khanna *et al*., 2004). Therefore, I investigated the expression of Ras, B-Raf, C-Raf, and p-ERK1/2 in *in vitro* and *in vivo* experiments for canine OS cells.

High metastatic HMPOS and OOS cells in culture condition expressed high Ras, B-Raf, and C-Raf, but low p-ERK1/2 when compared to non-metastatic CHOS cells. However, in the nude mouse model, primary tissues of IT-xenografted mice with HMPOS cells showed high expression of Ras, C-Raf, and p-ERK1/2 when compared to those of SC-xenografted mice or CHOS-xenografted mice. Moreover, the expressions of Ras, C-Raf, and p-ERK1/2 were correlated with the tumor volume, number of lung metastatic nodules, ezrin and PI. These results showed the effects of microenvironment at IT transplantation site on the increase of signal of Ras/Raf/ERK pathway for enhancing the primary tumor growth. The previous studies reported that Ras/Raf/ERK pathway plays important roles in survival, differentiation, and proliferation of tumor cells (Dhillon *et al*., 2007; Leicht *et al*., 2007).

The expression of p-ERM, gradually decreased in a time-dependent manner in section 1, was not correlated with PI, Ras, C-Raf, and p-ERK1/2 in section 2. Although the expressions of Ras and C-Raf were correlated with number of lung metastatic nodules, pERK1/2 expression was low in the lung lesions and was not correlated with

number of lung metastatic nodules and p-ERM expression. These results suggested that Ras/Raf/ERK pathway may be not associated with phosphorylation of ezrin and lung metastasis of OS cells.

Although the expression of p-ERM was correlated with B-Raf, its expression was not different between SC- and IT-xenografted mice; moreover, its expression was not correlated with any malignant behaviors and ezrin expression. Therefore, B-Raf expression may be not associated with the malignant behaviors and phosphorylation of ezrin in OS cells. However, ezrin in phosphorylated form may be involved in the shorter time at the beginning step for signal transduction of Ras/Raf/ERK pathway and then the dephosphorylated form may be involved in the later time for proliferation of OS. In the other way, ezrin may not be involved in the Ras/Raf/ERK pathway.

Ren, *et al*. reported that the dynamic regulation of ezrin phosphorylation was controlled through the classical PKC family (Ren *et al*., 2009). PKCα, one of the classical PKC family members, was shown to interact with ezrin, both *in vitro* and *in vivo*, and could phosphorylate ezrin *in vitro* (Ng *et al*., 2001). In this study, although PKCα was expressed in all canine OS cells, its expression was especially high in HMPOS cells. However, in HMPOS-xenografted mice, the expressions of PKCα and p-ERM were low in the primary tissues of SC-xenografted mice when compared to those in IT-xenografted mice. Moreover, PKCα was correlated with the tumor volume,

number of lung metastatic nodules, ezrin, p-ERM, and PI. According to immunohistochemical findings, the expressions of p-ERM and PKCα were low in central portions and expressed only at the leading edge or the invasive front of the primary and metastatic lesions in progression time at 4 weeks after transplantation. This result was similar to the previous study in murine OS cells, which the author demonstrated that PKCα was responsible for the phosphorylation of ezrin during cell migration and arrival in the lung at earlier phase and during the invasion of the metastatic lesion into the surrounding parenchyma of tumor in the later phase (Ren *et al.*, 2009). In addition, it also suggested that part of PKC-mediated effects on malignant behaviors of canine OS cells were mediated through interaction between phosphorylation of ezrin and microenvironment in IT-transplantation site.

PKCα has been connected with many aspects of metastatic progression, including migration and invasion (Herbert, 1993; Koivunen *et al.*, 2004; Musashi *et al.*, 2000; Sullivan *et al.*, 2000).

Taken together, the results in this section suggested that the Ras/Raf/ERK pathway and PKCα expression-depending on transplantation site may play important role in the malignant behaviors of canine OS cells.

However, the connection between ezrin, Ras/Raf/ERK pathway and PKCα was not clear. To extend understanding of PKC-mediated ezrin phosphorylation in canine OS, further study such as using a PKC inhibitor should be needed.

Variables	Ki-67
Tumor volume	$0.5301, p < 0.001$
Lung metastasis	$0.5603, p < 0.001$
Ezrin	$0.6905, p < 0.001$
P-ERM	NS

Table 2.2.1. Spearman's rank correlations between expression of Ki-67 and tumor volume, lung metastatic nodules, ezrin and p-ERM expressions in primary tissues of all mice. NS: not significant.

Variables	Ras	B-Raf	C-Raf	P-ERK1/2	PKCα
Tumor volume	0.5996	NS	0.5796	0.4102	0.5248
	$p < 0.001$		$p < 0.001$	$p < 0.05$	$p < 0.001$
Lung metastatsis	0.4993	NS	0.9243	NS	0.3599
	$p < 0.05$		$p < 0.001$		$p < 0.05$
Ezrin	0.4401	NS	0.4826	0.4393	0.6432
	$p < 0.05$		$p < 0.05$	$p < 0.05$	$p < 0.001$
P-ERM	NS	0.4283	NS	NS	0.3677
		$p < 0.05$			$p < 0.05$
Ki-67	0.7979	NS	0.8668	0.7171	0.5167
	$p < 0.001$		$p < 0.001$	$p < 0.001$	$p < 0.05$

Table 2.2.2. Spearman's rank correlations between expressions of Ras, B-Raf, C-Raf, p-ERK1/2, and PKCα and tumor volume, lung metastatic nodules, ezrin, p-ERM, and Ki-67 expressions in primary tissues of all mice. NS: not significant.
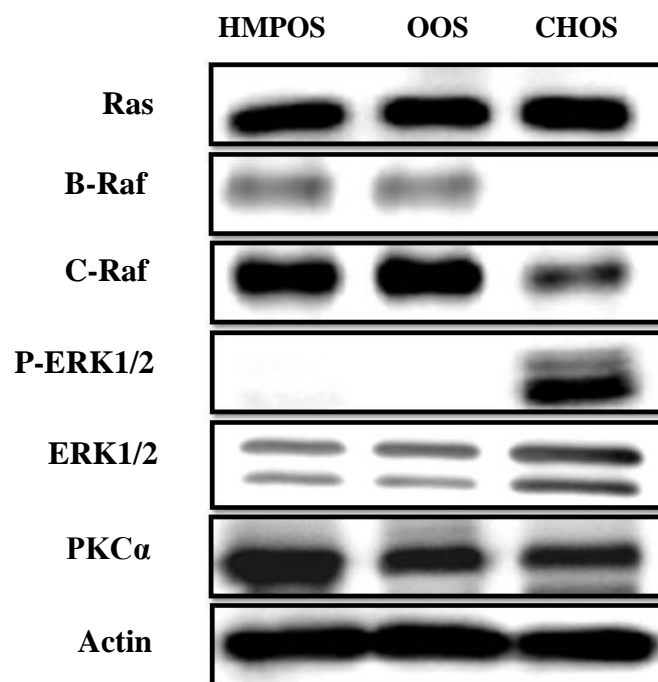
Figure 2.2.1 Western blot analysis shows expression of Ras, B-Raf, C-Raf, p-ERK1/2, ERK1/2, and PKCα in HMPOS, OOS, and CHOS cell lines. Ras and ERK1/2 expressions were detected in all cell lines. B-Raf was not detected in CHOS. C-Raf expression in HMPOS and OOS cells was stronger than that in CHOS cells. PKCα expression in HMPOS was stronger than that in OOS and CHOS cells. On the contrary, p-ERK1/2 was not expressed in HMPOS and OOS cells.
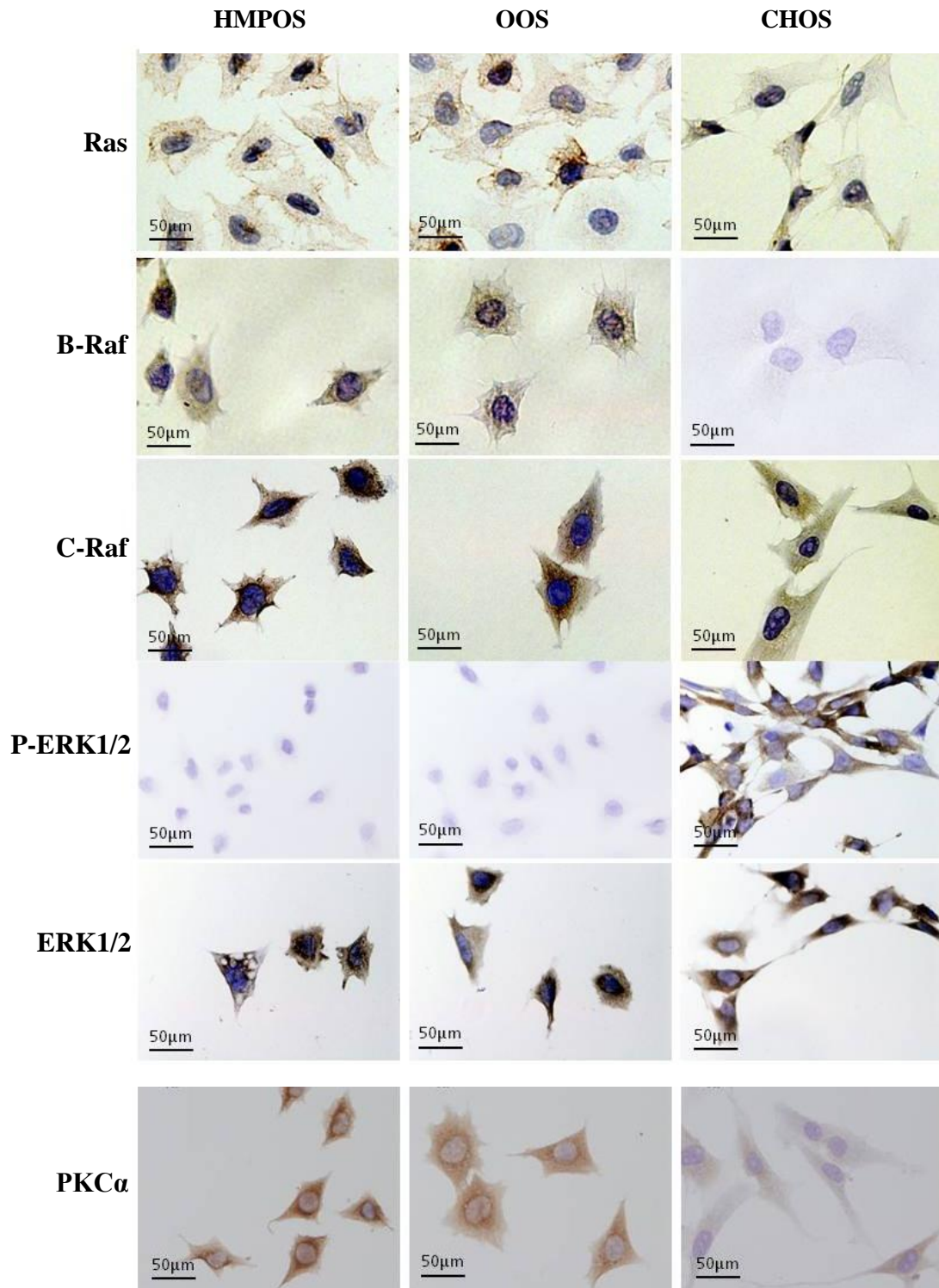
Figure 2.2.2. Immunocytochemistry for Ras, B-Raf, C-Raf, p-ERK1/2, ERK1/2, and PKCα of HMPOS, OOS, and CHOS cell lines. The expressions of Ras and ERK1/2 were detected in all cell lines. B-Raf was not detected in CHOS. C-Raf and PKCα expressions in HMPOS and OOS cells were stronger than those in CHOS cells. On the contrary, p-ERK1/2 was not expressed in HMPOS and OOS cells. Original magnification, 400×.
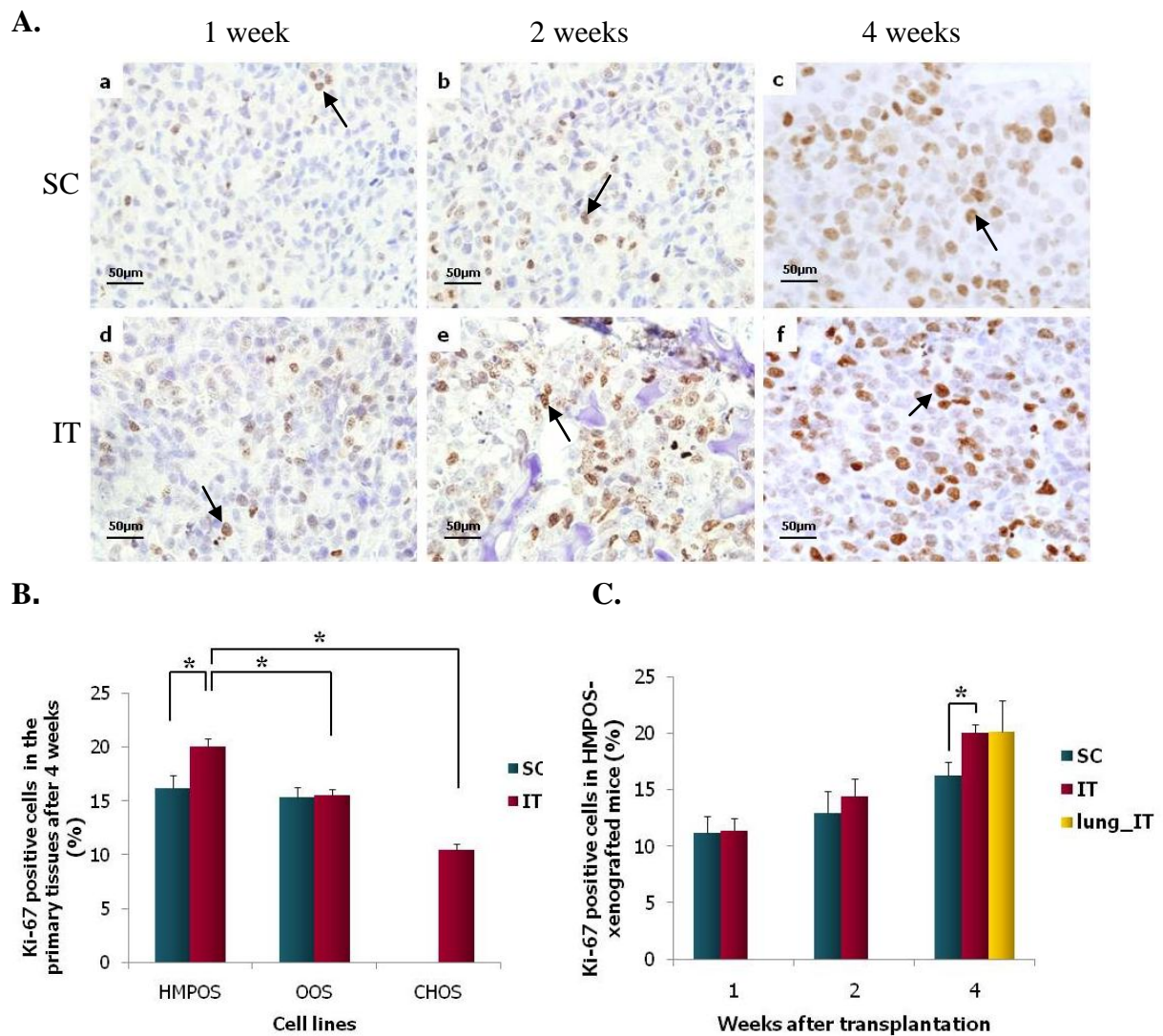
Figure 2.2.3. Ki-67 expression in primary and lung metastatic tissues.

(A) Immunohistochemistry for Ki-67-positive cells (arrows). Ki-67 expression was localized in nucleus

of OS cells in primary tissues of HMPOS-xenografted mice at 1, 2, and 4 weeks after transplantation via

SC (a,b,c) and IT (d,e,f) routes (original maginification, 400×). (B) The percentage of Ki-67-positive cells

at 4 weeks after transplantation in IT-xenografted mice with HMPOS was significantly higher ($p < 0.05$)

than that in mice xenografted with OOS and CHOS cells. (C) The percentage of Ki-67-positive cells in

SC-xenografted mice was significantly lower ($p < 0.05$) than IT-xenografted mice at 4 weeks, whereas

those tissues were not significantly different at 1 and 2 weeks after transplantation. The percentages of

Ki-67-positive cells were not significantly different between primary and metastatic lesions at 4 weeks

after transplantation. * Significant difference ($p < 0.05$); error bars represent SDs.
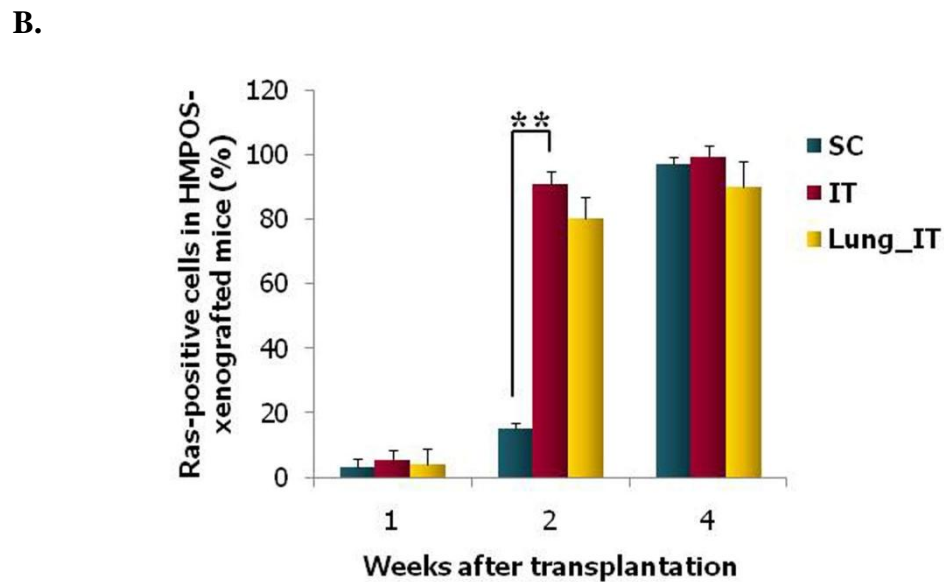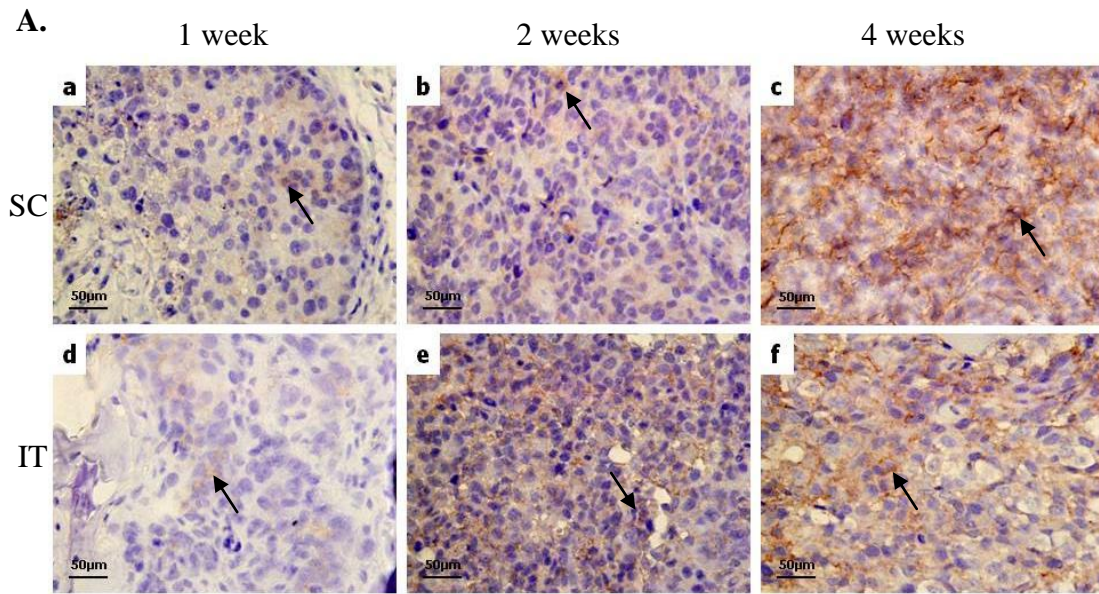
**Figure 2.2.4.** Ras expression in primary and lung metastatic tissues of HMPOS-xenografted mice.

(A) Immunohistochemistry for Ras-positive cells in the primary tissues (arrows). Ras expression was localized in the cytoplasm of OS cells at 1, 2, and 4 weeks after transplantation via SC (a,b,c) and IT (d,e,f) routes (original maginification, 400×). (B) The percentages of Ras-positive cells in the primary and lung metastatic tissues of HMPOS-xenografted mice. The expression of Ras in the IT xenograft was higher than that in the SC xenograft at 2 weeks after transplantation. Those in IT primary and lung metastatic tissues were not significantly different. ** Significant difference ($p < 0.01$); error bars represent SDs.
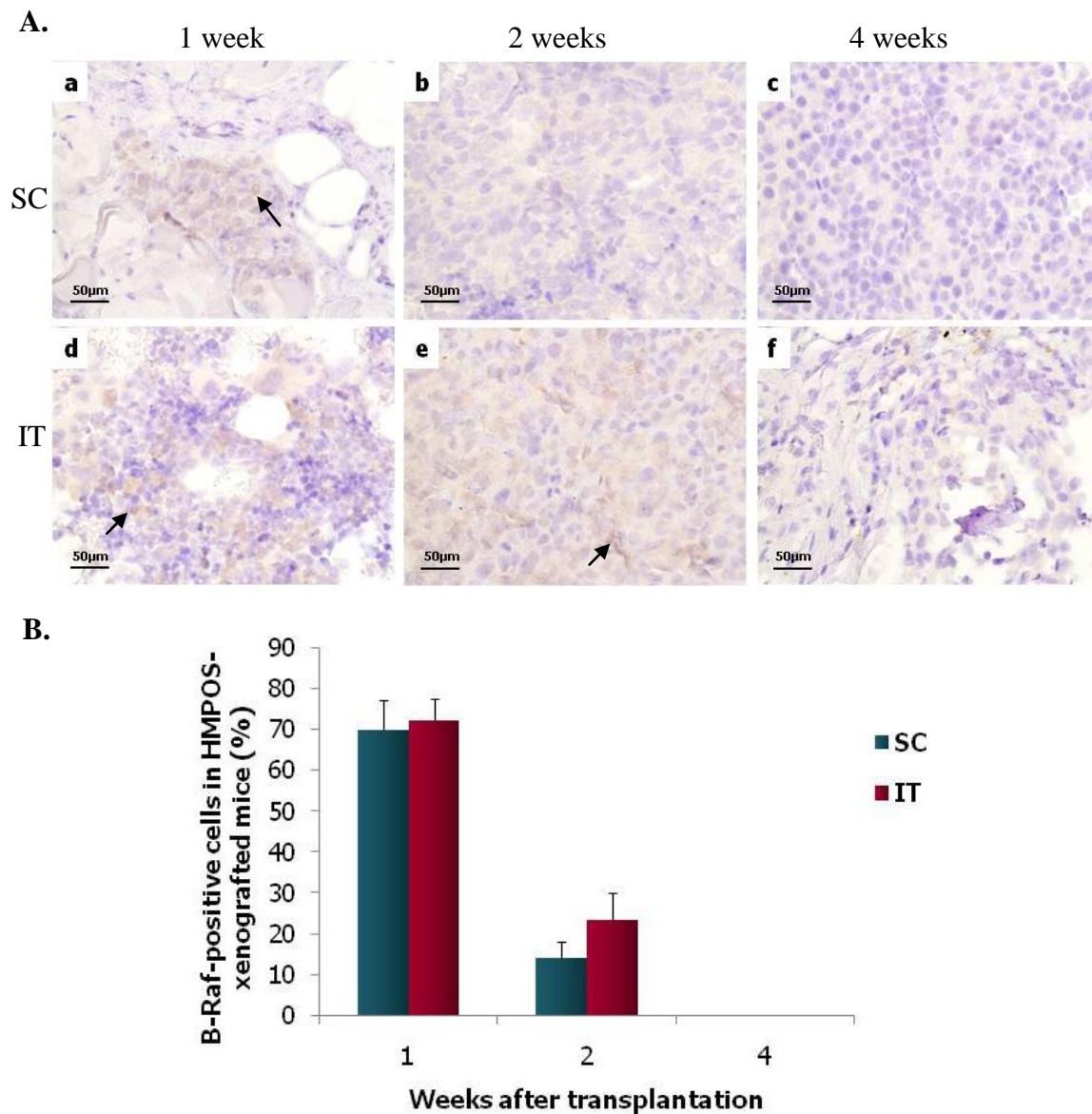
Figure 2.2.5. B-Raf expression in primary tissues of HMPOS-xenografted mice.

(A) Immunohistochemistry for B-Raf-positive cells in primary tissues (arrows). B-Raf expression was localized in the cytoplasm of OS cells at 1 and 2 weeks, but was not expressed at 4 weeks after transplantation via SC (a,b,c) and IT (d,e,f) routes (original maginification, 400×). (B) The percentage of B-Raf-positive cells in the primary tissues of HMPOS-xenografted mice. The expression of B-Raf was not significantly different between SC- and IT-xenografted mice. Error bars represent SDs.

A.

	1 week	2 weeks	4 weeks
SC	a	b	c
IT	d	e	f

B.
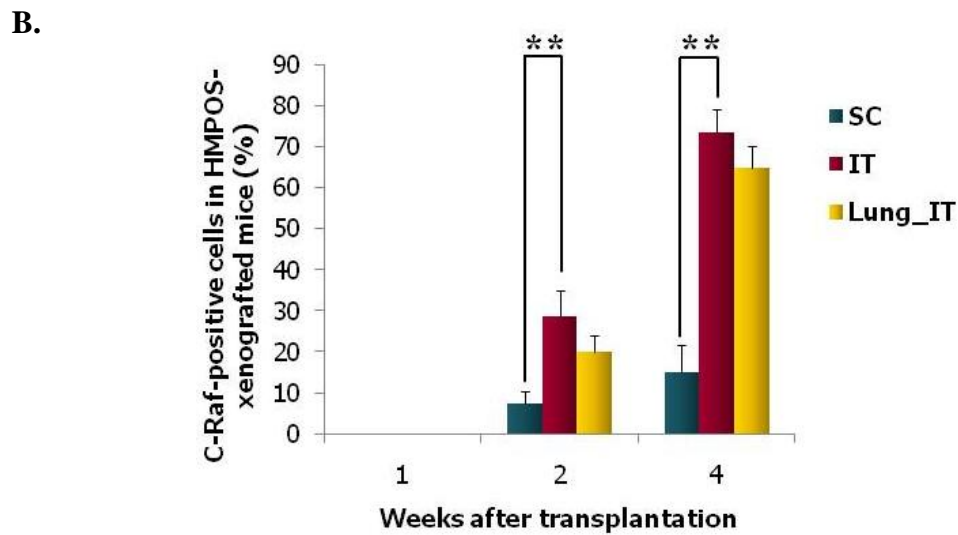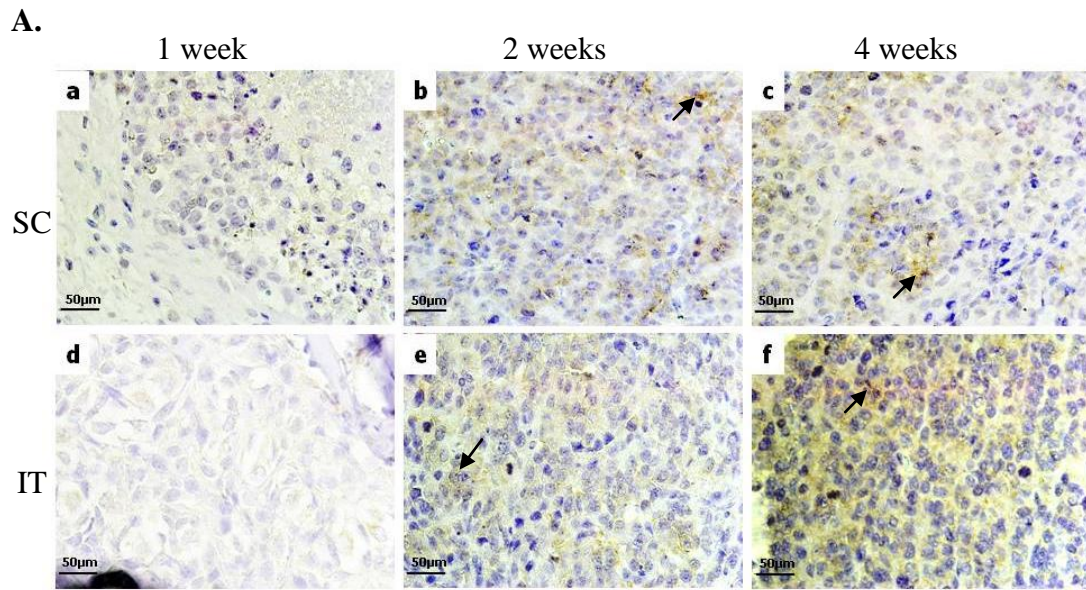
Figure 2.2.6. C-Raf expression in primary and lung metastatic tissues of HMPOS-xenografted mice.

(A) Immunohistochemistry for C-Raf-positive cells in primary tissues (arrows). C-Raf expression was localized in the cytoplasm of OS cells at 2 and 4 weeks, but was not expressed at 1 week after transplantation via SC (a,b,c) and IT (d,e,f) routes (original maginification, 400×). (B) The percentages of C-Raf-positive cells in the primary and lung metastatic tissues of HMPOS-xenografted mice. The expression of C-Raf in the IT xenograft was higher than that in the SC xenograft at 2 and 4 weeks after transplantation. Those in IT primary and lung metastatic tissues were not significantly different. ** Significant difference ($p < 0.01$); error bars represent SDs.
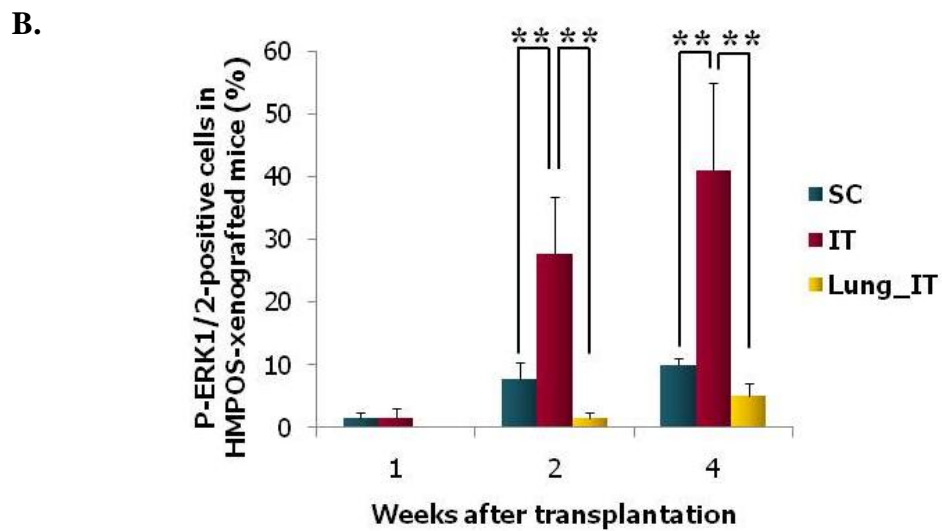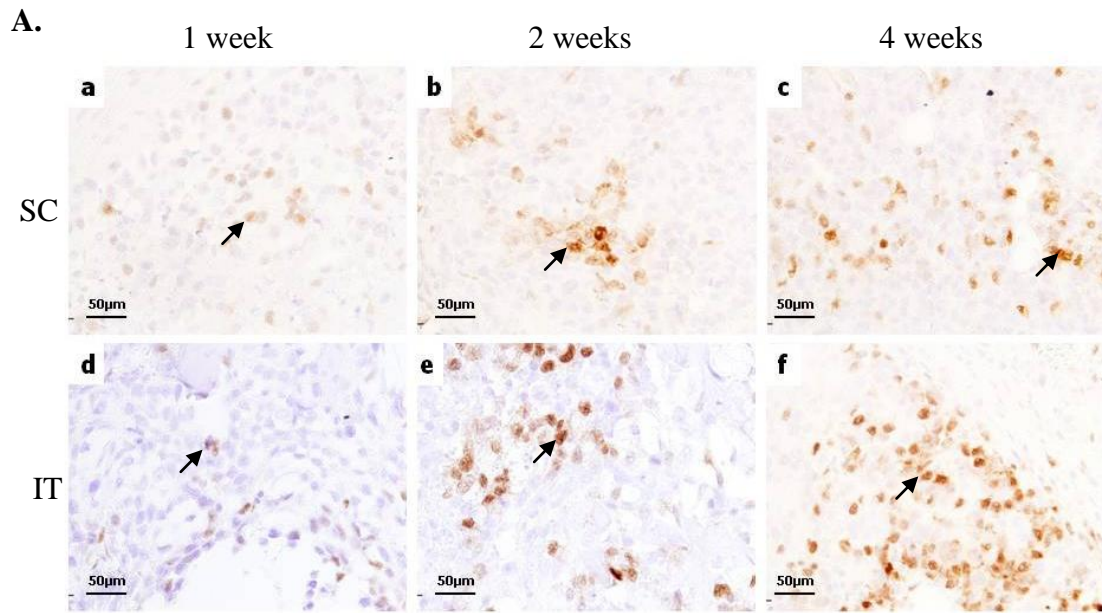
Figure 2.2.7. P-ERK1/2 expression in primary and lung metastatic tissues of HMPOS-xenografted mice.

(A) Immunohistochemistry for P-ERK1/2 -positive cells in primary tissues (arrows). P-ERK1/2 expression was localized in the nucleus and cytoplasm of OS cells at 1, 2, and 4 weeks after transplantation via SC (a,b,c) and IT (d,e,f) routes (original maginification, 400×). (B) The percentage of p-ERK1/2-positive cells in the primary tissues of HMPOS-xenografted mice. The expression of p-ERK1/2 in the IT xenograft was higher than that in the SC xenograft and lung metastatic tissues at 2 and 4 weeks after transplantation. ** Significant difference ($p < 0.01$); error bars represent SDs.
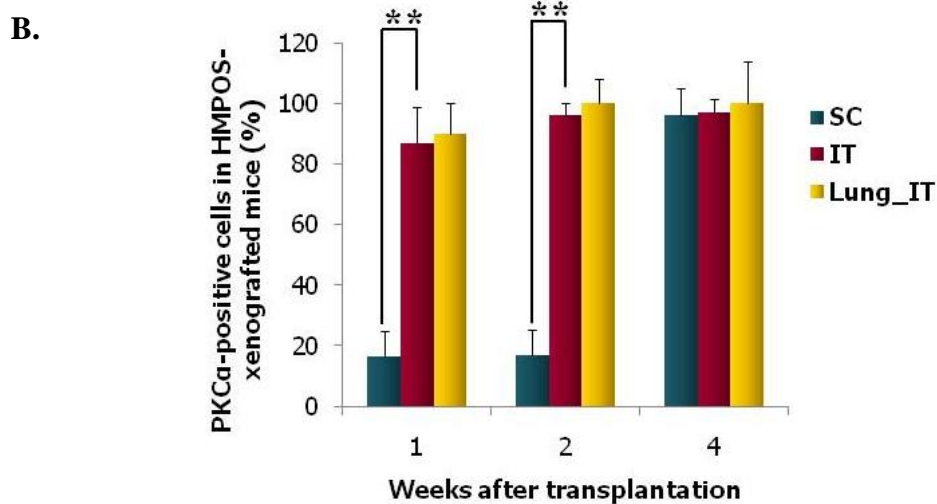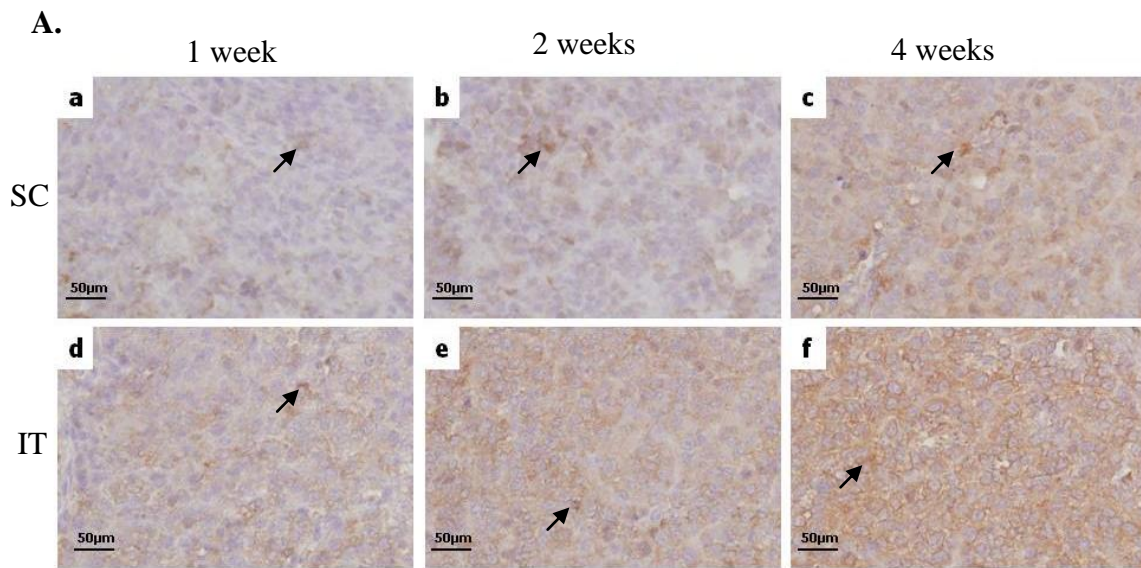
Figure 2.2.8. PKCα expression in primary tissues of HMPOS-xenografted mice.

(A) Immunohistochemistry for PKCα-positive cells in primary tissues (arrows). PKCα expression was localized in the cytoplasm and cell membrane of OS cells at 1, 2, and 4 weeks after transplantation via SC (a,b,c) and IT (d,e,f) routes (original maginification, 400×). (B) The percentages of PKCα-positive cells in the primary tissues of HMPOS-xenografted mice. The expression of PKCα in the IT xenograft was higher than that in the SC xenograft at 1 and 2 weeks after transplantation. Those in IT primary and lung metastatic tissues were not significantly different. **Significant difference ($p < 0.01$); error bars represent SDs.

Chapter 3

Regulation of p-ERM in canine OS cells by a PKC

inhibitor in both *in vitro* and *in vivo* orthotopic

xenografted mouse model

Introduction

Several kinases are implicated in the regulation of ERM protein function. PKCα is shown to interact with ezrin, both *in vitro* and *in vivo* (Ng *et al*., 2001). Several steps of the metastatic progression were linked to PKC, including resistance to apoptosis, migration and invasion (Herbert, 1993; Koivunen *et al*., 2004; Musashi *et al*., 2000; Sullivan *et al*., 2000). The promigratory effects of PKC were linked to ezrin phosphorylation in human and murine OS and ezrin in mouse OS cell lines may be blocked through the use of a PKC inhibitor (Ren *et al*., 2009).

Progression of OS is thought to result from cells migrating away from the primary tumor, surviving in the circulation, invading into lung tissue and establishing metastatic nodules in the lung. Thus, selective blocking this migratory and invasive ability, through targeted therapy of key metastatic molecules, should be an attractive strategy to inhibit tumor metastasis.

Chelerythrine chloride (benzophenanthridine alkaloid: CHE), a natural extract from *Chelidonium majus*, is a potent and specific inhibitor of protein kinase C. It has a variety of biological effects, including antibacterial, antifungal, antiviral, anti-inflammatory and antitumor activities (Chmura *et al*., 2000; Jarvis *et al*., 1994; Walterova *et al*., 1995). It was reported that CHE induced apoptosis in connection with

generation of reactive oxidative species and subsequent activation of c-Jun NH_2 terminal kinases (JNK), p38, and ERK1/2, which are members of MAPK family.

It is known that CHE induced apoptosis in various cancer cells, such as LNCaP and DU145 prostate cancer (Malikova *et al*., 2006), squamous cell carcinoma (Chmura *et al*.,2000), leukemia (Chmura *et al*., 1996; Freemerman*et al*., 1996), breast cancer (MCF-7), colon carcinoma (Chan *et al*., 2003) and uveal melanoma (OCM-1) in human (Kemeny-Beke *et al*., 2006). In OS, CHE-induced apoptosis is mediated through the activation of the RAF/MEK/ERK pathway. These results suggest that activating ERK may be a therapeutic strategy in OS.

In chapter 2, highly metastatic HMPOS and OOS cells exhibited the high expression of ezrin, p-ERM, and PKCα *in vitro*. Moreover, the expression of PKCα was correlated with the expression of ezrin and p-ERM with malignant behaviors in *in vivo* experiments. Although the low expression of p-ERK1/2 was detected *in vitro*, it was elevated in an orthotopic mouse model.

The objective of this chapter is to define the relationship among those molecules targeting to inhibit p-ERM by a PKC inhibitor in canine OS cell lines and a xenograft mouse model. In this chapter, the cell viability assay is used to determine the appropriate concentration of CHE for using in migration and invasion assays. Western blot analysis is used for linking among ezrin, Ras/Raf/ERK pathway and PKCα.

Moreover in *in vivo* experiments, the IT-xenograft mouse model with high metastatic

HMPOS cells is developed to determine the effect of CHE on malignant behaviors

correlated with the changes in expression of ezrin, Ras/Raf/ERK pathway and PKCα.

Materials and Methods

Drugs and reagents.

Cheleryhrine chloride (Sigma Chemical Corp.), CHE, was dissolved in sterile water immediately prior to use for *in vitro* and *in vivo* experiments for animal studies.

Cell viability assay

The MTT assay was performed using the cell proliferation kit I MTT (3-[4,5-dimethylthiazol-2-yi]-2,5-diphenyl tetrazolium bromide)-based kit (Roche Diagnostics GmbH, Mannheim, Germany) to determine the concentration of 50% growth inhibition (IC50) of CHE on each tumor cell. The cells were seeded in quadruplicate in 96-well plates at a density 5 x 10^3 cells per well (HMPOS and OOS cells) or 1 x 10^4 cells per well (CHOS cells) in FBS-containing RPMI media overnight to reach 80% to 90% confluence. The cells were treated with an equivalent amount of medium containing CHE at different concentrations (0.5, 1, 1.25, 2.5, 5, 10 and 20 μM). Distilled water was used as a vehicle for controls. After 24 hours of the incubation period, 10 μl of the MTT labeling reagent was added into the microplate. The cells were incubated for 4 hours in a humidified atmosphere. Cell viability was assessed by the absorbance measured with a

microplate ELISA reader. The viability of treated cells was related to a viability of

control vehicle-treated cells, which represented 100%.

Wound-healing migration assay

Cells were cultured to confluence in 24–well culture plates, on which a wound

scratch was made using a sterile 200 µl pipette tip in the middle of the cell monolayer.

Floating cells were removed by washing with phosphate-buffered saline (PBS) and 10%

FBS-RPMI medium containing 1 µM CHE was added. Cells were incubated at 37°C

with 5% CO_2 and images were recorded at 0 and 24 hours using a light microscope.

Transwell migration assay

The cell migration was performed using a 24-Multiwell Insert System (BD

Biosciences) containing polyethylene terephthalate membrane with an 8-µm pore.

RPMI medium containing 10% FBS was used as a chemoattractant in the bottom

chamber. Tumor cells of 2.5 x 10^4 per 500 µl resuspended in RPMI medium containing

5% FBS was added to the upper chamber in triplicate. CHE at 1 µM was added in both

upper and lower chambers. The cells were allowed to migrate for 22 hours in a

humidified incubator at 37°C with 5% CO_2 atmosphere. Non-migrated cells were

removed from the upper surface of the membrane by gently scrubbing with a cotton swab moistened with the medium. The cells were fixed and stained with 100% methanol for 1 minute and Wright-Giemsa for 15 minutes, respectively. The number of migrated cells per $100 \times$ magnification was determined by averaging the cell counts in 5 randomly-selected fields of each membrane.

Matrigel invasion assay

Matrigel cell invasion assay was performed using polycarbonate membrane with an 8-μm pore coated with Matrigel (BD Biosciences). The membrane was rehydrated in humidified incubator at $37^{\circ}C$ with 5% CO_2 for 2 hours. RPMI medium containing 10% FBS was used as a chemoattractant in the bottom chamber. Tumor cells of 2.5 x 10^4 per 500 μl were added into the upper chamber in triplicate. CHE at 5 μM was added in both upper and lower chambers. The cells were allowed to invade for 22 hours in a humidified incubator at $37^{\circ}C$ with 5% CO_2 atmosphere. Non-invading cells were removed from the upper surface of the membrane by gently scrubbing with a cotton swab moistened with the medium. The cells were fixed with 100% methanol and stained with Wright-Giemsa. The number of invading cells per $100\times$ magnification was determined by averaging the cells counts in 5 random fields of each membrane.

Real-time migration/invasion analysis

Real time monitoring of cell invasion and migration of HMPOS and CHOS cells were carried out using the Real-time Cell Analyzer double-plate (RTCA DP) instrument, xCELLigence System (Roche Diagnostics, GmbH, Germany), which was placed in a humidified incubator maintained at $37^{o}C$ with 5% CO_2. Cell invasion and migration were assessed using CIM-plate 16 (Roche Diagnostics GmbH) with 8 μm pores. These plates are similar to conventional transwell with the micro-electrodes located on the underside of the membrane of the upper chamber. Wells were coated on the upper surface of the transwell with Matrigel diluted 1:40 with FBS-free RPMI medium for measurement of cell invasion or without matrigel for measurement of cell migration, then placed in a humidified incubator maintained at $37^{o}C$ with 5% CO_2 for 4 hours. RPMI medium with 10% FBS was added in the lower chamber and cells were seeded into the upper chamber at 50,000 cells/well. Seeded cells with or without CHE 1 and 5 μM were added in tetraplicate. Cell Index (CI) values as a relative change in measured electrical impedance to integrated cellular status in culture were monitored every 15 minutes for 24 hours. Data analysis was carried out using RTCA Software version 1.2 supplied with the instrument.

Antibodies

The primary antibodies used in Western blot analysis were anti-ezrin, p-ERM, Ras, B-Raf, C-Raf, p-ERK1/2, ERK1/2, PKCα and actin, and those in immunohistochemistry were anti-ezrin, p-ERM, p-ERK1/2 and PKCα. They were used at the same dilutions as chapter 2.

Western blot analysis

Western blot analysis procedures were performed using the same as described in chapter 2.

In vivo **experiments**

To examine the effects of a PKC inhibitor on ezrin expression with primary tumor growth and metastasis *in vivo*, HMPOS (2×10^6 cells) were injected into 5-week-old female BALB/c nude mice via IT route.

Based on the results of lung metastatic potential in the xenografted mouse model in chapter 2, IT-xenografted mice with HMPOS cells showed early lung micrometastases at 1 week after transplantation. I hypothesized that CHE could delay

the time for formation of lung metastasis if mice would receive the treatment before developing lung metastasis. In addition, I also hypothesized that CHE could reduce the number of lung metastatic nodules if mice would receive the treatment after developing lung metastasis. The dosage and frequency of CHE-treatment to mice were similar to the previous study (Chmura *et al*., 2000).

Mice were divided into 3 groups as follows: mice in the control group (n=5) did not receive any treatments; mice in the treatment 1 group (n=5) were injected i.p. on days 0, 2, and 4 with 5 mg/kg CHE; and mice in the treatment 2 group (n=5) were injected i.p. on days 8, 10, and 12 with 5 mg/kg CHE. To determine the proper injection volume, the body weight of mice was measured before injection in each time. The side effect of CHE was considered when $\geq 10\%$ weight loss was observed in the treatment groups.

Evaluation of primary tumor growth and lung metastasis

Primary tumors and lung metastasis developed in nude mice were measured using the same procedures as in chapter 2.

Histology and immunohistochemistry

Histology and immunohistochemistry were performed using the same as described in chapter 2.

Statistical analysis

To compare the cell migration/invasion between the control and CHE-treated cells, statistical analysis was performed using a two-tailed Student's *t*-test. The means, SDs, and SEs of primary tumor volumes, the number of lung metastatic nodules, the body weight and the percentages of ezrin-, p-ERM-, Ki-67, p-ERK1/2, and PKCα positive cells were calculated. The Tukey-Kramer multiple comparison test and analysis of variance (ANOVA) were used for statistical analysis among the different groups. Statistical difference was set at $p < 0.05$. Data analysis was carried out using NCSS 2007 (Kaysville, UT, USA).

Results

Cell viability assay

HMPOS, OOS, and CHOS cell lines treated with CHE for 24 hours underwent cell death (Figure 3.1). When CHE concentrations were less than or equal to 5 μM, most of cell lines survived, while that was more than 5 μM, all the cell lines did not survive. The IC50 values of CHE were 7.42, 7.10, and 7.56 μM for HMPOS, OOS, and CHOS cell lines, respectively. Therefore, CHE concentrations at 1 and 5 μM were selected for the following assays.

Wound-healing migration assay

Figure 3.2 shows the effect of CHE on cell migration using a wound-healing migration assay. The migration of HMPOS seemed to be faster than OOS and CHOS cells, however, there was no significant difference. After exposure to 1μM CHE, HMPOS and OOS cells had a delay in migration compared with control cells, however, there was no significant difference.

Transwell migration assay

Figure 3.3 shows the effect of CHE on cell migration using a transwell migration assay. The cell migration of HMPOS and OOS cells were significantly faster ($p < 0.01$) than CHOS cells. Exposure of CHE at 1 μM to HMPOS and OOS cells caused a significant delay in migration compared with control cells. In contrast, CHE had no effect on the migration of CHOS cells.

Matrigel invasion assay

Figure 3.4 shows the effect of CHE on cell invasion using a Matrigel invasion assay. The potential in cell invasion of HMPOS cells was higher ($p < 0.01$) than OOS and CHOS cells. Exposure of all cells to CHE at 5 μM caused a significant delay in invasion when compared with control cells.

Real-time migration/invasion assays

The real time effect of CHE on migration and invasion of HMPOS cells is shown in Figure 3.5. Exposure of HMPOS cells to CHE at 1 μM caused a significant delay in migration from 6 hours until 24 hours compared to the control cells as shown in Figure 3.5A. CHE at 1 μM had no effect on the invasion of HMPOS cells.

Exposure of HMPOS cells to CHE at 5 μM caused a significant delay in migration from 1 hour until 24 hours and invasion from 2 hours until 24 hours compared to the control cells as shown in Figure 3.5B.

Western blot analysis on expressions of ezrin, p-ERM, Ras, C-Raf, p-ERK1/2, ERK1/2, and PKCα in HMPOS cells

Figure 3.6 shows the expressions of ezrin, p-ERM, Ras, C-Raf, p-ERK1/2, ERK1/2, and PKCα in HMPOS cells after incubation with CHE at 5 μM for 0.5,1, 2, 12, and 24 hours.

CHE suppressed the expression of p-ERM and PKCα from 1 to 24 hours. In contrast, B-Raf and p-ERK1/2 expressions were increased from 0.5 to 24 hours in a time-dependent manner. The expressions of ezrin, Ras, and C-Raf in HMPOS cells were detected and not changed at all incubation times.

In vivo **experiment**

Body weight

Figure 3.7 shows the change in body weight of mice in the control, treatment 1 and 2 groups. Slight decrease in body weight was found after treatment with CHE at 1

and 2 weeks after transplantation in the treatment 1 and 2 groups, but slightly increased again thereafter. These results suggested that the toxicity of this drug was low and could be used without serious side effects in this mouse model.

Tumor growth

Figure 3.8 shows the typical gross findings of primary tumors at 4 weeks after transplantation in IT-xenografed mice in the control and treatment groups. Primary tumors and lung metastasis could be observed in all mice.

Figure 3.9 shows the change in tumor volume in mice of all groups. There was no significant difference in tumor volume among the groups.

Pulmonary metastasis

Table 3.1 shows the number of mice with lung metastasis in each group. No gross pulmonary metastasis was detected in all groups at 1 week after transplantation, however on histology, the lung micrometastases were detected in all mice of the control and treatment 2 groups. In the treatment 1 group, no micrometastasis was detected in any mice at 1 week after transplantation. At 2 weeks after transplantation, gross metastatic nodules on lung surfaces of all mice were detected in the control and the

treatment 2 group, while 60% (3/5) of mice in the treatment 1 group showed lung metastatic nodules. However at 4 weeks after transplantation, mice in all groups developed lung metastasis.

Figure 3.10 shows the number of gross lung metastatic nodules at 2 and 4 weeks after transplantation. At 2 weeks after transplantation, there was no significant difference in the number of lung metastatic nodules between the control and treatment groups. At 4 weeks after transplantation, the number of lung metastatic nodules in the control group was significantly more than those in the treatment groups.

Immunohistochemistry for ezrin, p-ERM, p-ERK1/2, and PKCα in primary and lung metastatic tissues

Figures 3.11-14 show the immunohistochemical findings for ezrin, p-ERM, p-ERK1/2, and PKCα, respectively, in the primary tissues of IT-xenografted mice with HMPOS cells in the control and treatment groups at 1 week after transplantation. Expression patterns for these proteins were almost similar to those in chapter 2. Moreover, the graphs in these figures show the changes in the percentage of positive cells for ezrin, p-ERM, p-ERK1/2, and PKCα at 1, 2, and 4 weeks after transplantation.

The percentage of ezrin-positive cells was not different among all groups (Figure 3.11).

The percentage of p-ERM-positive cells in the treatment group 1 was significantly lower ($p < 0.01$) than those in the control group at 1 week after transplantation. At 2 and 4 weeks after transplantation, the percentages of p-ERM-positive cells in the treatment groups were lower than those of the control group. That of the treatment group 2 was significantly lower ($p < 0.05$) than that of the control group at 2 weeks after transplantation (Figure 3.12).

The percentage of p-ERK1/2-positive cells was not different among all groups (Figure 3.13).

The percentage of PKCα-positive cells in the treatment group 1 was significantly lower ($p < 0.05$) than those in the control group at 1 week after transplantation. At 2 weeks after transplantation, the percentage of PKCα-positive cells in treatment group 2 was significantly lower ($p < 0.05$) than those in the control group (Figure 3.14).

Figure 3.15 shows the immunohistochemical findings for p-ERM, PKCα, and p-ERK1/2 on the lung metastatic lesions of mice in the control group at 1 week after transplantation and in the treatment groups 1 and 2 at 2 weeks after transplantation. The expressions of those molecules were localized in OS cells as shown in chapter 2.

P-ERM-positive cells was not detected on the lung metastatic nodules of the treatment group 1 and the percentage of p-ERM-positive cells in the treatment group 2 was significantly lower ($p < 0.05$) than that of the control group at 2 weeks after

transplantation. However at 4 weeks after transplantation, all groups showed low p-ERM expression and there was no significant difference among groups (Figure 3.16A). In contrast, the percentage of p-ERK1/2-positive cells was not different from the control group at 2 and 4 weeks after transplantation (Figure 3.16B). The percentage of PKCα-positive cells in the lung metastatic nodules was similar to p-ERM expression. The percentages of PKCα-positive cells in the treatment groups 1 and 2 were significantly lower ($p < 0.05$) than the control group at 2 weeks after transplantation. However at 4 weeks after transplantation, all groups showed high PKCα expression and there was no significant difference among groups (Figure 3.16C).

Discussion

CHE, a potent and specific inhibitor of protein kinase C, was used in this chapter to study the regulation of ezrin phosphorylation in both *in vitro* and *in vivo*.

In *in vitro* experiments, metastatic phenotypes including cell viability, migration, and invasion were evaluated in 3 canine OS cell lines after exposure to CHE.

CHE inhibited cell viability at a dose-dependent manner in all cell lines. Exposure to this drug for 24 hours at a dosage of less than or equal to 5 μM did not decrease the cell viability, while that more than 5 μM suppressed. These findings are in agreement with the previous studies using various cancer cell lines, including human head and neck squamous cell carcinoma, mouse lymphocytic leukemia and human prostate cancer cell lines (Chmura *et al*., 2000; Kaminskyy *et al*., 2008; Malikova *et al*., 2006).

Cell migration after the treatment with CHE was evaluated using 3 methods to provide more accurate results. For many years, transwell assay and wound-healing assay were widely available formats to study cell migration. However, new technologies such as xCELLigence system has recently emerged as alternative migration and invasion assays that provide additional or complementary information.

Using wound-healing migration assay, cell migration of HMPOS, OOS, and CHOS cells following exposure to CHE was observed. However, the distance of migration between the control and CHE-treated cells was not significantly different. Wound-healing assay provided several advantages: (1) the assay can be performed in any readily available plate configuration; (2) cells move in a defined direction to close the wound; and (3) the movement and morphology of the cells can be visually observed and images captured throughout the experiment thereby permitting velocity measurements. However, there are some disadvantages of this system: (1) the size, shape, and spacing of the scratches can vary leading to assay variability; (2) difficult to ensure that control and treated-cells are at the same degree of confluence; (3) results can be compromised by the release of factors from damaged cells; (4) chemotaxis was not used; and it is difficult to obtain statistically significant quantitative results (Hulkower and Herber, 2011; Kam *et al*., 2008).

Transwell migration assay was used to count the number of migrated cells. Among OS cells, migration of HMPOS and OOS cells were faster than CHOS cells. Anti-migratory effect of CHE was more clearly observed in HMPOS and OOS cells than CHOS cells. These data suggested that CHE suppressed the migration of HMPOS and OOS cells. Transwell migration assay offers the advantages: (1) the assay can analyze migration in response to a chemotactic gradient; and (2) it can achieve the

quantitative results. However, the disadvantage is difficult to visualize the cells and observe morphology during the experiments (Hulkower and Herber, 2011).

Because there has been no way to quantitatively monitor cell migration in real time of wound-healing and transwell assays, the xCELLigence system enables accurate real time monitoring of cell migration without any need to removing them from the plate which may alter cell function (Keogh, 2010). The xCELLigence system was used to determine the anti-migratory effect in HMPOS and CHOS cells for 24 hours in every 15 minute immediately after exposure of cells to CHE. Migration of HMPOS cells was faster than CHOS cells. Migrations of treated HMPOS cells were suppressed from 6 to 24 hours when compared to control cells. In addition, with the increased dosage at 5 µM, migration of treated HMPOS cells was suppressed in the earlier phase from 1 to 24 hours. This result suggested that the anti-migratory effect of CHE was dose-dependent.

These *in vitro* results distinguished the different levels of aggressive behaviors for cell migration of 3 different cell lines which corresponded to the results in chapter 2, that showed metastatic potential of HMPOS and OOS cells and non-metastatic potential of CHOS cells. Moreover, the results suggested that CHE inhibited the migration of metastatic OS cells.

Matrigel invasion assay was used to count the number of invaded cells through the Matrigel-coating membrane after the treatment with CHE at 5 μM. Among cell lines, HMPOS cells had a high potential of invasion more than OOS and CHOS cells. All treated cells were significantly decreased in invasive potential when compared to control cells. Both advantage and disadvantage for this assay were similar to those in transwell migration assay.

Therefore, real time xCELLigence system was also used to evaluate the cell invasion. According to the results in this real time assay, there was no inhibitory effect of CHE at 1 μM on cell invasion. Therefore, the dosage was increased to 5 μM, in which the invasion of CHE-treated HMPOS cells was suppressed from 2 to 24 hours.

Cell invasion, a process typically associated with cancer cell metastasis (Frield and Wolf, 2003), refers to 3-dimensional migration of cells as they penetrate an extracellular matrix (ECM) or Matrigel, thus the effective dose of CHE to inhibit invasion of OS cells in this study was higher than that in migration assay. However, I concluded that CHE inhibited the invasion of OS cells.

Cell migration and invasion are important phenotypes for early events in the metastatic cascade. High potential in these phenotypes facilitates tumor cells to overcome the local adhesive forces, migrate towards the microvasculature, and invade

the vessel. As expected, the highly tumorigenic and metastatic HMPOS cells had higher cell migration and invasion potential, while low-tumorigenic and non-metastatic CHOS cells demonstrated lower migration and invasion potential. The higher motility and invasion of HMPOS cells may be in part related to high expression of ezrin and p-ERM.

The influence of CHE, a PKC inhibitor, on expression of PKCα, ezrin and ezrin-related molecules in HMPOS cells was analyzed by Western blot analysis. The dose of CHE at 5 μM was selected because it suppressed both migration and invasion of HMPOS cells *in vitro*. After the treatment, expression of PKCα and p-ERM, but not ezrin, was down regulated in a time-dependent manner started from 1 hour after exposure to CHE. Together with the previous results, PKC-mediated effects on cell migration and invasion were mediated through phosphorylation of ERM.

Several of the steps associated with metastatic progression have been linked between PKCα and ezrin and related not only to migration and invasion but also resistance to apoptosis (Koivunen *et al*., 2004; Musashi *et al*., 2000; Sullivan *et al*., 2000) that may associate with p-ERK1/2 (Khanna *et al*., 2004). Therefore, I evaluated the expression of molecules relating to the pathway of Ras/Raf/ERK. CHE stimulated the expression of B-Raf and phosphorylation of ERK1/2 in a time-dependent manner. Ras-dependent ERK1/2 activation by receptor tyrosine kinase or Ras-independent activation through PKC was reported previously (Chong *et al*., 2003; Yang *et al*., 2008).

116

In this study, CHE-induced ERK1/2 activation seems to be Ras/Raf-dependent and not regulated by PKC or ezrin. This result was similar to the previous study in human OS cell lines and the author suggested that activating ERK, rather than inhibiting it, may be the therapeutic merit in OS (Yang *et al*., 2008). However, this should be investigated in the future.

Taken together the results in *in vitro* studies, it was suggested that anti-migratory and anti-invasive effects of a PKC inhibitor were related to down regulation of p-ERM but not p-ERK1/2, which may be therapeutic strategies in canine OS. These data encouraged the value of the continued study of this PKC inhibitor targeting the ezrin-ERK-PKC phenotype in a xenografted mouse model.

A xenograft orthotopic model with highly metastatic HMPOS cells in nude mice was used to determine the effect of this PKC inhibitor on tumor growth and lung metastatic potential as well as the expression of p-ERM and p-ERK1/2. I hypothesized that CHE could inhibit phosphorylation of ERM and ERK1/2 that resulted in decreased tumor growth and lung metastatic potential.

Importantly, no signs of toxicity were observed in CHE *in vivo* as in the previous report (Chmura *et al*., 2000). In the treatment 1 group, there was no lung micrometastasis at 1 week and lung metastatic nodules were detected only 3 of 5 mice

in this group at 2 weeks after transplantation. This delayed lung metastasis was similar

to the previous study in *in vivo* mouse model of breast cancer, where lung metastasis

was suppressed by a PKCα inhibitor (Kim *et al*., 2011), suggesting that CHE may play

roles in inhibition of migration and invasion and may be used to develop as the

protective agent for lung metastasis.

The treatment 2 group was designed as in clinical canine patients, where they

had already developed lung micrometastasis. CHE suppressed expression of p-ERM and

PKCα at 2 weeks after transplantation. Although lung metastatic nodules were detected

in all mice at 2 and 4 weeks after transplantation, number of lung metastatic nodules

was lower than those in the control group. Therefore, CHE may be used to decrease the

lung metastatic potential. This result was similar to the previous phase I trials of the

other PKC inhibitor (Bryostatin) in metastatic melanoma and colorectal cancer (Propper

et al., 1998; Zonder *et al*., 2001).

The expressions of p-ERK1/2 in the treatment 1 and 2 groups were not

significantly different from the control group and were not related to suppression of

PKCα and p-ERM on primary and lung metastatic lesions. However at 4 weeks after

transplantation, the expressions of p-ERM and PKCα were not different from the

control group. This inhibition may affect transiently at an earlier phase of migration and

invasion but not kill the OS cells. Therefore, OS cells could still survive for

proliferating in primary and lung metastatic lesions. However, it was suggested that CHE did not change in tumor volume and differed from the previous study that CHE delayed the tumor growth in human squamouse cell carcinoma (Chmura *et al*., 2000).

In conclusion, CHE suppressed lung metastatic potential but not tumor growth, which may be explained with the regulation of the phosphorylation of ERM and PKCα, but not the Ras/Raf/ERK pathway.

In the future, study the connection between PKC and ezrin may be managed through the other pharmacological PKC inhibitor or change the treatment protocol to be a long-term intermittent dosing that may not effectively regulated only lung metastasis, but also tumor growth.

Group	1 week after transplantation	2 weeks after transplantation	4 weeks after transplantation
Control	5/5	5/5	5/5
Treatment 1	0/5	3/5	5/5
Treatment 2	5/5	5/5	5/5

Table 3.1. Number of mice in each groups that developed (micro/macroscopic) lung metastasis. Development of lung metastasis was delayed in mice of treatment 1 group.
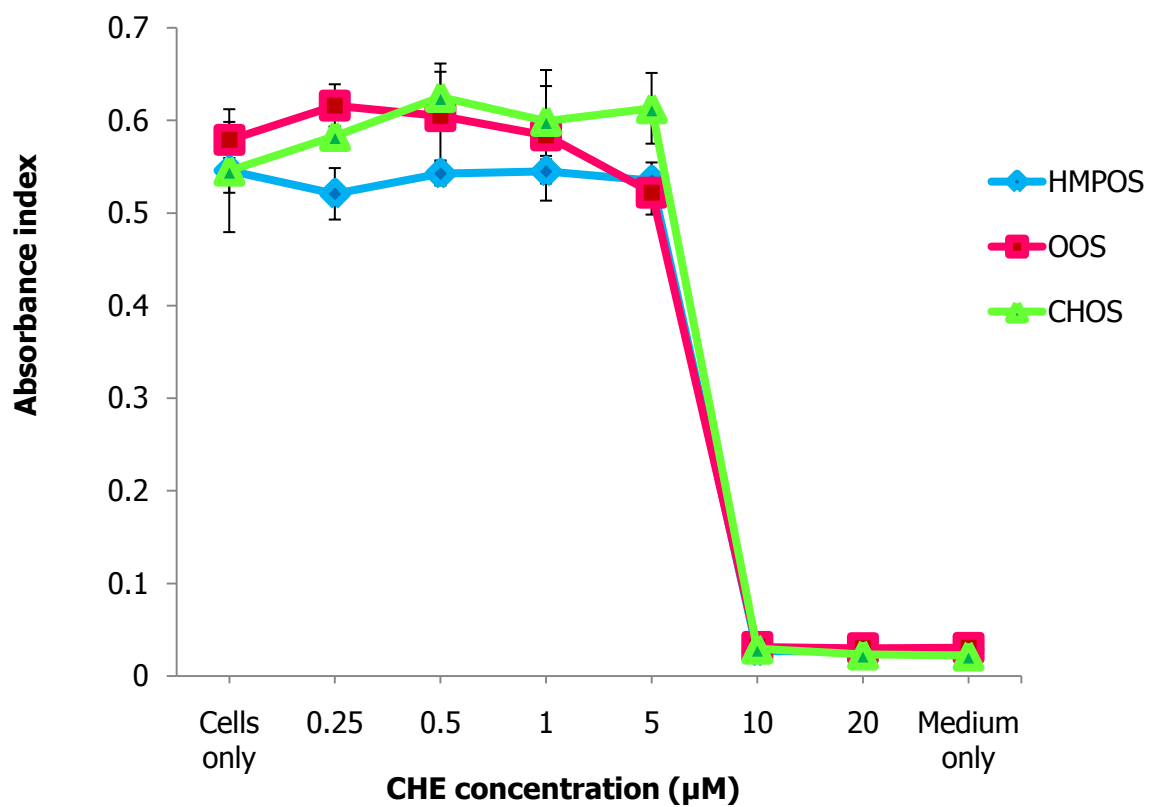
Figure 3.1. Cell viability assay of HMPOS, OOS, and CHOS cells after incubation with CHE for 24 hours. When the CHE concentrations were less than or equal to 5 μM, all cell lines survived. Error bars represent SDs.
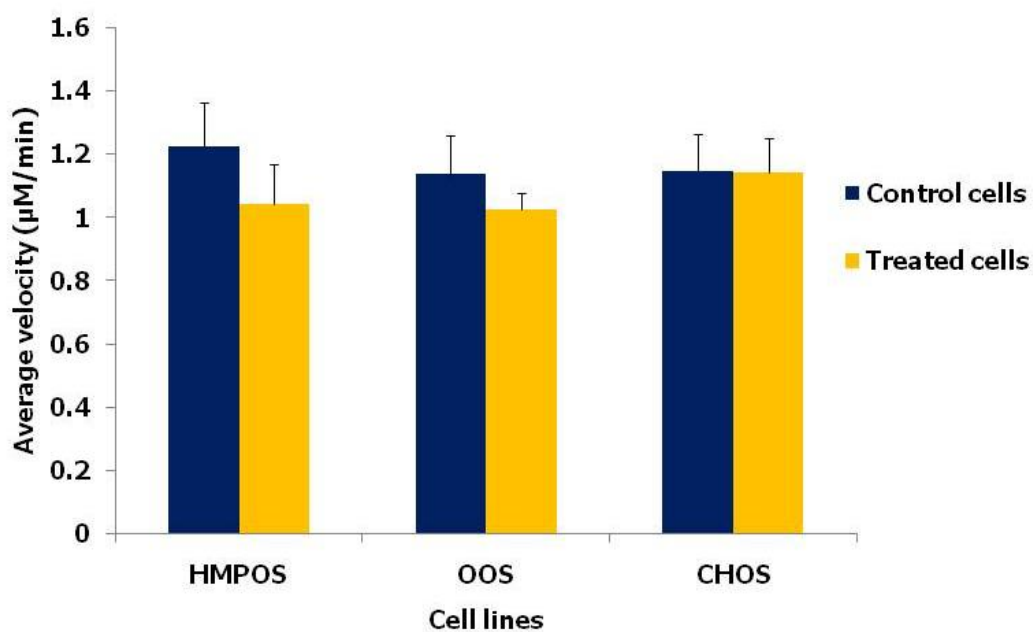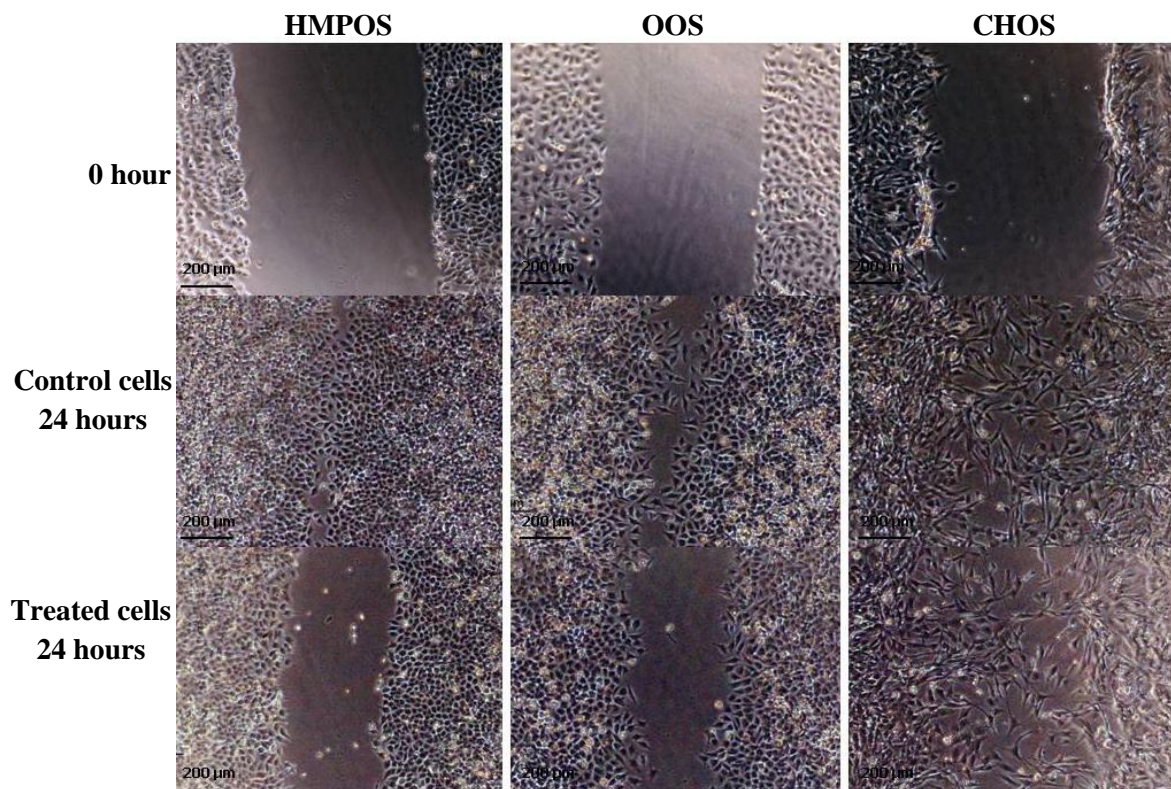
Figure 3.2. Wound-healing migration assay for HMPOS, OOS, and CHOS cells after incubation with CHE for 24 hours. Migration of treated cells showed a lower velocity than control cells. However, statistical analysis was not significantly different between control and CHE-treated cells. Error bars represent SDs.
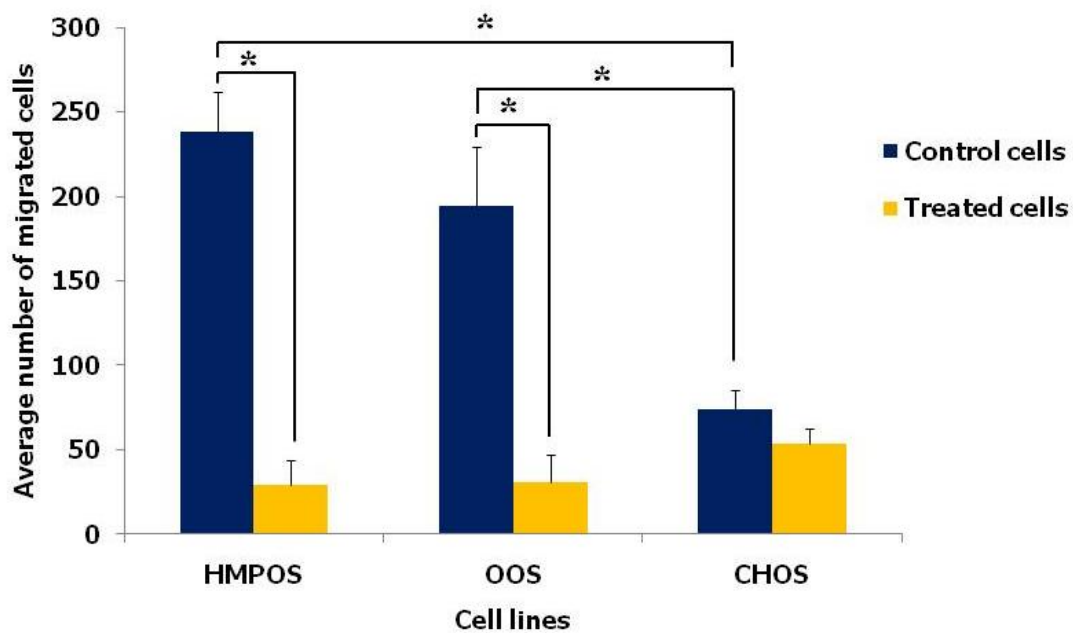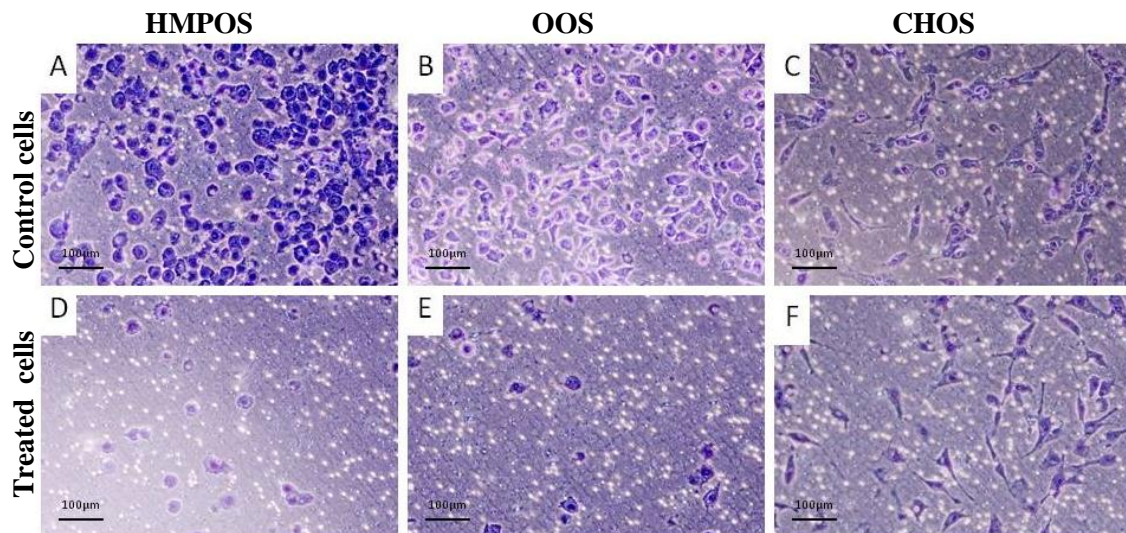
Figure 3.3. Effect of CHE on cell migration using a transwell chamber. The representative fields of the lower chamber were photographed under a light microscope (original magnification, 100×). (A,B,C) HMPOS, OOS, and CHOS cell lines without CHE and (D,E,F) with CHE after 24 hours. The cell migration of HMPOS and OOS cells were significantly faster ($p < 0.01$) than CHOS cells. Exposure of CHE at 1 μM to HMPOS and OOS cells caused a significant delay in migration compared to control cells. CHE had no effect on the migration of CHOS cells. * Significant difference ($p < 0.01$) between control and treated cells; error bars represent SDs.
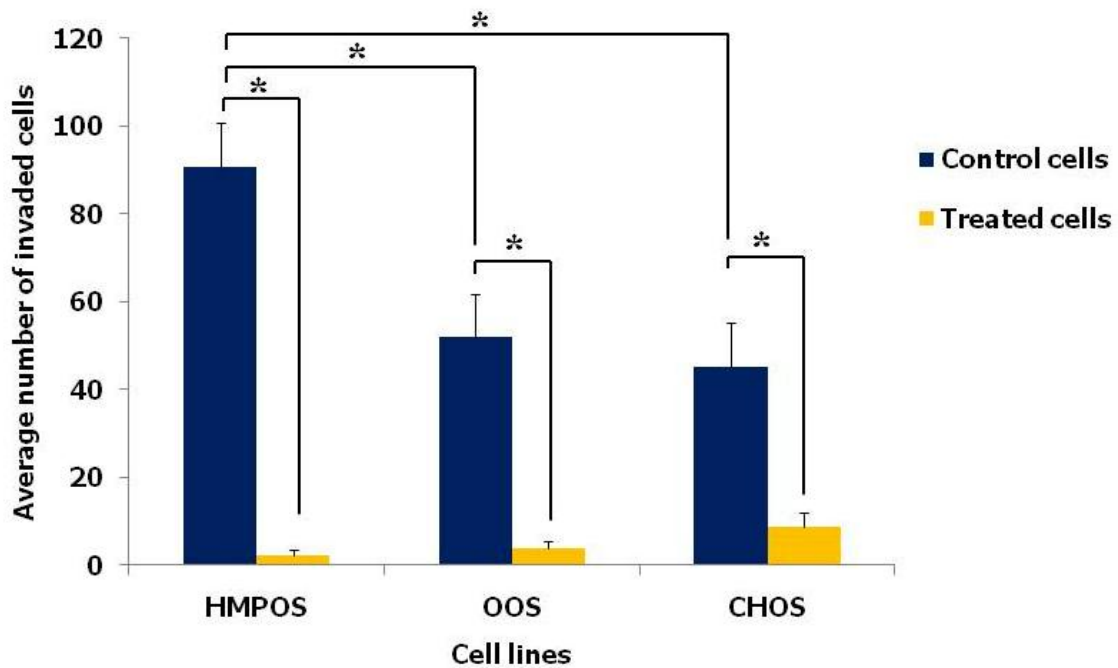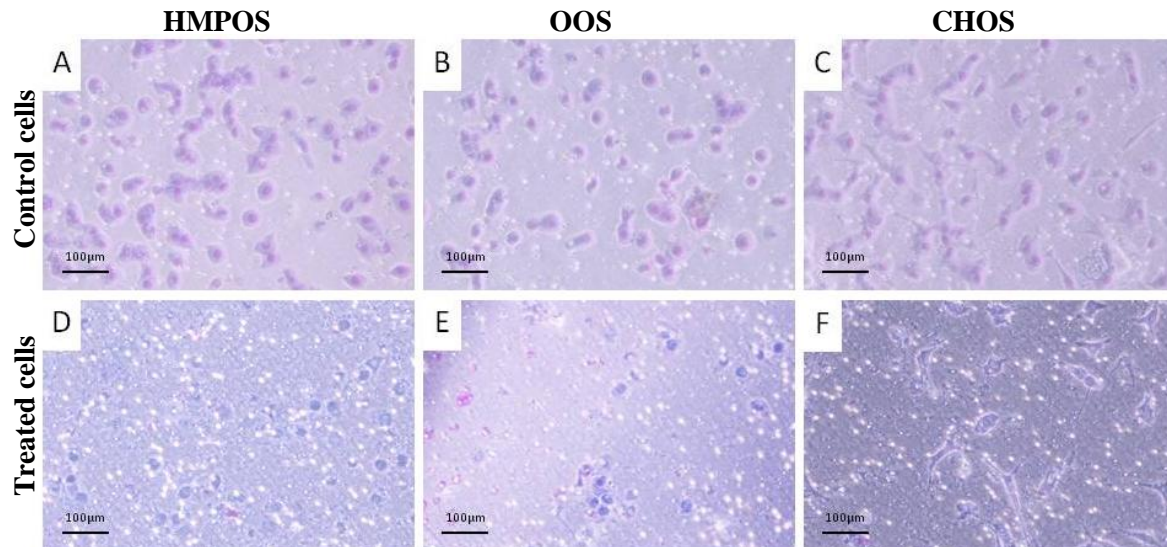
Figure 3.4. Effect of CHE on cell invasion using a Matrigel invasion assay. The representative fields of the lower chamber were photographed under a light microscope (original magnification, ×100). (A, B, C) HMPOS, OOS, and CHOS cell lines without CHE and (D, E, F) with CHE after 24 hours. The cell invasion of HMPOS cells was significant higher ($p < 0.01$) than OOS and CHOS cells. Exposure of all cell lines to CHE at 5 μM caused a significant delay ($p < 0.01$) in invasion compared to control cells. * Significant difference ($p < 0.01$) between control and treated cells; error bars represent SDs.

A.
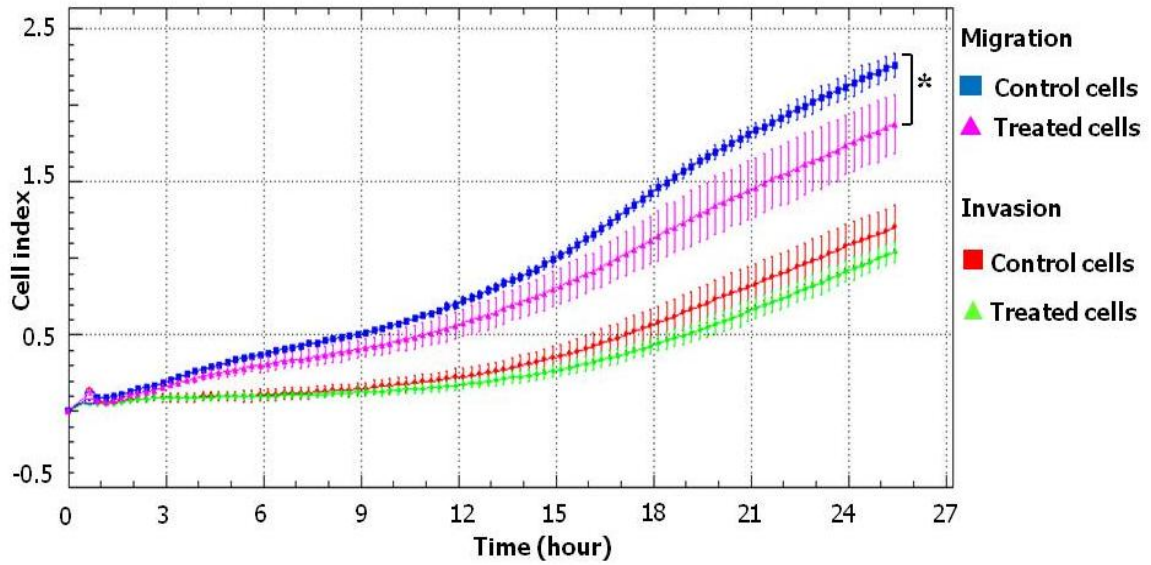
B.
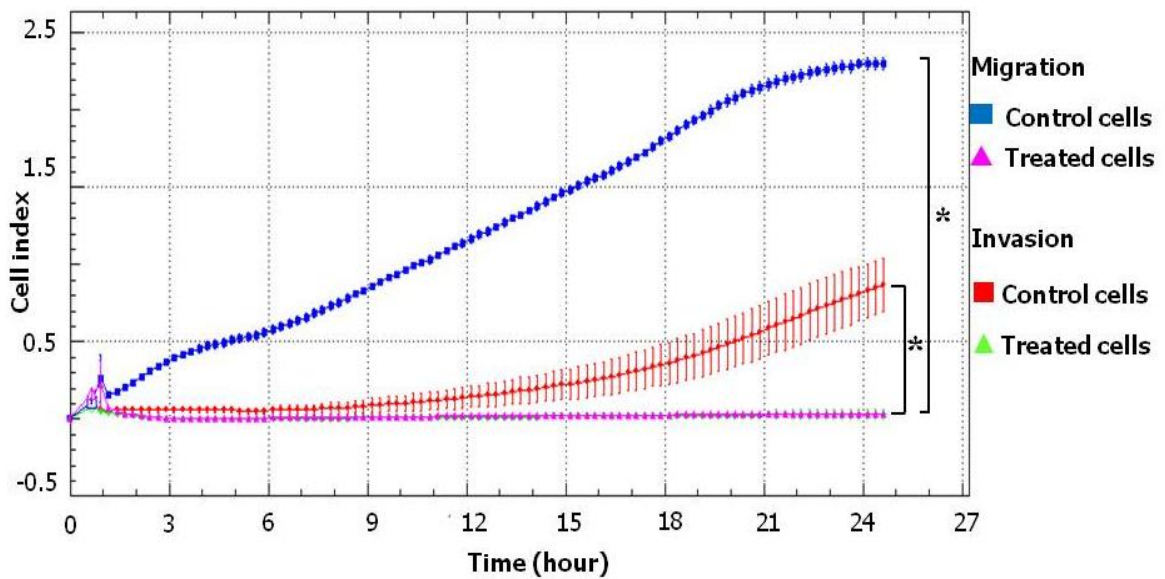
Figure 3.5. The real time effect of CHE on migration and invasion of HMPOS cells by xCELLigence system. (A) CHE at 1 μM caused a significant delay in migration from 6 hours until 24 hours. (B) CHE at 5 μM caused a significant delay ($p < 0.01$) in migration from 1 hour until 24 hours and invasion from 2 hours until 24 hours. * Significant difference ($p < 0.01$) between treated and control cells; error bars represent SDs.
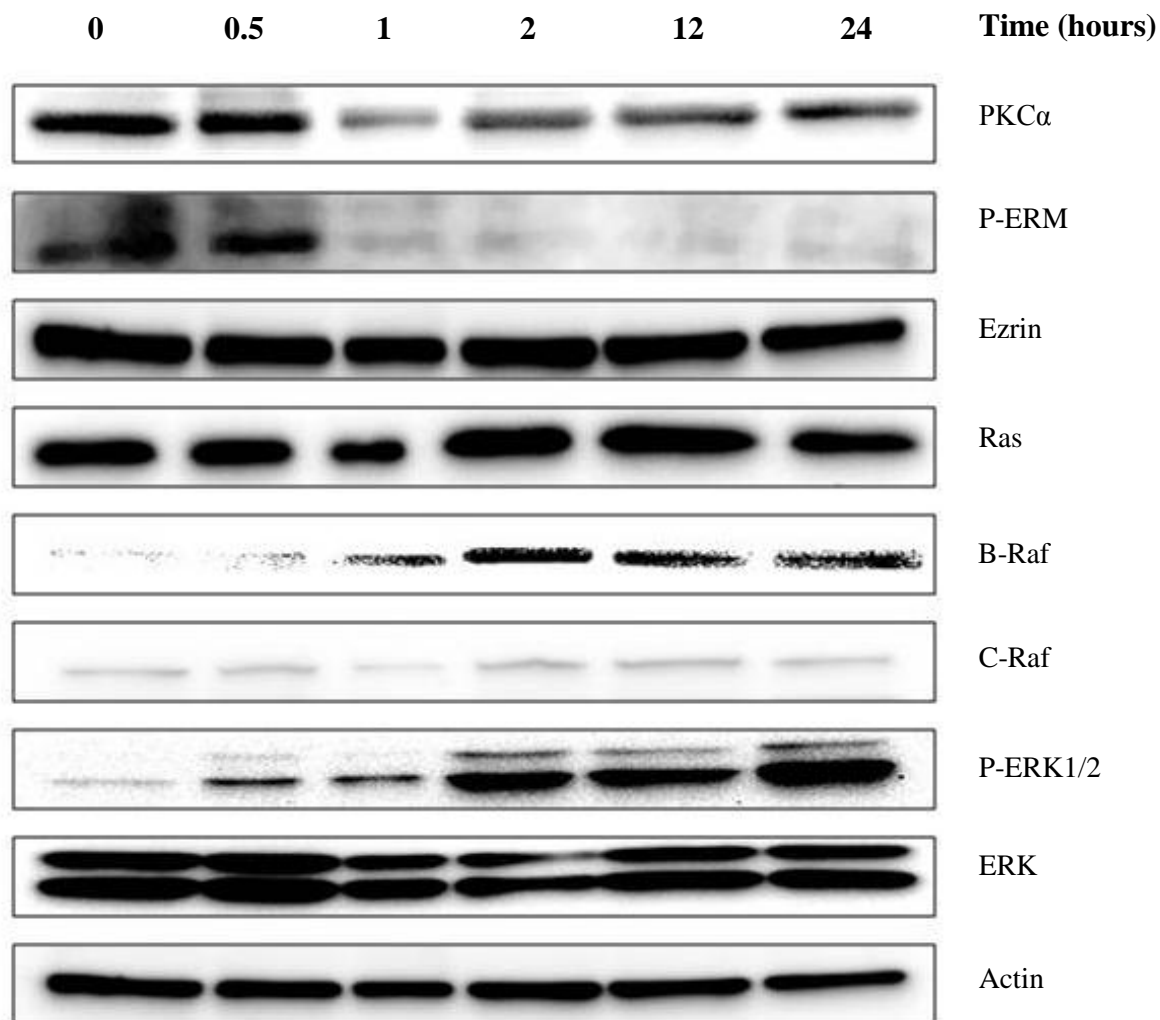
Figure 3.6. Western blot analysis for HMPOS cells after exposure to CHE 5 μM. CHE-treatment decreased the expressions of PKCα and p-ERM from 1 to 24 hours. CHE-treatment increased the expressions of B-Raf and p-ERK1/2 from 0.5 to 24 hours.
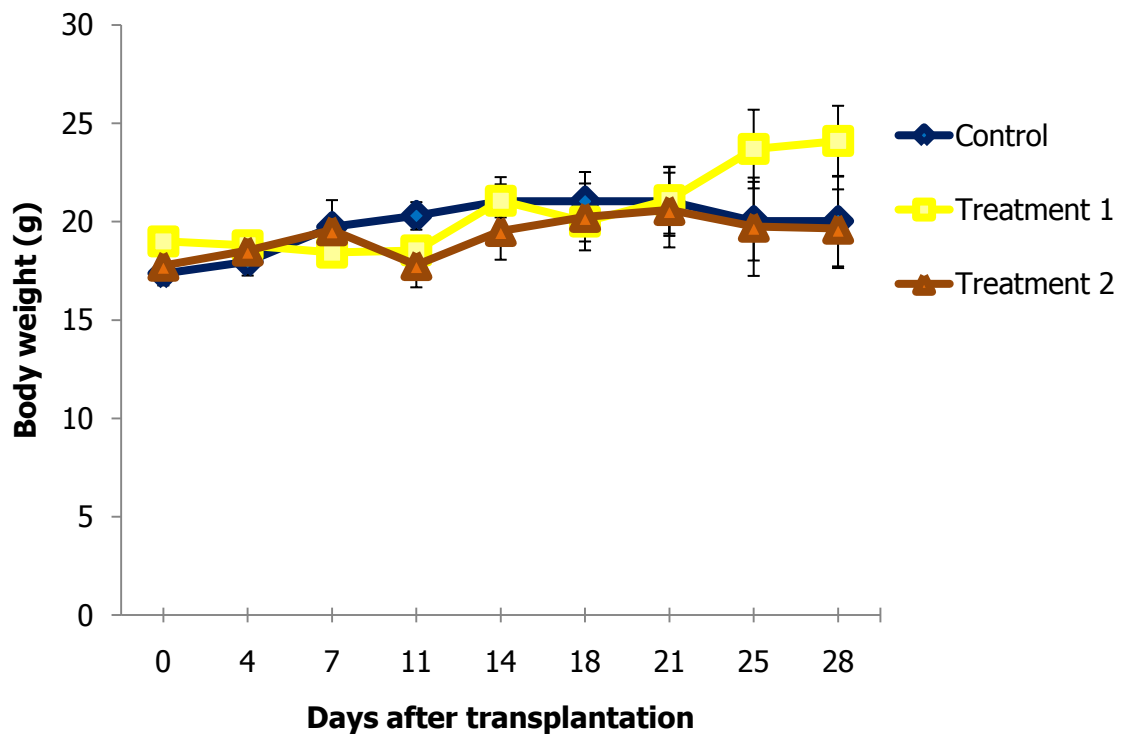
Figure 3.7. Body weight of mice in each group. Slightly decreased body weight (<10% of initial body weight) was found after treatment with CHE at 1 and 2 weeks after transplantation in the treatment 1 and 2 groups. Error bars represent SDs.
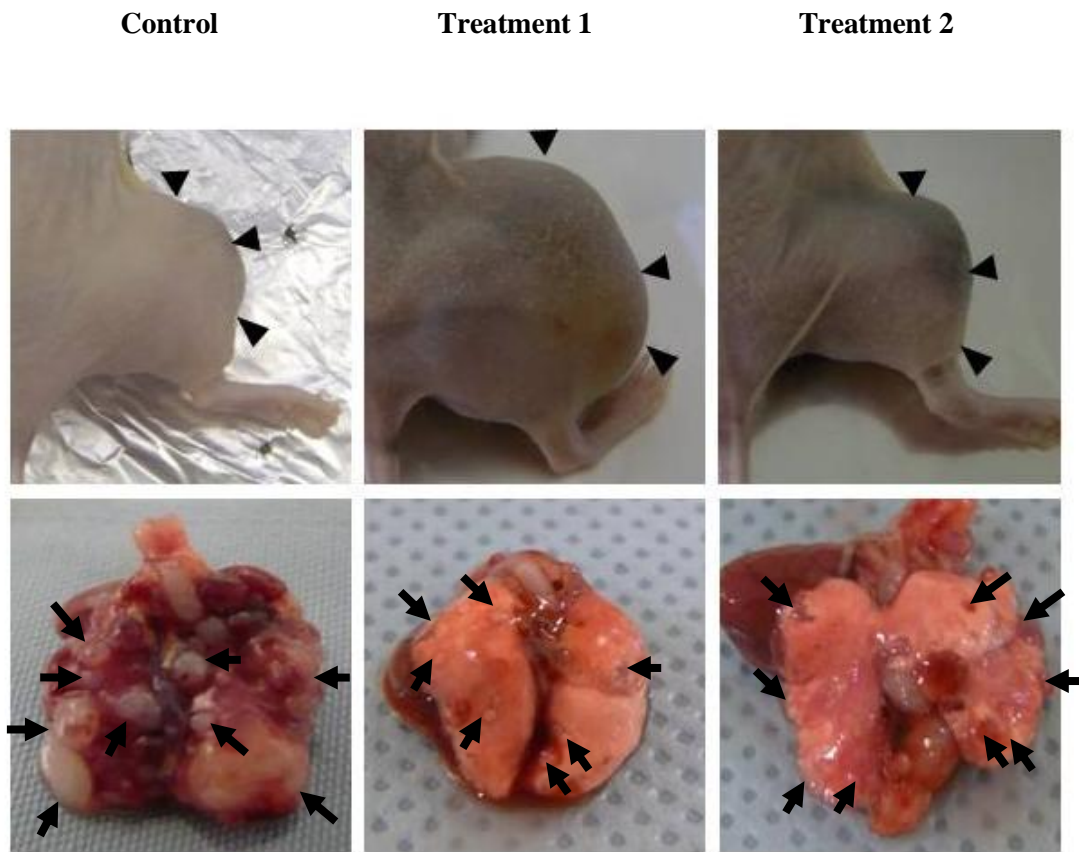
Figure 3.8. Typical gross findings of primary tumors and lung metastasis at 4 weeks after transplantation in IT-xenografted mice of the control and treatment groups. Primary tumors and lung metastasis could be observed in all mice.
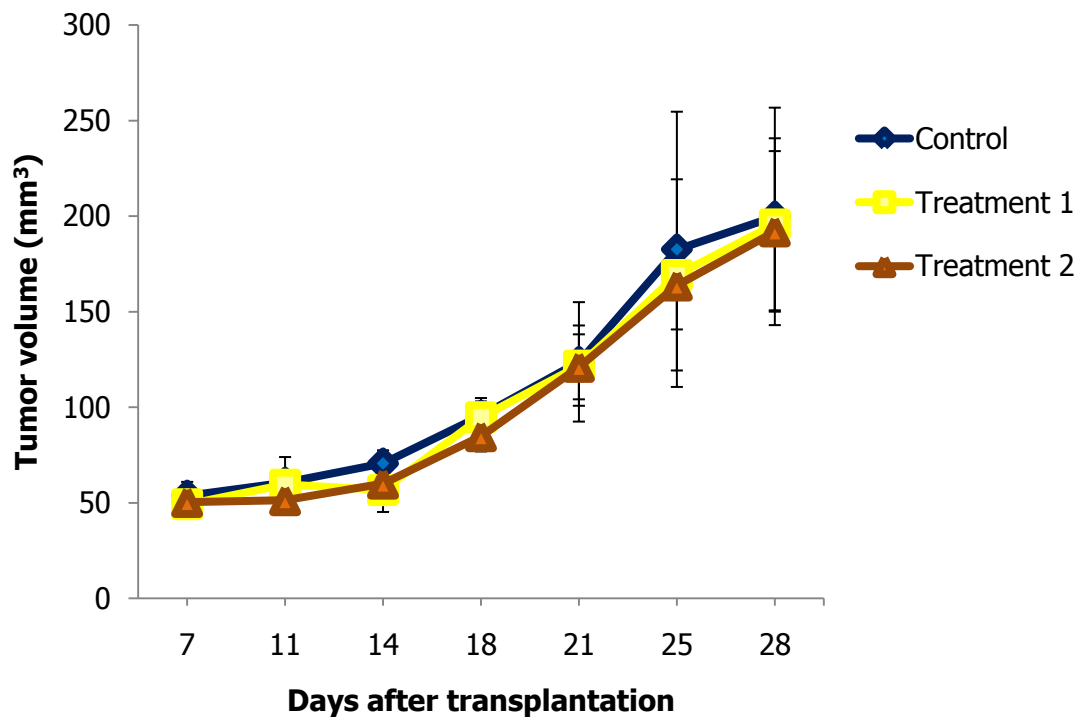
Figure 3.9. Tumor volume of mice in each group. There was no significant difference in tumor volume among the groups. Error bars represent SDs.
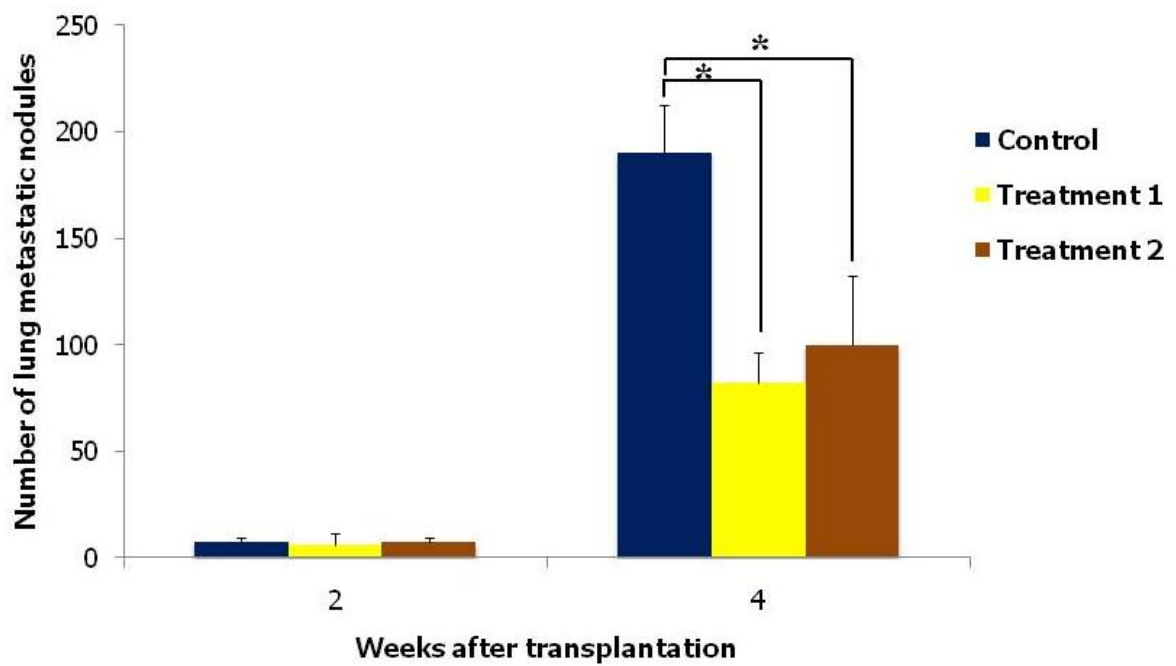
Figure 3.10. Number of gross lung metastatic nodules. Number of lung metastatic nodules produced in mice of both treatment groups was significantly lower ($p < 0.05$) than the control group. *Significant difference ($p < 0.05$) between the control and treatment groups; error bars represent SDs.
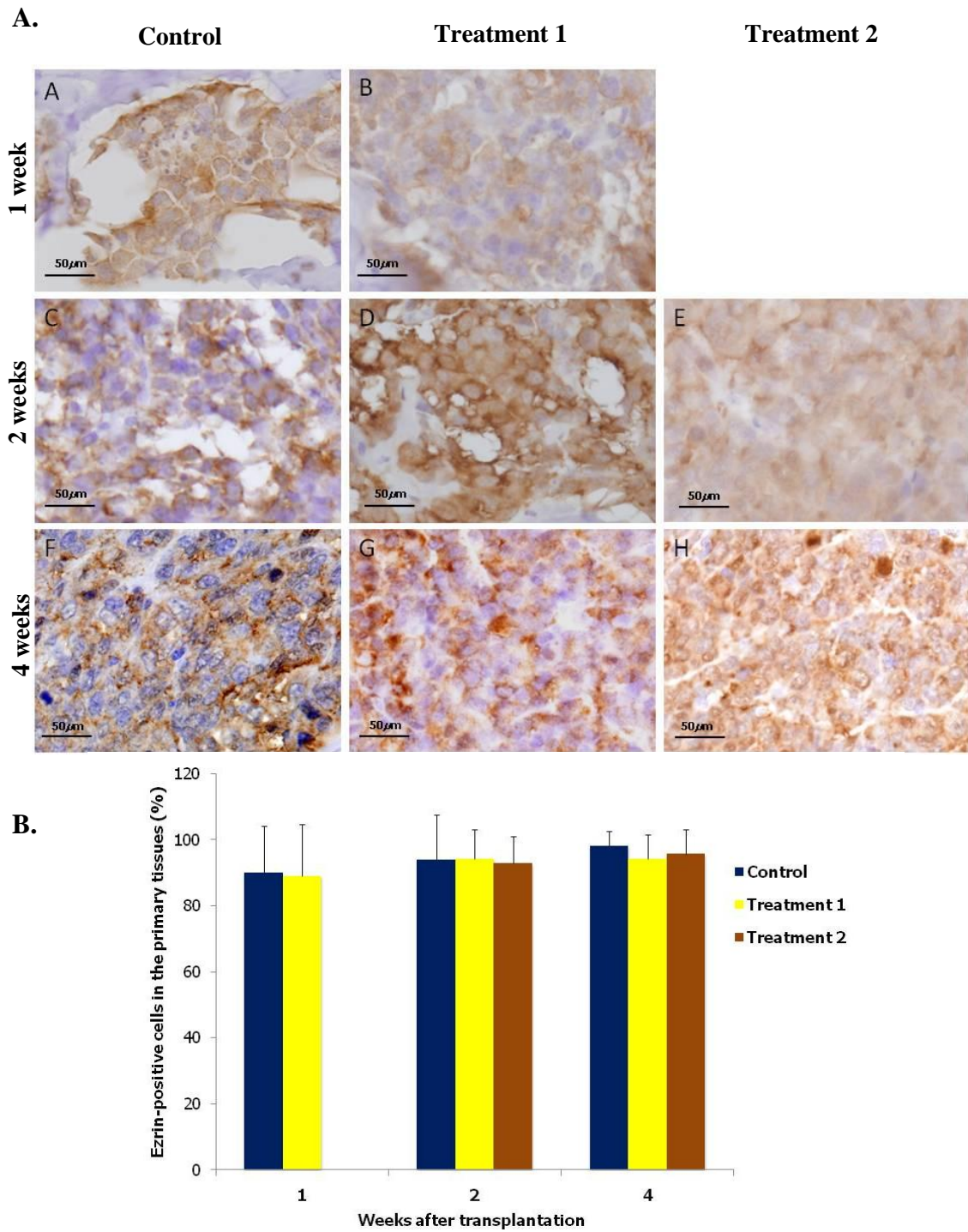
Figure 3.11. Expression of ezrin in the primary tissues. (A) Typical immunohistochemical staining for ezrin in primary tissues in each group after 1 week (A,B), 2 weeks (C,D,E), and 4 weeks (F,G,H) after transplantation**.** Original magnification, 400×. (B) The percentage of ezrin-positive cells was not significantly different between the control and treatment groups. Error bars represent SDs.
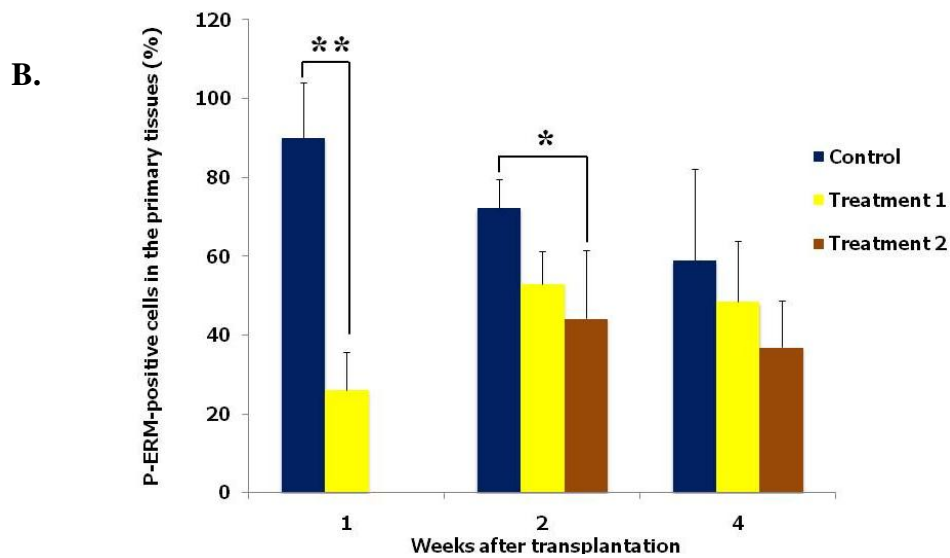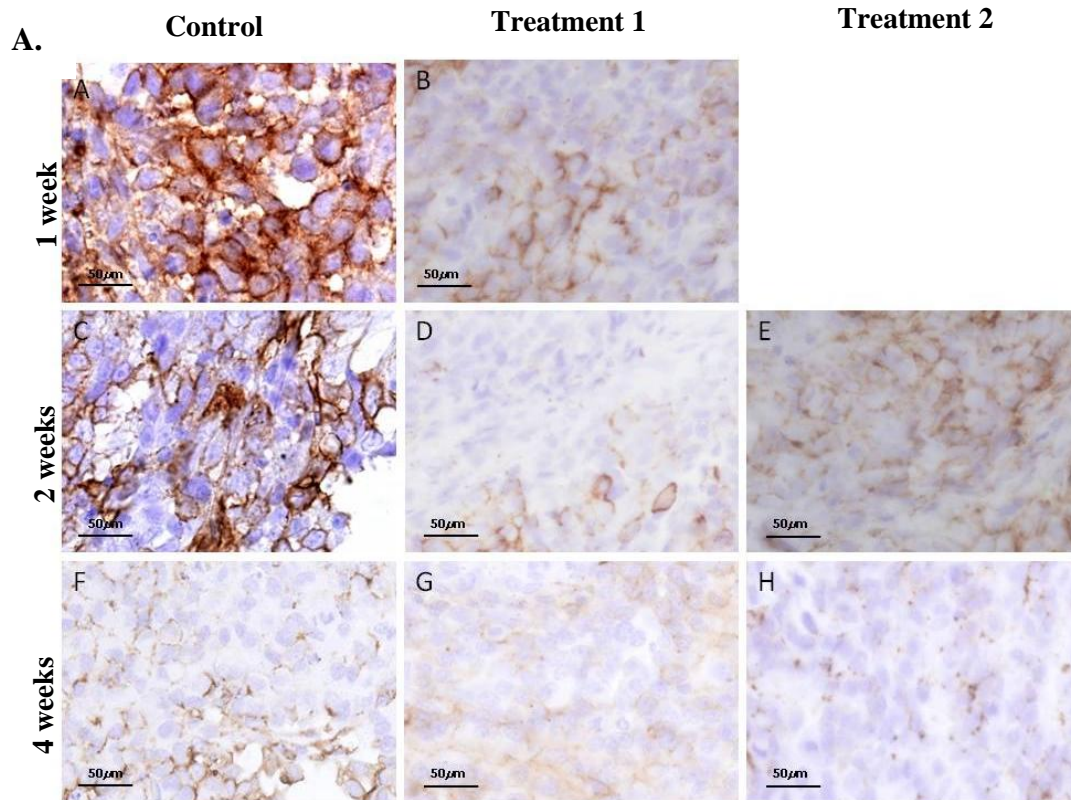
Figure 3.12. Expression of p-ERM in the primary tissues. (A) Typical immunohistochemical staining for p-ERM at primary tissues in each group after 1 week (A,B), 2 weeks (C,D,E), and 4 weeks (F,G,H) after transplantation. Original magnification, 400×. (B) The percentage of p-ERM-positive cells in the treatment 1 group was significantly lower ($p < 0.01$) than the control group at 1 week. The percentage of p-ERM-positive cells in the treatment 2 group was significantly lower ($p < 0.05$) than the control group at 2 weeks after transplantation. Significant difference (*$p < 0.05$, **$p < 0.01$) between the control and treatment groups; error bars represent SDs.
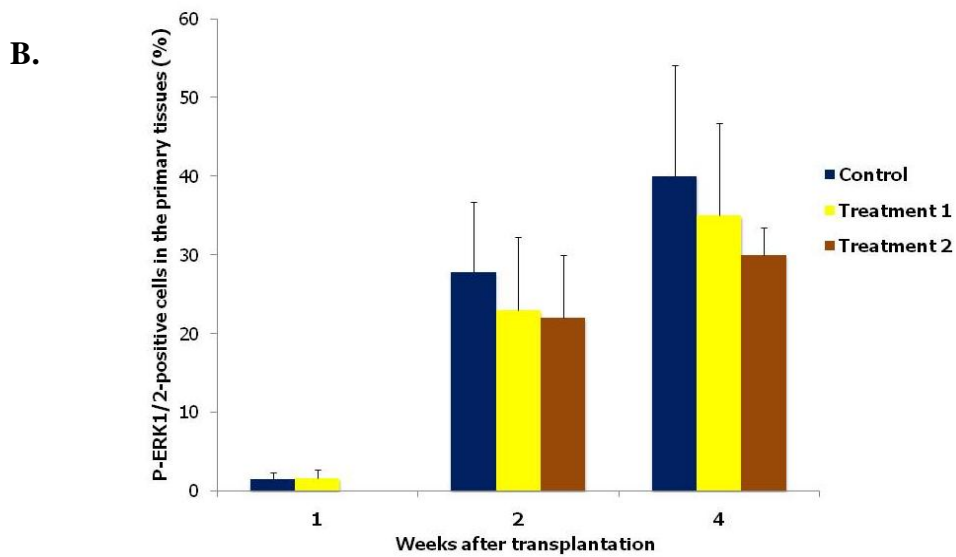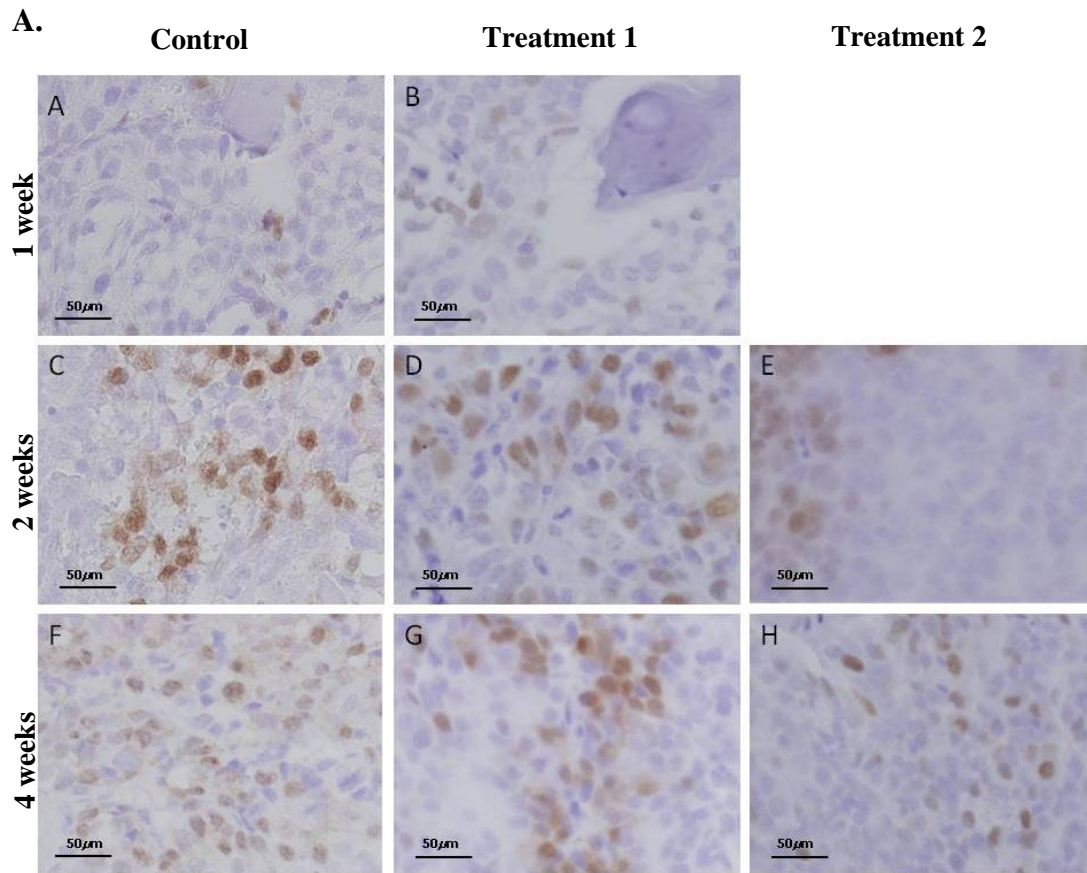
Figure 3.13 Expression of p-ERK1/2 in the primary tissues. (A) Typical immunohistochemical staining for p-ERK1/2 in primary tissues in each group after 1 week (A,B), 2 weeks (C,D,E), and 4 weeks (F,G,H) after transplantation. Original magnification, ×400. (B) The percentage of p-ERK1/2 was not significantly different between the control and treatment groups. Error bars represent SDs.
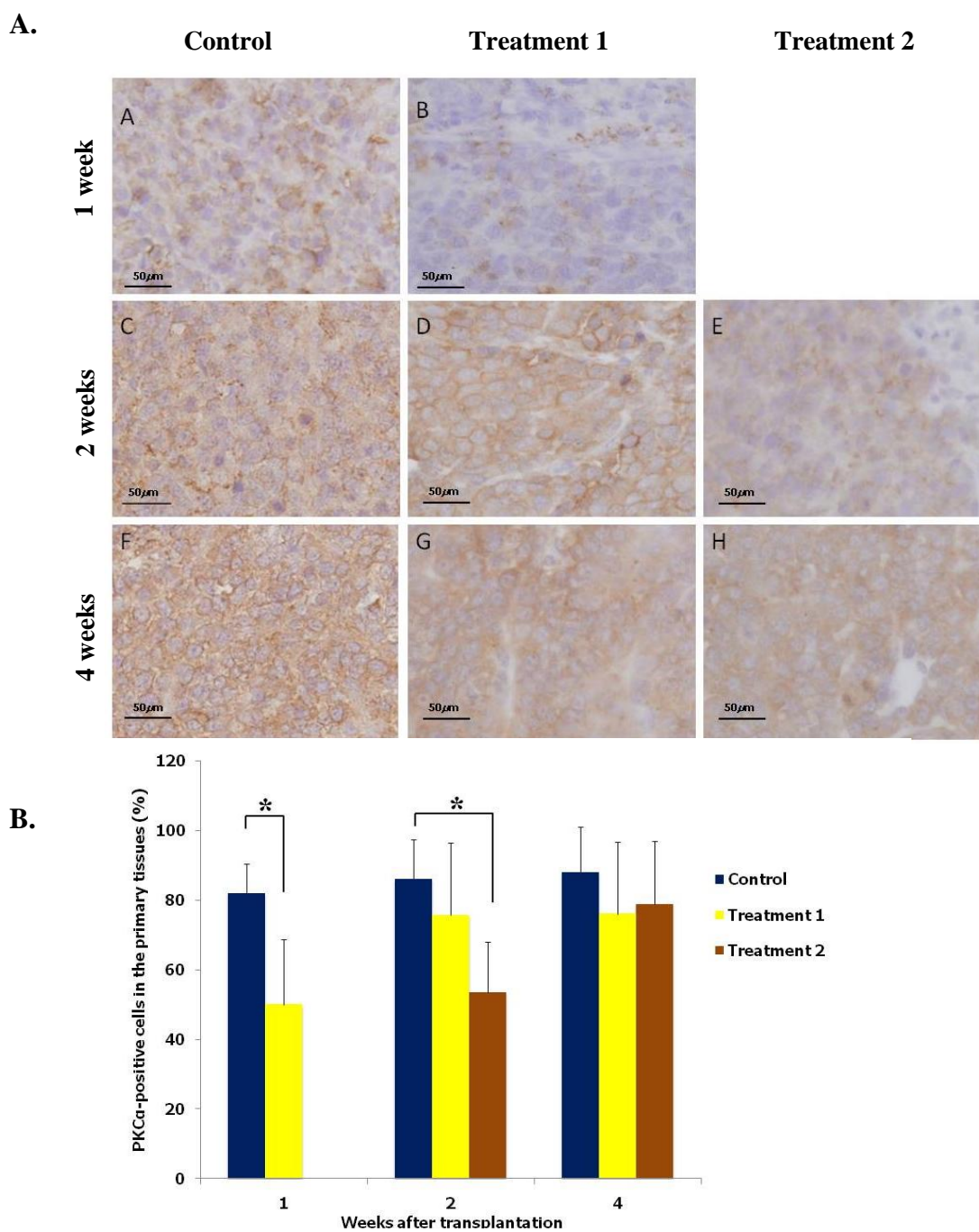
Figure 3.14 Expression on PKCα in the primary tissues. (A) Typical immunohistochemical staining for PKCα in primary tissues in each group after 1 week (A,B), 2 weeks (C,D,E), and 4 weeks (F,G,H) after transplantation. Original magnification, 400×. (B) The percentage of PKCα-positive cells in the treatment 1 group was significantly lower ($p < 0.05$) than the control group at 1 week and the percentage of PKCα-positive cells in the treatment 2 group was significantly lower ($p < 0.05$) than the control group at 2 weeks after transplantation. *Significant difference ($p < 0.05$) between the control and treatment groups; error bars represent SDs.
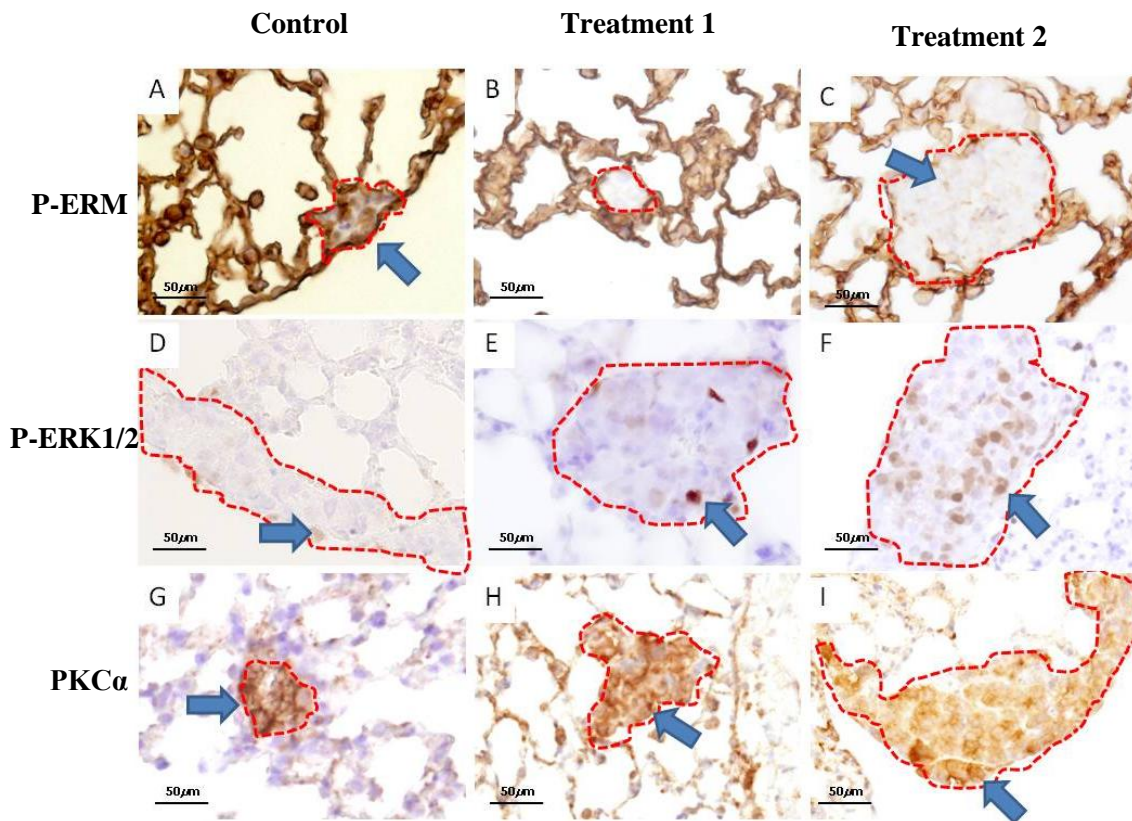
Figure 3.15 Immunohistochemical findings for p-ERM- (A,B,C), p-ERK1/2- (D,E,F), and PKCα-(G,H,I) positive cells (arrows) in the lung metastatic tissues of mice in the control group at 1 week and in the treatment 1 and 2 groups at 2 weeks after transplantation. Red dot lines indicate the tumor lesions in the lung tissues. Original magnification, 400×. P-ERM-positive cells was not detected on the lung metastatic nodules of the treatment group 1 and the percentage of p-ERM-positive cells in the treatment group 2 was low at 2 weeks after transplantation. p-ERK1/2-positive cells in the treatment 1 and 2 groups were not different from the control group. PKCα-positive cells in the treatment 1 and 2 groups were lower than the control group.
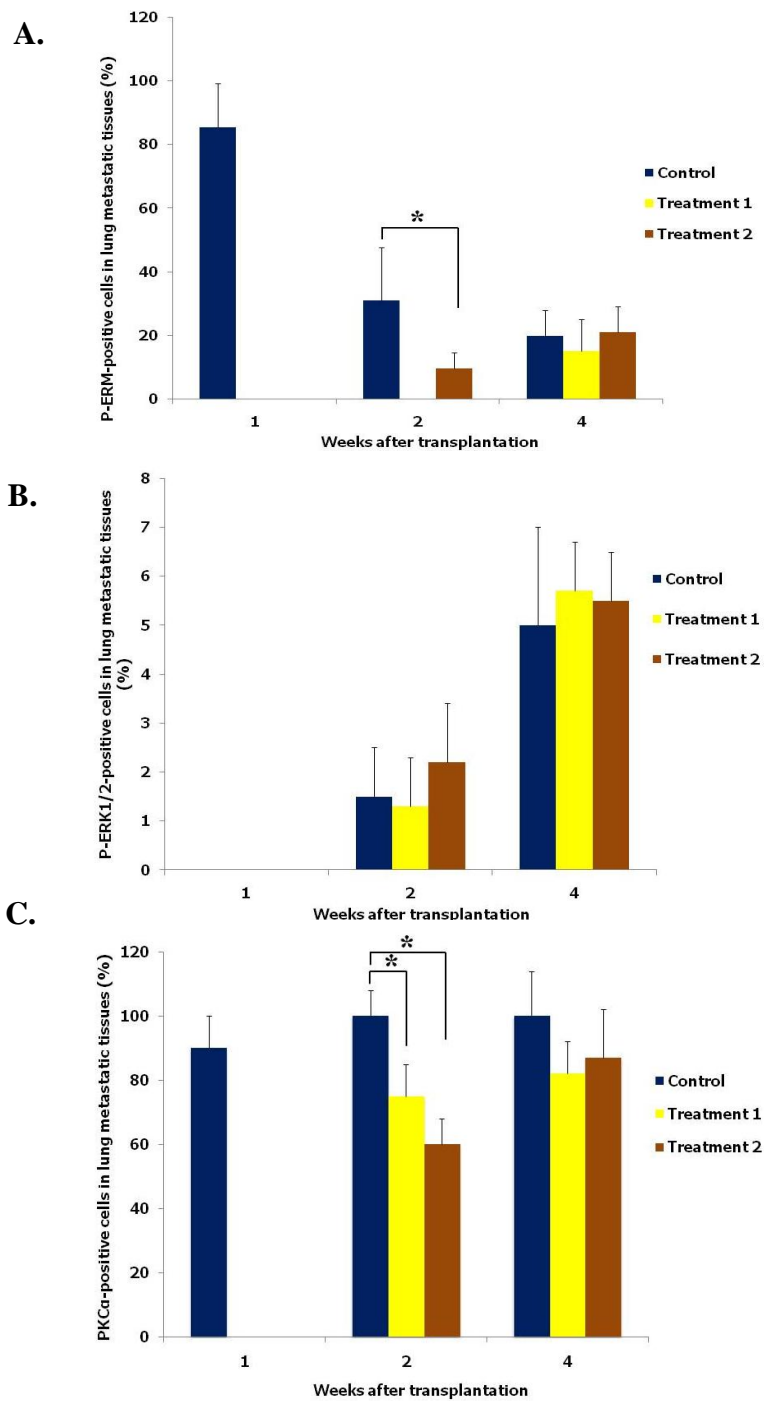
Figure 3.16 Expressions of p-ERM, p-ERK1/2, and PKCα in lung metastatic tissues. (A) The percentages of p-ERM-positive cells in the treatment 1 and 2 groups were significantly lower ($p < 0.05$) than that of the control group at 2 weeks after transplantation. There was no significant difference among all groups at 4 weeks after transplantation. (B) The percentages of p-ERK1/2-positive cells in each groups were not significantly different at 2 and 4 weeks after transplantation. (C) The percentages of PKCα-positive cells in the treatment 1 and 2 groups were significantly lower ($p < 0.05$) than that of the control group at 2 weeks after transplantation. There was no significant difference between the control and treatment groups at 4 weeks after transplantation.

Conclusion

Conclusion

OS is the most common malignant primary bone tumor in dogs and humans. Despite of advances in diagnosis and treatments for the primary tumor, development of lung metastasis continues to be the most significant cause of death in both species. Phosphorylation of ezrin is reported to be regulated by PKC (Ng *et al*., 2001; Ren *et al*., 2009) and described to have the crucial functions in metastatic process, including motility, invasion, adherence, survival of OS cells (Hunter, 2004; Khanna *et al*., 2004), and integration of membrane transport with signaling pathways, including MAPK pathway (del Pozo *et al*., 1996; Orian-Rousseau *et al*., 2007). Recently, several studies of ezrin's role in metastasis have been reported but they were limited to mouse and human OS (Khanna *et al*., 2001; Khanna *et al*., 2004; Ren *et al*., 2009). Therefore, the aim of this study was to investigate whether ezrin activity was associated with malignant behaviors of canine OS. For this purpose, canine OS specimens, cell lines, and xenografted mouse model were used in this study.

In chapter 1, primary tissues of canine OS patients obtained by surgical excision were used to determine the expression of ezrin and phosphorylated form of ezrin at C-terminal threonine 567 which detected through the expression of p-ERM. Moreover, PI was also used to evaluate the correlation between the proliferation potential of OS

tissues and the expression of ezrin and p-ERM. I hypothesized that the expression of ezrin and p-ERM was correlated with the negative prognostic factors of OS, including age, sex, breed, age, anatomical site, histology type, ALP, lung metastasis, survival time, and PI. Ezrin and p-ERM expressions were high in 87% of primary tissues of OS. I demonstrated that canine OS patients with high expressions of ezrin and p-ERM tended to be associated with a shorter survival time compared to those with low ezrin expression.

This suggested the possibility that the aggressive behavior of canine OS may not be dependent on any clinicopathological characteristics or the proliferation of the primary lesions and it may be used to answer the question why the lung metastasis often develops at the early time in the course of disease progression. However, it was difficult to conclude that ezrin and p-ERM expression in canine OS patients was a prognostic factor, but these proteins may be indicated to predict the outcome of canine OS patients. The roles of ezrin and p-ERM expressions in malignant behavior and the mechanism should be further clarified.

In section 1 of chapter 2, ezrin was expressed in all 3 cell lines (HMPOS, OOS, and CHOS), p-ERM was not expressed in CHOS cells, a least malignant OS cell line. As expected, CHOS cells could not produce any lung metastasis with either IT or SC transplantation. However, IT xenograft appeared to facilitate OS cell growth and lung

metastasis more than that of SC xenograft in HMPOS and OOS cells. These results suggested that the tumor growth and metastasis in this mouse model was dependent on the character of the cell lines despite of the transplantation site. In addition, transplantation sites may influence on the malignant behavior of metastatic OS cells, though the site could not change any potential of non-metastatic OS cells (CHOS).

IT transplantation with HMPOS and OOS cells exhibited higher expressions of ezrin and p-ERM when compared to SC transplantation of those cell lines. Interestingly, p-ERM may be essential in the earlier phase of progression because p-ERM expression in the primary and lung metastatic lesions decreased according to the time after transplantation.

In section 2 of chapter 2, high metastatic HMPOS and OOS cells expressed high B-Raf and C-Raf expressions but low p-ERK1/2 expression when compared to non-metastatic CHOS cells. PI, Ras, C-Raf, and p-ERK1/2 expressions in the primary lesions of IT-xenografted mice increased in a time-dependent manner and were significantly higher than SC- xenografted mice at the later progression time after transplantation and correlated with tumor growth. Although the expression of PKCα in primary tissues of IT-xenografted mice was high at all time points, in the earlier phase of progression, it was significantly higher than SC-xenografted mice.

These data suggested that phosphorylation of ezrin may be associated with PKCα. Moreover, the connection between ezrin and Ras/Raf/ERK pathway should be clarified.

Finally in chapter 3, CHE, a broad range PKC inhibitor, was used to regulate phosphorylation of ezrin. PKC was known to phosphorylate ezrin. The results in *in vitro* studies, the anti-migratory and anti-invasive effects of a PKC inhibitor were related to down regulation of p-ERM but not p-ERK1/2, which may be important information for therapeutic strategies in canine OS. This result was similar to the previous study in mouse and human OS cell lines (Ren *et al*., 2009; Yang *et al*., 2008).

The *in vivo* results suggested that CHE delayed development of lung metastasis in mice that had not yet developed lung micrometastases. Moreover, it suppressed lung metastatic potential in mice that had already developed lung micrometastases. In contrast, it had no effect on tumor growth. Taken together with the *in vitro* results, it may explain the relationship between the malignant behaviors and ezrin activity in that PKCα may be responsible for phosphorylation of ERM, including ezrin. In addition, P-ERM and PKCα, but not Ras/Raf/ERK pathway were regulated by CHE during migration and invasion to the lung, but not survival of OS cells. Therefore, PKC inhibitors may be especially active in canine patients that were dependent on ezrin at

high risk for metastasis. These data supported the value of the continued study on novel

therapeutic approaches that target ezrin-PKC phenotype in canine OS.

Acknowledgements

References

Barroga, E.F., Kadosawa, T., Okumura, M., Fujinaga, T., 1999, Establishment and characterization of the growth and pulmonary metastasis of a highly lung metastasizing cell line from canine osteosarcoma in nude mice. J Vet Med Sci 61, 361-367.

Bergman, P.J., MacEwen, E.G., Kurzman, I.D., Henry, C.J., Hammer, A.S., Knapp, D.W., Hale, A., Kruth, S.A., Klein, M.K., Klausner, J., Norris, A.M., McCaw, D., Straw, R.C., Withrow, S.J., 1996, Amputation and carboplatin for treatment of dogs with osteosarcoma: 48 cases (1991 to 1993). J Vet Intern Med 10, 76-81.

Berlin, O., Samid, D., Donthineni-Rao, R., Akeson, W., Amiel, D., Woods, V.L., Jr., 1993, Development of a novel spontaneous metastasis model of human osteosarcoma transplanted orthotopically into bone of athymic mice. Cancer Res 53, 4890-4895.

Bohling, T., Turunen, O., Jaaskelainen, J., Carpen, O., Sainio, M., Wahlstrom, T., Vaheri, A., Haltia, M., 1996, Ezrin expression in stromal cells of capillary hemangioblastoma. An immunohistochemical survey of brain tumors. Am J Pathol 148, 367-373.

Boston, S.E., Duerr, F., Bacon, N., Larue, S., Ehrhart, E.J., Withrow, S., 2007, Intraoperative radiation for limb sparing of the distal aspect of the radius without transcarpal plating in five dogs. Vet Surg 36, 314-323.

Boston, S.E., Ehrhart, N.P., Dernell, W.S., Lafferty, M., Withrow, S.J., 2006, Evaluation of survival time in dogs with stage III osteosarcoma that undergo treatment: 90 cases (1985-2004). J Am Vet Med Assoc 228, 1905-1908.

Bretscher, A., Edwards, K., Fehon, R.G., 2002, ERM proteins and merlin: integrators at the cell cortex. Nat Rev Mol Cell Biol 3, 586-599.

Bussard, K.M., Gay, C.V., Mastro, A.M., 2008, The bone microenvironment in metastasis; what is special about bone? Cancer Metastasis Rev 27, 41-55.

Cant, S.H., Pitcher, J.A., 2005, G protein-coupled receptor kinase 2-mediated phosphorylation of ezrin is required for G protein-coupled receptor-dependent reorganization of the actin cytoskeleton. Mol Biol Cell 16, 3088-3099.

Chackal-Roy, M., Niemeyer, C., Moore, M., Zetter, B.R., 1989, Stimulation of human prostatic carcinoma cell growth by factors present in human bone marrow. J Clin Invest 84, 43-50.

Chambers, A.F., Naumov, G.N., Vantyghem, S.A., Tuck, A.B., 2000, Molecular biology of breast cancer metastasis. Clinical implications of experimental studies on metastatic inefficiency. Breast Cancer Res 2, 400-407.

Chmura, S.J., Dolan, M.E., Cha, A., Mauceri, H.J., Kufe, D.W., Weichselbaum, R.R., 2000, In vitro and in vivo activity of protein kinase C inhibitor chelerythrine chloride induces tumor cell toxicity and growth delay in vivo. Clin Cancer Res 6, 737-742.

Chong, H., Vikis, H.G., Guan, K.L., 2003, Mechanisms of regulating the Raf kinase family. Cell Signal 15, 463-469.

Cui, Y., Li, T., Zhang, D., Han, J., 2010, Expression of Ezrin and phosphorylated Ezrin (pEzrin) in pancreatic ductal adenocarcinoma. Cancer Invest 28, 242-247.

Cui, Z.Y., Ahn, J.S., Lee, J.Y., Kim, W.S., Lim, H.Y., Jeon, H.J., Suh, S.W., Kim, J.H., Kong, W.H., Kang, J.M., Nam do, H., Park, K., 2006, Mouse Orthotopic Lung Cancer Model Induced by PC14PE6. Cancer Res Treat 38, 234-239.

Dass, C.R., Ek, E.T., Contreras, K.G., Choong, P.F., 2006, A novel orthotopic murine model provides insights into cellular and molecular characteristics contributing to human osteosarcoma. Clin Exp Metastasis 23, 367-380.

del Pozo, M.A., Sanchez-Mateos, P., Sanchez-Madrid, F., 1996, Cellular polarization induced by chemokines: a mechanism for leukocyte recruitment? Immunol Today 17, 127-131.

Dhillon, A.S., Hagan, S., Rath, O., Kolch, W., 2007, MAP kinase signalling pathways in cancer. Oncogene 26, 3279-3290.

Dickerson, M.E., Page, R.L., LaDue, T.A., Hauck, M.L., Thrall, D.E., Stebbins, M.E., Price, G.S., 2001, Retrospective analysis of axial skeleton osteosarcoma in 22 large-breed dogs. J Vet Intern Med 15, 120-124.

Elliott, B.E., Meens, J.A., SenGupta, S.K., Louvard, D., Arpin, M., 2005, The membrane cytoskeletal crosslinker ezrin is required for metastasis of breast carcinoma cells. Breast Cancer Res 7, R365-373.

Elzagheid, A., Korkeila, E., Bendardaf, R., Buhmeida, A., Heikkila, S., Vaheri, A., Syrjanen, K., Pyrhonen, S., Carpen, O., 2008, Intense cytoplasmic ezrin immunoreactivity predicts poor survival in colorectal cancer. Hum Pathol 39, 1737-1743.

Evans, L.B., 1983, Osteosarcoma in a young Great Dane dog. J S Afr Vet Assoc 54, 271-273.

Ferracini, R., Di Renzo, M.F., Scotlandi, K., Baldini, N., Olivero, M., Lollini, P., Cremona, O., Campanacci, M., Comoglio, P.M., 1995, The Met/HGF receptor is over-expressed in human osteosarcomas and is activated by either a paracrine or an autocrine circuit. Oncogene 10, 739-749.

Fievet, B.T., Gautreau, A., Roy, C., Del Maestro, L., Mangeat, P., Louvard, D., Arpin, M., 2004, Phosphoinositide binding and phosphorylation act sequentially in the activation mechanism of ezrin. J Cell Biol 164, 653-659.

Friedl, P., Wolf, K., 2003, Tumor-cell invasion and migration: Diversity and escape mechanisms. Nature Reviews Cancer 3, 362-374.

Garzotto, C.K., Berg, J., Hoffmann, W.E., Rand, W.M., 2000, Prognostic significance of serum alkaline phosphatase activity in canine appendicular osteosarcoma. J Vet Intern Med 14, 587-592.

Hameetman, L., Kok, P., Eilers, P.H., Cleton-Jansen, A.M., Hogendoorn, P.C., Bovee, J.V., 2005, The use of Bcl-2 and PTHLH immunohistochemistry in the diagnosis of peripheral chondrosarcoma in a clinicopathological setting. Virchows Arch 446, 430-437.

Hammer, A.S., Weeren, F.R., Weisbrode, S.E., Padgett, S.L., 1995, Prognostic factors in dogs with osteosarcomas of the flat or irregular bones. J Am Anim Hosp Assoc 31, 321-326.

Heidecker, G., Huleihel, M., Cleveland, J.L., Kolch, W., Beck, T.W., Lloyd, P., Pawson, T., Rapp, U.R., 1990, Mutational activation of c-raf-1 and definition of the minimal transforming sequence. Mol Cell Biol 10, 2503-2512.

Herbert, J.M., 1993, Protein kinase C: a key factor in the regulation of tumor cell adhesion to the endothelium. Biochem Pharmacol 45, 527-537.

Hillers, K.R., Dernell, W.S., Lafferty, M.H., Withrow, S.J., Lana, S.E., 2005, Incidence and prognostic importance of lymph node metastases in dogs with appendicular osteosarcoma: 228 cases (1986-2003). J Am Vet Med Assoc 226, 1364-1367.

Hirschfeld, S., Helman, L., 1994, Diverse roles of insulin-like growth factors in pediatric solid tumors. In Vivo 8, 81-90.

Hong, S.H., Kadosawa, T., Mochizuki, M., Matsunaga, S., Nishimura, R., Sasaki, N., 1998, Establishment and characterization of two cell lines derived from canine spontaneous osteosarcoma. J Vet Med Sci 60, 757-760.

Hulkower, I.K., Herber, R.L., 2011, Cell migration and invasion assays as tools for drug discovery. pharmaceutics 3, 107-124.

Hunter, K.W., 2004, Ezrin, a key component in tumor metastasis. Trends Mol Med 10, 201-204.

Ilmonen, S., Vaheri, A., Asko-Seljavaara, S., Carpen, O., 2005, Ezrin in primary cutaneous melanoma. Mod Pathol 18, 503-510.

Jarvis, W.D., Turner, A.J., Povirk, L.F., Traylor, R.S., Grant, S., 1994, Induction of apoptotic DNA fragmentation and cell death in HL-60 human promyelocytic leukemia cells by pharmacological inhibitors of protein kinase C. Cancer Res 54, 1707-1714.

Kam, Y., Guess, C., Estrada, L., Weidow, B., Quaranta, V., 2008, A novel circular invasion assay mimics in vivo invasive behavior of cancer cell lines and distinguishes single-cell motility in vitro. BMC Cancer 8, 198.

Kaminskyy, V., Lin, K.W., Filyak, Y., Stoika, R., 2008, Differential effect of sanguinarine, chelerythrine and chelidonine on DNA damage and cell viability in primary mouse spleen cells and mouse leukemic cells. Cell Biol Int 32, 271-277.

Keogh, R.J., 2010, New technology for investigating trophoblast function. Placenta 31, 347-350.

Khanna, C., Helman, L.J., 2006, Molecular approaches in pediatric oncology. Annu Rev Med 57, 83-97.

Khanna, C., Hunter, K., 2005, Modeling metastasis in vivo. Carcinogenesis 26, 513-523.

Khanna, C., Khan, J., Nguyen, P., Prehn, J., Caylor, J., Yeung, C., Trepel, J., Meltzer, P., Helman, L., 2001, Metastasis-associated differences in gene expression in a murine model of osteosarcoma. Cancer Res 61, 3750-3759.

Khanna, C., Prehn, J., Yeung, C., Caylor, J., Tsokos, M., Helman, L., 2000, An orthotopic model of murine osteosarcoma with clonally related variants differing in pulmonary metastatic potential. Clin Exp Metastasis 18, 261-271.

Khanna, C., Wan, X., Bose, S., Cassaday, R., Olomu, O., Mendoza, A., Yeung, C., Gorlick, R., Hewitt, S.M., Helman, L.J., 2004, The membrane-cytoskeleton linker ezrin is necessary for osteosarcoma metastasis. Nat Med 10, 182-186.

Killion, J.J., Radinsky, R., Fidler, I.J., 1998, Orthotopic models are necessary to predict therapy of transplantable tumors in mice. Cancer Metastasis Rev 17, 279-284.

Kim, C., Shin, E., Hong, S., Chon, H.J., Kim, H.R., Ahn, J.R., Hong, M.H., Yang, W.I., Roh, J.K., Rha, S.Y., 2009, Clinical value of ezrin expression in primary osteosarcoma. Cancer Res Treat 41, 138-144.

Kim, J., Thorne, S.H., Sun, L., Huang, B., Mochly-Rosen, D., 2011, Sustained inhibition of PKCalpha reduces intravasation and lung seeding during mammary tumor metastasis in an in vivo mouse model. Oncogene 30, 323-333.

Kim, M.S., Song, W.S., Cho, W.H., Lee, S.Y., Jeon, D.G., 2007, Ezrin expression predicts survival in stage IIB osteosarcomas. Clin Orthop Relat Res 459, 229-236.

Kirpensteijn, J., Kik, M., Rutteman, G.R., Teske, E., 2002, Prognostic significance of a new histologic grading system for canine osteosarcoma. Vet Pathol 39, 240-246.

Koivunen, J., Aaltonen, V., Koskela, S., Lehenkari, P., Laato, M., Peltonen, J., 2004, Protein kinase C alpha/beta inhibitor Go6976 promotes formation of cell junctions and inhibits invasion of urinary bladder carcinoma cells. Cancer Res 64, 5693-5701.

Krishnan, K., Bruce, B., Hewitt, S., Thomas, D., Khanna, C., Helman, L.J., 2006, Ezrin mediates growth and survival in Ewing's sarcoma through the AKT/mTOR, but not the MAPK, signaling pathway. Clin Exp Metastasis 23, 227-236.

Kubota, T., 1994, Metastatic models of human cancer xenografted in the nude mouse: the importance of orthotopic transplantation. J Cell Biochem 56, 4-8.

Kuo, T.H., Kubota, T., Watanabe, M., Furukawa, T., Kase, S., Tanino, H., Saikawa, Y., Ishibiki, K., Kitajima, M., Hoffman, R.M., 1993, Site-specific chemosensitivity of human small-cell lung carcinoma growing orthotopically compared to subcutaneously in SCID mice: the importance of orthotopic models to obtain relevant drug evaluation data. Anticancer Res 13, 627-630.

Laprie, C., Abadie, J., Amardeilh, M.F., Net, J.L., Lagadic, M., Delverdier, M., 2001, MIB-1 immunoreactivity correlates with biologic behaviour in canine cutaneous melanoma. Vet Dermatol 12, 139-147.

Leicht, D.T., Balan, V., Kaplun, A., Singh-Gupta, V., Kaplun, L., Dobson, M., Tzivion, G., 2007, Raf kinases: function, regulation and role in human cancer. Biochim Biophys Acta 1773, 1196-1212.

Ling, G.V., Morgan, J.P., Pool, R.R., 1974, Primary bone rumors in the dog: a combined clinical, radiographic, and histologic approach to early diagnosis. J Am Vet Med Assoc 165, 55-67.

Liptak, J.M., Dernell, W.S., Straw, R.C., Rizzo, S.A., Lafferty, M.H., Withrow, S.J., 2004, Proximal radial and distal humeral osteosarcoma in 12 dogs. J Am Anim Hosp Assoc 40, 461-467.

Loukopoulos, P., Robinson, W.F., 2007, Clinicopathological relevance of tumour grading in canine osteosarcoma. J Comp Pathol 136, 65-73.

Luu, H.H., Kang, Q., Park, J.K., Si, W., Luo, Q., Jiang, W., Yin, H., Montag, A.G., Simon, M.A., Peabody, T.D., Haydon, R.C., Rinker-Schaeffer, C.W., He, T.C., 2005, An orthotopic model of human osteosarcoma growth and spontaneous pulmonary metastasis. Clin Exp Metastasis 22, 319-329.

Malikova, J., Zdarilova, A., Hlobilkova, A., Ulrichova, J., 2006, The effect of chelerythrine on cell growth, apoptosis, and cell cycle in human normal and cancer cells in comparison with sanguinarine. Cell Biol Toxicol 22, 439-453.

Matsui, T., Maeda, M., Doi, Y., Yonemura, S., Amano, M., Kaibuchi, K., Tsukita, S., 1998, Rho-kinase phosphorylates COOH-terminal threonines of ezrin/radixin/moesin (ERM) proteins and regulates their head-to-tail association. J Cell Biol 140, 647-657.

McNeill, C.J., Overley, B., Shofer, F.S., Kent, M.S., Clifford, C.A., Samluk, M., Haney, S., Van Winkle, T.J., Sorenmo, K.U., 2007, Characterization of the biological behaviour of appendicular osteosarcoma in Rottweilers and a comparison with other breeds: a review of 258 dogs. Vet Comp Oncol 5, 90-98.

Meng, Y., Lu, Z., Yu, S., Zhang, Q., Ma, Y., Chen, J., 2010, Ezrin promotes invasion and metastasis of pancreatic cancer cells. J Transl Med 8, 61.

Misdorp, W., Hart, A.A., 1979, Some prognostic and epidemiologic factors in canine osteosarcoma. J Natl Cancer Inst 62, 537-545.

Mohammed, R.A., Green, A., El-Shikh, S., Paish, E.C., Ellis, I.O., Martin, S.G., 2007, Prognostic significance of vascular endothelial cell growth factors -A, -C and -D in breast cancer and their relationship with angio- and lymphangiogenesis. Br J Cancer 96, 1092-1100.

Moilanen, J., Lassus, H., Leminen, A., Vaheri, A., Butzow, R., Carpen, O., 2003, Ezrin immunoreactivity in relation to survival in serous ovarian carcinoma patients. Gynecol Oncol 90, 273-281.

Moore, A.S., Dernell, W.S., Ogilvie, G.K., Kristal, O., Elmslie, R., Kitchell, B., Susaneck, S., Rosenthal, R., Klein, M.K., Obradovich, J., Legendre, A., Haddad, T., Hahn, K., Powers, B.E., Warren, D., 2007, Doxorubicin and BAY 12-9566 for the treatment of osteosarcoma in dogs: a randomized, double-blind, placebo-controlled study. J Vet Intern Med 21, 783-790.

Morrison, D.K., Cutler, R.E., 1997, The complexity of Raf-1 regulation. Curr Opin Cell Biol 9, 174-179.

Musashi, M., Ota, S., Shiroshita, N., 2000, The role of protein kinase C isoforms in cell proliferation and apoptosis. Int J Hematol 72, 12-19.

Nakajima, M., Morikawa, K., Fabra, A., Bucana, C.D., Fidler, I.J., 1990, Influence of organ environment on extracellular matrix degradative activity and metastasis of human colon carcinoma cells. J Natl Cancer Inst 82, 1890-1898.

Nakamura, N., Oshiro, N., Fukata, Y., Amano, M., Fukata, M., Kuroda, S., Matsuura, Y., Leung, T., Lim, L., Kaibuchi, K., 2000, Phosphorylation of ERM proteins at filopodia induced by Cdc42. Genes Cells 5, 571-581.

Nakamura, T., Fidler, I.J., Coombes, K.R., 2007, Gene expression profile of metastatic human pancreatic cancer cells depends on the organ microenvironment. Cancer Res 67, 139-148.

Ng, T., Parsons, M., Hughes, W.E., Monypenny, J., Zicha, D., Gautreau, A., Arpin, M., Gschmeissner, S., Verveer, P.J., Bastiaens, P.I., Parker, P.J., 2001, Ezrin is a

downstream effector of trafficking PKC-integrin complexes involved in the control of cell motility. EMBO J 20, 2723-2741.

Norrdin, R.W., Powers, B.E., Torgersen, J.L., Smith, R.E., Withrow, S.J., 1989, Characterization of osteosarcoma cells from two sibling large-breed dogs. Am J Vet Res 50, 1971-1975.

Ohta, G., Sakai, H., Kachi, S., Hirata, A., Yonemaru, K., Kitajima, A., Yanai, T., Masegi, T., 2004, Assessment of proliferative potentials of canine osteosarcomas and chondrosarcomas by MIB-1 immunohistochemistry and bromodeoxyuridine incorporation. J Comp Pathol 131, 18-27.

Orian-Rousseau, V., Morrison, H., Matzke, A., Kastilan, T., Pace, G., Herrlich, P., Ponta, H., 2007, Hepatocyte growth factor-induced Ras activation requires ERM proteins linked to both CD44v6 and F-actin. Mol Biol Cell 18, 76-83.

Park, H.R., Jung, W.W., Bacchini, P., Bertoni, F., Kim, Y.W., Park, Y.K., 2006, Ezrin in osteosarcoma: comparison between conventional high-grade and central low-grade osteosarcoma. Pathol Res Pract 202, 509-515.

Pearson, M.A., Reczek, D., Bretscher, A., Karplus, P.A., 2000, Structure of the ERM protein moesin reveals the FERM domain fold masked by an extended actin binding tail domain. Cell 101, 259-270.

Pietromonaco, S.F., Simons, P.C., Altman, A., Elias, L., 1998, Protein kinase C-theta phosphorylation of moesin in the actin-binding sequence. J Biol Chem 273, 7594-7603.

Propper, D.J., Macaulay, V., O'Byrne, K.J., Braybrooke, J.P., Wilner, S.M., Ganesan, T.S., Talbot, D.C., Harris, A.L., 1998, A phase II study of bryostatin 1 in metastatic malignant melanoma. Br J Cancer 78, 1337-1341.

Ren, L., Hong, S.H., Cassavaugh, J., Osborne, T., Chou, A.J., Kim, S.Y., Gorlick, R., Hewitt, S.M., Khanna, C., 2009, The actin-cytoskeleton linker protein ezrin is regulated during osteosarcoma metastasis by PKC. Oncogene 28, 792-802.

Ru, G., Terracini, B., Glickman, L.T., 1998, Host related risk factors for canine osteosarcoma. Vet J 156, 31-39.

Sakai, H., Noda, A., Shirai, N., Iidaka, T., Yanai, T., Masegi, T., 2002, Proliferative activity of canine mast cell tumours evaluated by bromodeoxyuridine incorporation and Ki-67 expression. J Comp Pathol 127, 233-238.

Sakai, H., Yamane, T., Yanai, T., Shirai, N., Masegi, T., 2001, Expression of cyclin kinase inhibitor p27(Kip1) in skin tumours of dogs. J Comp Pathol 125, 153-158.

Salas, S., Bartoli, C., Deville, J.L., Gaudart, J., Fina, F., Calisti, A., Bollini, G., Curvale, G., Gentet, J.C., Duffaud, F., Figarella-Branger, D., Bouvier, C., 2007, Ezrin and alpha-smooth muscle actin are immunohistochemical prognostic markers in conventional osteosarcomas. Virchows Arch 451, 999-1007.

Salas, S., de Pinieux, G., Gomez-Brouchet, A., Larrousserie, F., Leroy, X., Aubert, S., Decouvelaere, A.V., Giorgi, R., Fernandez, C., Bouvier, C., 2009, Ezrin immunohistochemical expression in cartilaginous tumours: a useful tool for differential diagnosis between chondroblastic osteosarcoma and chondrosarcoma. Virchows Arch 454, 81-87.

Seitz, P.K., Zhu, B.T., Cooper, C.W., 1992, Effect of transforming growth factor beta on parathyroid hormone receptor binding and cAMP formation in rat osteosarcoma cells. J Bone Miner Res 7, 541-546.

Selvarajah, G.T., Kirpensteijn, J., van Wolferen, M.E., Rao, N.A., Fieten, H., Mol, J.A., 2009, Gene expression profiling of canine osteosarcoma reveals genes associated with short and long survival times. Mol Cancer 8, 72.

Slayter, M.V., Boosinger, T.R., Pool, R.R., Dammrich, K., Misdorp, W., Larsen, S. 1994. Histological Classification of Bone and Joint Tumors of Domestic Animals (Washinton, D.C.), 7-11.

Soderstrom, M., Palokangas, T., Vahlberg, T., Bohling, T., Aro, H., Carpen, O., 2010, Expression of ezrin, Bcl-2, and Ki-67 in chondrosarcomas. APMIS 118, 769-776.

Spodnick, G.J., Berg, J., Rand, W.M., Schelling, S.H., Couto, G., Harvey, H.J., Henderson, R.A., MacEwen, G., Mauldin, N., McCaw, D.L., *et al*., 1992, Prognosis for dogs with appendicular osteosarcoma treated by amputation alone: 162 cases (1978-1988). J Am Vet Med Assoc 200, 995-999.

Straw, R.C., Withrow, S.J., 1996, Limb-sparing surgery versus amputation for dogs with bone tumors. Vet Clin North Am Small Anim Pract 26, 135-143.

Straw, R.C., Withrow, S.J., Powers, B.E., 1990, Management of canine appendicular osteosarcoma. Vet Clin North Am Small Anim Pract 20, 1141-1161.

Sullivan, R.M., Stone, M., Marshall, J.F., Uberall, F., Rotenberg, S.A., 2000, Photo-induced inactivation of protein kinase calpha by dequalinium inhibits motility of murine melanoma cells. Mol Pharmacol 58, 729-737.

Togo, S., Shimada, H., Kubota, T., Moossa, A.R., Hoffman, R.M., 1995, Host organ specifically determines cancer progression. Cancer Res 55, 681-684.

Wald, F.A., Oriolo, A.S., Mashukova, A., Fregien, N.L., Langshaw, A.H., Salas, P.J., 2008, Atypical protein kinase C (iota) activates ezrin in the apical domain of intestinal epithelial cells. J Cell Sci 121, 644-654.

Walterova, D., Ulrichova, J., Valka, I., Vicar, J., Vavreckova, C., Taborska, E., Harjrader, R.J., Meyer, D.L., Cerna, H., Simanek, V., 1995, Benzo[c]phenanthridine alkaloids sanguinarine and chelerythrine: biological activities and dental care applications. Acta Univ Palacki Olomuc Fac Med 139, 7-16.

Welch, D.R., 1997, Technical considerations for studying cancer metastasis in vivo. Clin Exp Metastasis 15, 272-306.

Weng, W.H., Ahlen, J., Astrom, K., Lui, W.O., Larsson, C., 2005, Prognostic impact of immunohistochemical expression of ezrin in highly malignant soft tissue sarcomas. Clin Cancer Res 11, 6198-6204.

Withrow, S.J., MacEwen, G. 1989. Clinical Veterinary Oncology. In Tumors of the skeletal system, La Rue, S.M., Withrow, S.J., eds. (Philadephia, JB Lippincott), 234-252.

Withrow, S.J., Vail, D.M. 2007. Small Animal Clinical Oncology. In Tumors of the skeletal system, Dernell, W.S., Ehrhart, N.P., Straw, R.C., Vail, D.M., eds. (St. Louis, SAUNDERS), 540-582.

Xu-Dong, S., Zan, S., Shui-er, Z., Li-na, T., Wen-xi, Y., Feng, L., Yang, Y., 2009, Expression of Ezrin correlates with lung metastasis in Chinese patients with osteosarcoma. Clin Invest Med 32, E180-188.

Yang, R., Piperdi, S., Gorlick, R., 2008, Activation of the RAF/mitogen-activated protein/extracellular signal-regulated kinase kinase/extracellular signal-regulated kinase pathway mediates apoptosis induced by chelerythrine in osteosarcoma. Clin Cancer Res 14, 6396-6404.

Yu, Y., Khan, J., Khanna, C., Helman, L., Meltzer, P.S., Merlino, G., 2004, Expression profiling identifies the cytoskeletal organizer ezrin and the developmental homeoprotein Six-1 as key metastatic regulators. Nat Med 10, 175-181.

Yuan, J., Ossendorf, C., Szatkowski, J.P., Bronk, J.T., Maran, A., Yaszemski, M., Bolander, M.E., Sarkar, G., Fuchs, B., 2009, Osteoblastic and osteolytic human osteosarcomas can be studied with a new xenograft mouse model producing spontaneous metastases. Cancer Invest 27, 435-442.

Zonder, J.A., Shields, A.F., Zalupski, M., Chaplen, R., Heilbrun, L.K., Arlauskas, P., Philip, P.A., 2001, A phase II trial of bryostatin 1 in the treatment of metastatic colorectal cancer. Clin Cancer Res 7, 38-42.